

St. John's University

St. John's Scholar

Theses and Dissertations

2019

**INVESTIGATION OF COMPACTION BEHAVIOR OF
PHARMACEUTICAL POWDERS: AN ELUCIDATION BASED ON
PERCOLATION THEORY**

Saurabh Maheshwari Mishra

Follow this and additional works at: https://scholar.stjohns.edu/theses_dissertations

**INVESTIGATION OF COMPACTION BEHAVIOR OF PHARMACEUTICAL
POWDERS:
AN ELUCIDATION BASED ON PERCOLATION THEORY**

A dissertation submitted in partial fulfillment of the
requirements for the degree of

DOCTOR OF PHILOSOPHY

to the faculty of the department of

GRADUATE DIVISION

COLLEGE OF PHARMACY AND HEALTH SCIENCES

at

ST. JOHN'S UNIVERSITY

New York

by

SAURABH M. MISHRA

Date Submitted: _____ Date Approved: _____

Saurabh M. Mishra

Bhagwan D. Rohera, Ph.D.

ABSTRACT

INVESTIGATION OF COMPACTION BEHAVIOR OF PHARMACEUTICAL POWDERS: AN ELUCIDATION BASED ON PERCOLATION THEORY

Saurabh M. Mishra

Pharmaceutical product development has evolved from conventional empirical approach towards the more systematic and science based approach over the past decades. However, the process of tableting and compaction behavior of pharmaceutical powders is still ambiguous and not well understood. In the present study, a comprehensive attempt has been made to understand this complex and dynamic process of compaction of disordered pharmaceutical powders using percolation phenomenon. Commonly used pharmaceutical powder materials, spheres and their binary mixtures of different particle sizes, crystal structure and deformation behavior were compressed at varying compression loads at different relative densities. Mechanical strength of tablets, namely radial tensile strength, compressive strength and elastic modulus, were evaluated and studied according to the classical models of powder compaction and percolation phenomenon. It was found that percolation phenomenon has a significant effect on the compaction of powder materials and can be used to characterize deformation and bonding behavior of powder materials. A model developed on the fundamentals of percolation theory was found to predict the compactibility of disordered powder materials and their binary mixtures with higher accuracy compared to the established classical compaction models. Moreover, it was found that the developed model can predict the dilution capacity of excipients and can be used as a material-sparing tool in the initial formulation development of tablet dosage forms. It was also found that percolation theory can help to understand mechanics of tablet

formation more clearly by establishing a relationship between compressibility and compactibility phenomena of powder materials. Further, a closer look at tableting process reveals that process of tableting closely mimics 3-dimensional correlated diffusive percolation phenomenon with a universal critical exponent value of $q = 2$ and percolation thresholds, $\rho_c = 0.634$ ($z = 12$) and 0.366 ($z = 6$) depending on the type of material used. Similar results were also observed in the case of powders compacted using an industrial scale rotary tablet press thus confirming that tableting of pharmaceutical powders is far from an equilibrium process depending upon the variability of time and space. Thus it can be concluded that comprehensive application of percolation theory can serve as a single effective tool in the study of compaction behavior of pharmaceutical powders and can be effectively used in the current quality by design (QbD) practice to establish robust design space for the formulation development of tablet dosage forms.

ACKNOWLEDGEMENTS

First and foremost, I wish to express my gratitude to my mentor and thesis research supervisor, Dr. Bhagwan D. Rohera, for his immense support and encouragement throughout my graduate studies at St. John's University College of Pharmacy and Health Sciences during the period 2013-2015 (M.S.) and 2015-2019 (Ph.D.). My association with him for these six years would always remain as the most memorable and wonderful period of my life. During these years, he not only acted as a mentor and thesis research supervisor but also guided and prepared me for the future and taught me the principles which I would always try to emulate in my life. Under his guidance, I not only grew as a science scholar but also became a better and confident person.

I would also like to thank my co-mentor Dr. Hans Leuenberger, Professor Emeritus of Pharmaceutical Technology, University of Basel, Switzerland and, presently, Adjunct Professor of Pharmaceutics, Florida University College of Pharmacy, Orlando, FL for his guidance, contribution as well his passion towards this research project. I would always consider myself as one of the very few fortunate PhD students having completed his PhD under two esteemed persons of the field.

I am grateful to Dr. Senshang Lin, Dr. Tanaji Talele, Dr. Ketan Patel and Dr. Nitesh Kunda for serving as members of my thesis research committee and for their insightful comments and suggestions that helped me widen my research from various perspectives. I would also like to thank Dr. Sandra Reznik for agreeing to serve as chair of the defense committee. My sincere thanks to all other faculty members who helped me develop other skills through course work and assignments. I would also like to acknowledge the financial

support in the form of teaching/doctoral fellowship from St. John's University during my graduate studies.

I would like to extend my thanks to Dr. Florin Catrina, St. John's College for allowing me to take calculus classes during the early stage of my doctoral thesis research as well as his patience to understand my research project and clarifying various math questions. I would also like to thank Dr. Nikhil Gupta and Yi Yang, NYU Tandon School of Engineering, Brooklyn for permitting me to use Instron Testing Instrument that made a part of this study possible.

I would also like to extend my special thanks to Dr. Michael Levin, MCC Corporation, East Hanover, NJ for providing rotary press data of Avicel[®] PH 101 and Emcompress[®] that made a part of this study possible. Along with this, I would like to thank the BASF Corporation (Ludwigshafen, Germany), FMC Biopolymers (Newark, DE), JRS Pharma (Patterson, NY), Pharmatrans Sanaq AG (Basel, Switzerland), Freund Corporation (Shinjuku-Ku, Japan) for kindly providing the gift samples of several polymeric excipients and sugar spheres to carry out this research.

I owe a big thanks to my friends Hemanth Mamidi, Siddhant Palekar, Pulkit Khatri and others for their perpetual help and support. I also wish to thank everyone who helped me during my thesis research.

I would like to express my utmost gratitude to my grandparents (Late Dr. Mukutdhari Mishra and Shyama Mishra), parents (Dr. Maheshwari Kumar Mishra and Geeta Mishra) and sisters (Shubhi and Shuchi) for their blessings, love, and support. I would also like to extend a special thanks to my wife, Sweta, for her endless love, support, and well wishes. It is those endless moments that my family sacrificed to harbor and

culminate the principles that make me the person I am. I faithfully owe my gratitude to them for their invaluable place in my life.

In addition, I would like to extend my sincere thanks to the entire powder and tablet technologists as well as other pharmaceutical scientists who have been constantly and diligently working in this area for the progress and advancement of this field.

Last but not least, I would like to thank *Lord Shri Ramchandra* for giving me this wonderful life and the sole reason for my very existence.

I dedicate this work to my grandfather, Dr. Mukutdhari Mishra, a great scholar and academician who always taught me the importance of keeping deservedness over desirability and earning over craving. His love, teaching and knowledge have helped me understand the importance of education, humanity and spirituality in my life. A big thank you Panditji.

TABLE OF CONTENTS

1. Introduction	1
1.1 History and Background	1
1.2. The Complexity of Pharmaceutical Powders	10
1.2.1. Powder: A 4 th State of matter	10
1.2.2. Phenomenon of Powder Compression	11
1.3. Powder Properties and their characterization	14
1.3.1. Compressibility of powder	14
1.3.2. Compactibility of Powder	18
1.4. Compaction of Powder mixtures: Failure of Classical models.....	22
1.5. Fundamentals of Percolation Theory	24
1.5.1. Theoretical Section	29
1.5.2. Mathematical Aspects of Percolation Theory	32
1.5.3. Percolation Phenomenon in Powder Technology.....	33
1.6. Research Objectives.....	37
2. Materials and Methods	39
2.1. Materials	39
2.2. Methods	39
2.2.1. Physical Characterization of Powder Materials	39
2.2.2. True Density	40
2.2.3. Compression of Powders and Evaluation of Tablet Properties	41
2.2.4. Relative Density and Porosity	43
2.2.5. Radial Tensile Strength	43

2.2.6. Young's or Elastic Modulus, E	44
2.2.7. Compressive strength of compact	44
2.2.8. Compressibility of powder materials	47
2.2.9. Compactibility of Powder materials	50
2.3. Estimation of Young's modulus/Elastic modulus at zero porosity.....	53
2.3.1. Estimation of bond and site percolation threshold.....	53
2.3.2. Percolation Model	54
2.3.3. Universality of critical exponent, q	57
2.3.4. Critical exponent for powder compression	60
2.3.5. Approximation to Bethe Lattice assuming $q=1$	63
2.3.6. Assuming the value of critical exponent based on mechanical lattices	65
2.3.7. Correlated Percolation Phenomenon	66
2.3.8. Statistical Evaluation and Nonlinear Regression Analysis	68
3. Results and Discussion	72
3.1. Chapter I: Compaction Behavior of Single component Powder and Understanding Mechanics of Tablet Formation by Classical Models and Percolation Theory	72
3.1.1. Compressibility and Compression Behavior of Powder Materials	73
3.1.2. Compactibility of Powder Materials	81
3.1.3. Compactibility of Binary Mixtures	91
3.1.4. Chapter Summary	97
3.2. Chapter II: Compaction behavior of disordered binary powder mixtures	100
3.2.1. Percolation threshold and compactibility of single components	101
3.2.2. Percolation threshold of binary mixtures	109

3.2.3. Compactibility of binary mixtures	114
3.2.4. Significance of Percolation model and its application in QbD	123
3.2.5. Chapter Summary	125
3.3. Chapter III: Relationship between Mechanical Properties and Anisotropy of compact	127
3.3.1. Effect of Compression load on Elastic modulus, compressive strength and Tensile strength	128
3.3.2. Establishing a relationship between mechanical properties	131
3.3.3. Elastic modulus at zero porosity	135
3.3.4. Compressive strength and tensile strength at zero porosity	142
3.3.5. Chapter Summary	149
3.4. Chapter IV: A Closer Look at Tableting Process: An Order Out of Chaos	150
3.4.1. Spheres and powder materials	153
3.4.2. Effect of particle size on percolation threshold	157
3.4.3. Effect of crystalline nature of microcrystalline cellulose on percolation threshold	157
3.4.4. A simple experimental set up for studying processes far-from-equilibrium conditions	163
3.4.5. Chapter Summary	164
3.5. Chapter V: Consolidation of Powder and Elucidation of Bonding Area and Bonding Strength Using Percolation Theory.....	166
3.5.1. A Modified model to define compactibility of powder materials	166
3.5.2. Compressibility of powder materials and their binary mixtures	167

3.5.3. Compactibility of Powder materials and their binary mixtures	174
3.5.4. Elucidation of Bonding Area and Bonding Strength by Percolation Theory	183
3.5.5. Chapter Summary	187
4. Conclusions	188
References	189
Appendix	204

LIST OF TABLES

Table 1: Values of bond and site percolation thresholds of ideal systems (Isichenko 1992)	28
Table 2: Values of critical exponent of lattice in various dimensions	62
Table 3: Various statistical parameters that describe a nonlinear regression analysis	71
Table 4: Values of bond and site percolation thresholds estimated using Heckel equation (Eq. 15)	76
Table 5: Physical properties of powder materials	80
Table 6: Values of compactibility parameters determined using Leuenberger equation (Eq. 28), Ryshkewitch Duckworth equation (Eq. 29) and Percolation model (Eq. 40).....	86
Table 7: Percolation model parameters of the single components determined by assuming $q > 0$ and $q = 2.7$ using Eq. 5.	102
Table 8: Values of parameters of single component powders determined using percolation model (Eq. 40) and Ryshkewitch-Duckworth model (Eq. 29).	108
Table 9: Values of compactibility parameter and percolation threshold of binary mixtures determined using percolation model (Eq. 40) assuming the value of the critical exponent, $q = 2.7$	112
Table 10: Values of parameters of single component powders determined using percolation model (Eq. 41) and Sprigg's model (Eq. 32).	139
Table 11: Values of parameters of single component powders determined for tensile strength using percolation model (Eq. 40) and Ryshkewitch-Duckworth model (Eq. 29).	143

Table 12: Values of parameters of single component powders determined for tensile strength using percolation model (Eq. 40) and Ryshkewitch-Duckworth model (Eq. 29).	144
Table 13: Value of percolation threshold, ρ_c , calculated by assuming the value of critical exponent, $q = 2$	159
Table 14: Value of percolation threshold, ρ_c , calculated by assuming the value of critical exponent, $q = 2$	160
Table 15: Calculated value of percolation threshold, ρ_c , calculated by assuming the value of critical exponent, $q = 2$ for various grades of microcrystalline cellulose	161
Table 16: Calculated value of percolation threshold, ρ_c , calculated by assuming the value of critical exponent, $q = 2$ for microcrystalline cellulose (Avicel PH 101) and dicalcium phosphate (Emcompress) using industrial scale rotary press at different tableting speed.....	162
Table 17: Calculated compressibility and compactibility parameters of binary mixtures of carbamazepine (CBZ) and lactose monohydrate (LM) with microcrystalline cellulose (MCC).....	172
Table 18: Calculated Akaike Information Criterion (AIC) values for binary mixtures of carbamazepine and lactose with microcrystalline cellulose using Eq. 4 and Eq.8. The numbers of adjusting parameters (n) for both the model were 2. .	182

LIST OF FIGURES

Figure 1: Quality by design (QbD) approach for the formulation development of typical tablet formulations. Adapted from Mishra and Rohera (2)	4
Figure 2: Compression Susceptibility of binary mixtures of plastic material (PEG 4000 and Sodium stearate) and brittle material (Caffeine). Adapted from Leuenberger and Rohera and Leuenberger, Rohera and Haas (16,50).	7
Figure 3: Response surface plot depicting the effect of independent variables on various CQAs of ODT. Adapted from Mishra and Rohera (2).	9
Figure 4: Schematic representation of Powder compression	13
Figure 5: Typical stress-strain curve of a material	16
Figure 6: Deformation behavior of solid under compression load	17
Figure 7: Transition of powder bed in a solid compact with respect to application of compression load	21
Figure 8: (A) Square lattice, (B) Square lattice with 50% open sites, (C) Square lattice with 67% open sites. In 1(c), infinite clusters are shown by dark bonds and isolated clusters are shown with light bonds. (Reproduced with permission from ref. 16; Copyright 1998 Kluwer Academic Publishers.).....	26
Figure 9: Body centered simple cubic structure. Indigo and green represents occupation of two components A and B in 3 Dimensional Structure.	27
Figure 10: (A) Mixture of conductive and non-conductive grains assuming black discs of conductive and white discs of non-conductive nature. Adapted from (46). (B) Variation of electrical conductivity as a function of filler content of urea-formaldehyde embedded in cellulose composites. (○) Tin, (●) Copper, (■)	

Zinc. Adapted from (47)	31
Figure 11: Schematic representation of uniaxial compression to develop stress strain curve.....	45
Figure 12: Schematic representation of load displacement and stress strain curve	46
Figure 13: A schematic representation of powder compaction by uniaxial compression.	61
Figure 14: A typical example of small Bethe lattice with coordination number, $Z = 3$. ..	64
Figure 15: Heckel plot of carbamazepine, microcrystalline cellulose, crospovidone and croscarmellose sodium (Eq. 15).....	75
Figure 16: Plot of tensile strength vs. product of compression load and relative density of compacts according to Leuenberger equation (Eq. 28)	83
Figure 17: Plot of tensile strength vs. porosity of compacts according to Ryshkewitch Duckworth equation (Eq. 29).....	84
Figure 18: Plot of tensile strength vs. normalized relative density of compacts according to Percolation model (Eq. 40).	85
Figure 19: (R^2) values along with standard deviation determined by Leuenberger equation (Eq. 28), Ryshkewitch Duckworth equation (Eq. 29) and percolation model (Eq. 40). The red line indicates reference line of $R^2 = 1$	89
Figure 20: Tensile strength of compacts of carbamazepine and microcrystalline cellulose binary mixtures with increasing volume fraction of carbamazepine	92
Figure 21: Tensile strength of compacts of carbamazepine and croscarmellose sodium binary mixtures with increasing volume fraction of carbamazepine	93
Figure 22: Tensile strength of compacts of carbamazepine and crospovidone binary mixtures with increasing volume fraction of carbamazepine	94

Figure 23: Compactibility of carbamazepine, microcrystalline cellulose and crospovidone using percolation model (Eq. 40)	106
Figure 24: Plot of tensile strength of compacts as a function of compact porosity for determination of compactibility parameter of carbamazepine, microcrystalline cellulose and crospovidone according to Ryshkewitch-Duckworth model (Eq. 29)	107
Figure 25: Relationship between estimated percolation thresholds (ρ_{cm}) with increasing volume fraction of well compactable material in binary mixtures a) v/v of microcrystalline cellulose, (B) v/v of crospovidone.	113
Figure 26: Maximum tensile strength at zero porosity or compactibility of binary mixture at each volume fraction of well compactable material as per Eq. 40. (A) v/v of microcrystalline cellulose, (B) v/v of crospovidone	117
Figure 27: Plot of maximum tensile strength of compacts as a function of volume fraction of well compactible component in the binary mixture according to Ryshkewitch-Duckworth model (Eq. 29). The solid line represents compactibility parameter of binary mixture according to linear mixing model (Eq. 30) and dotted line represents compactibility parameter according to power mixing model (Eq. 31)	120
Figure 28: Effect of increasing compression load on elastic modulus of microcrystalline cellulose and lactose monohydrate	129
Figure 29: Effect of increasing compression load on mechanical strength of microcrystalline cellulose and lactose monohydrate. (A) Effect on compressive strength. (B) Effect on tensile strength.	130

Figure 30: Relationship between elastic modulus with compressive strength and tensile strength (A) microcrystalline cellulose, (B) lactose monohydrate	132
Figure 31: Relationship between compressive strength and tensile strength. (A) microcrystalline cellulose, (B) lactose monohydrate.....	134
Figure 32: Effect of porosity on elastic modulus of microcrystalline cellulose and lactose monohydrate using Sprigg's equation (Eq. 32)	140
Figure 33: Effect of relative density on elastic modulus of microcrystalline cellulose and lactose monohydrate as per percolation model (Eq. 41).....	141
Figure 34: Effect of porosity on compressive strength of microcrystalline cellulose and lactose monohydrate using Ryshkewitch Duckworth equation (Eq. 29).....	145
Figure 35: Effect of porosity on tensile strength of microcrystalline cellulose and lactose monohydrate using percolation model	146
Figure 36: Effect of porosity on tensile strength of microcrystalline cellulose and lactose monohydrate using Ryshkewitch Duckworth model.....	147
Figure 37: Effect of relative density on tensile strength of microcrystalline cellulose and lactose monohydrate using Percolation model	148
Figure 38: Percolation threshold of binary mixtures of carbamazepine and microcrystalline cellulose assuming $q = 2$	156
Figure 39: Compression load vs. relative density of binary mixtures using modified Heckle equation (Eq. 23). (A) Binary mixture of carbamazepine and microcrystalline cellulose (CBZ:MCC). (B) Binary mixture of lactose monohydrate and microcrystalline cellulose (LM:MMC).....	171
Figure 40: Relationship of compressibility parameters, $1/c$ (MPa) and percolation	

threshold, ρ_{c1} calculated by Eq. 23 of both model binary mixtures (carbamazepine and microcrystalline cellulose (CBZ: MCC) and lactose monohydrate and microcrystalline cellulose: (LM: MCC) with increasing concentration of microcrystalline cellulose.....173

Figure 41: Tensile strength vs. relative density of binary mixtures using new model (Eq. 49). (A) Binary mixture of carbamazepine and microcrystalline cellulose. (B) Binary mixture of lactose monohydrate and microcrystalline cellulose .176

Figure 42: Tensile strength vs. relative density of binary mixtures using percolation model (Eq. 40). (A) Binary mixture of carbamazepine and microcrystalline cellulose. (B) Binary mixture of lactose monohydrate and microcrystalline cellulose178

Figure 43: Relationship of compactibility parameters, σ_0 (MPa) and percolation threshold, ρ_{c2} calculated by Eq. 40 of both model binary mixtures (carbamazepine and microcrystalline cellulose (CBZ: MCC) and lactose monohydrate and microcrystalline cellulose: (LM: MCC) with increasing concentration of microcrystalline cellulose179

Figure 44: Elucidation of bonding area and bonding strength in both model binary mixtures of carbamazepine and microcrystalline cellulose (CBZ: MCC), lactose monohydrate and microcrystalline cellulose (LM: MCC). (A) Relationship between compressibility, c and compactibility. (B) Relationship between percolation thresholds of compressibility and compactibility.....186

Glossary

a = Intercept of the linear segment of Heckel plot

k = Slope of the linear segment of Heckel plot

E = Elastic modulus/Young's Modulus

E_0 = Elastic modulus/Young's modulus at zero porosity

F = Crushing strength of tablet (kg)

D = Diameter of tablet (mm)

h = Thickness of tablet (mm)

l = length of sample

I = Interaction between particles

M = Mechanical strength of tablet (MPa)

N = Load (Newton)

P = Occupational or percolation probability in a lattice

ρ_c = Percolation threshold in lattice

ρ_{cb} = Bond percolation threshold of powder material

ρ_{cs} = Site percolation threshold of powder material

ρ_b = Relative bulk density of powder material

ρ_t = Relative tapped density of powder material

ρ = True density of powder material (g/cc)

ρ_m = True density of the binary mixture of powder materials (g/cc)

ρ_{cm} = Percolation threshold of binary mixtures

v_A = Volume fraction of component A

v_B = Volume fraction of component B

v/v = Volumetric ratio of single component in binary mixture

ρ_r = Relative density of tablet

σ_c = Compression load (MPa)

σ_t = Tensile strength of tablet (MPa)

σ_0 = Maximum tensile strength or compactibility of single component powder material at zero porosity (MPa)

σ_{0m} = Maximum tensile strength or compactibility of the binary mixture at zero porosity (MPa)

σ_{cs} = Compressive strength of tablet (MPa)

σ_{cs0} = Compressive strength of tablet at zero porosity (MPa)

σ_{0m} = Maximum tensile strength or compactibility of the binary mixture at zero porosity (MPa)

b = Bonding propensity of powder materials

S = Scaling factor in power law equation (MPa)

γ = Compression susceptibility of powder material (MPa⁻¹)

P_y = Mean yield pressure of powder material (MPa)

q = Critical exponent in power law equation

Z = Coordination number

1. Introduction:

In a recent survey of new molecular entities (NMEs) approved by the US Food and Drug Administration (US FDA) in 2014, 46% were solid dosage form products (1). Among these, at least 80% of solid dosage form products were approved as tablet dosage forms. Thus tablet is still one of the most preferred dosage forms because of its ease of administration, higher patient compliance and ease of production (2).

1.1 History and Background:

The first powder press was patented in 1843, and was hand operated. It was initially designed for producing superior graphite for pencils, but its pharmaceutical potential was soon realized and led to it being patented (3). An obvious problem with the hand-operated tablet press was that the applied pressure depended on the machine operator. Thus mechanical properties and other pharmaceutical properties were largely dependent on the physical strength and judgment of the operator. To standardize and better control the tableting process, simple pressure gauges were attached with tablet presses in late 1930s. Further advancements in tableting were made in the 1950s with the introduction of industrial electronics and equipment (4). Nowadays, tableting machines are computerized and can produce large number of tablets per hour, for example, the GEA Performa™ P can produce at least 157,000 tablets per hour and the GEA Performa™ S can produce up to 405,000 tablets per hour. Apart from industrial scale tableting machines, technological advancements have resulted in the introduction of material testing instruments to characterize and evaluate the powder compression behavior during preformulation studies

(3). However, formulation development of tablets has remained more of an art than science with little change since its inception. With poor understanding of formulation factors along with empirical knowledge of the process, a large batch-to-batch variability in the quality of the products can be observed (5). FDA soon recognized these problems, and with the initiative of International Society of Pharmaceutical Engineers (ISPE) launching Product Quality Life Cycle Implementation (PQLI), quality by design (QbD) was introduced (6).

According to the ICH Q8(R2) guidelines, quality by design (QbD) can be defined as the systematic, scientific, risk-based, holistic and proactive approach to pharmaceutical development that begins with the predefined objective and emphasis on product and process understanding and process control (7). Although relatively new in practice in pharmaceutical industry, application of QbD and its elements can be traced back to 100 years when factorial design was first used as experimental design in agricultural sciences for better yield and consistent production. Since the mid 20th century, United States Military has used risk-based approaches, such as Failure Mode Effective Analysis (FMEA), to validate military equipment and their failures (8). Similarly, quality by design (QbD) approach in pharmaceutical industry deals with the study of suitability of drug substances and drug products for their intended use (9).

The objective of quality by design (QbD) is to understand how pharmaceutical formulation and process parameters influence the overall desired quality of the product and to ensure the quality during product shelf-life (10). After the initial risk assessment and analysis of potential factors that have high impact on quality attributes of the product, one needs to establish them robust with a minimal variation called as a design space. ICH Q8 guidelines define design space as multi-dimensional combination and interaction of input

variables, such as material attributes and process parameters, on the quality of product (7). It is the multi-dimensional region meeting with all the specifications of Critical Quality Attributes (CQAs) during shelf-life of the product with respect to the process parameters at high assurance (11). To establish design space from a knowledge space, elements of QbD, such as defining Target Product Profile, Critical Quality Attributes, to identifying Critical Material Attributes and Critical Process Parameters, risk assessment, control strategy are used (Fig. 1).

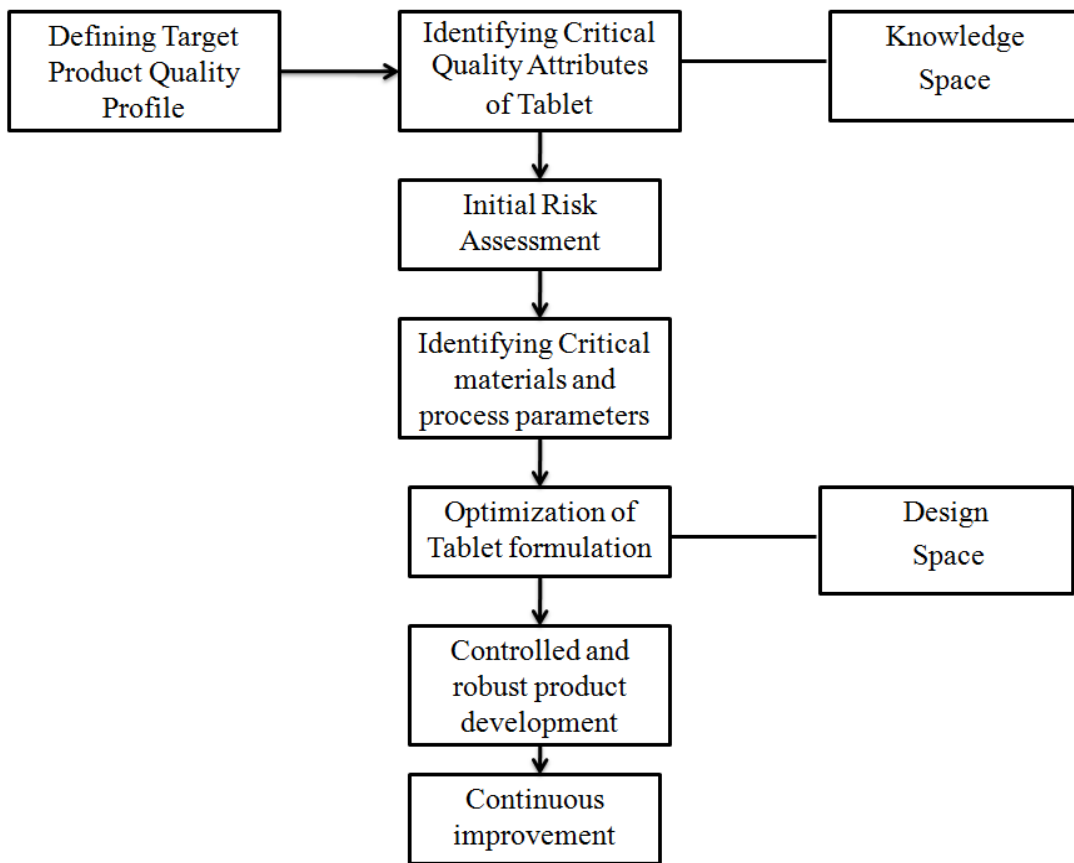


Figure 1: Quality by design (QbD) approach for the formulation development of typical tablet formulations. Adapted from Mishra and Rohera (2)

The use of scientific approaches establishing design space, such as the statistical design of experiments (DoE), optimization modeling, multivariate data analysis, and chemometrics in combination with the knowledge management system, is reported extensively in the literature (12). The purpose of this program was to facilitate a common understanding of the systematic and science-based approach to product and process development of pharmaceuticals (8). Under this new framework, the identification of critical material attributes and process parameters and their relationship with the product quality enable the use of process analytical technology (PAT) to assure consistent product quality. The ultimate goal of this framework is to achieve a world-class, i.e. a six sigma (6σ), quality of the products with practically no defective goods compared to traditional two sigma (2σ) quality with the possibility of 5% failure of the product (13). Along with the initiative of various regulatory agencies, individual ingenuity from the scientific community has also been reported. Notable among them are manufacturing classification system (MCS) and material science tetrahedron (MST) (5, 14). These approaches emphasized more on understanding the material properties and process parameters and their bearing on successful development of the product with less variability. However, pharmaceutical tablet dosage forms are heterogeneous and disordered particulate systems often demonstrating the non-linear and non-monotonous behavior (15). This complexity of tablet dosage form often leads to failure in establishing design space and, with that failure, to achieve a robust product development strategy.

The unanticipated behavior of tablet properties is not a new phenomenon in pharmaceuticals. Such behavior was reported by Leuenberger and Rohera (16) in binary systems consisting of powder components of dissimilar compaction behavior that

exhibited phase inversion (Figure 2). This behavior of phase inversion was compared with that of an emulsion in which beyond a critical ratio of two immiscible liquids, further addition of liquid that makes up internal phase causes inversion of internal phase to external phase.

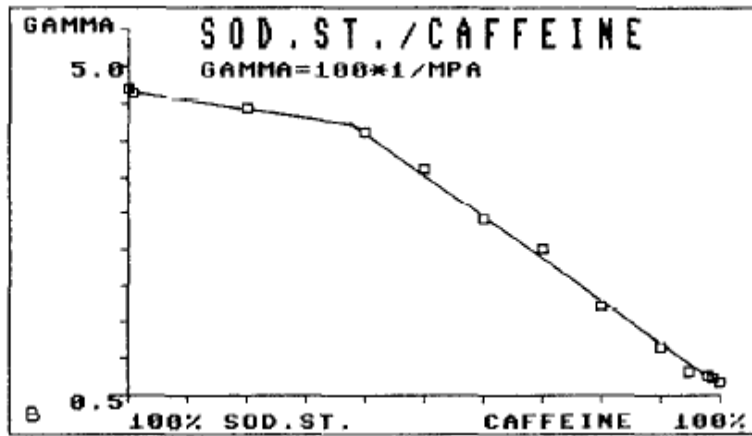
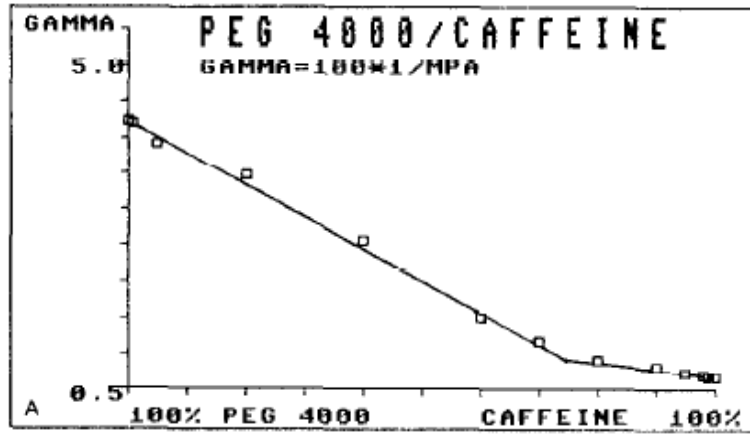


Figure 2: Compression susceptibility of binary mixtures of plastic materials (PEG 4000 and sodium stearate) and brittle material (Caffeine). Adapted from Leuenberger and Rohera and Leuenberger, Rohera and Haas (16,50).

The similar unanticipated behavior of tablet properties, such as tablet crushing strength, friability and water absorption time, was observed in one of our earlier studies (2). By application of Box-Behnken response surface methodology as DoE tool, various quality attributes of ODTs, such as tablet crushing strength, tablet porosity, water absorption time and tablet friability, exhibited significant ($P < 0.05$) quadratic or non-linear behavior (Figure 3). The significance of these non-linear models using DoE tools has been reported by other researchers too. However, limited information is available to understand the exact reason for such behavior (17, 18). As these uncertainties may lead to the failure of DoE model, attempts should be made to understand the cause of their unanticipated behavior. This can be achieved by an extensive risk assessment of materials and processes involved in the formulation development of the product. The purpose of risk assessment prior to the development studies is to identify potentially high-risk formulation and process variables that can possibly impact the quality of the drug product. It helps to prioritize which studies need to be conducted and is often driven by knowledge gaps or uncertainty. ICH Q9 provides a list of common risk assessment tools, such as Ishikawa fishbone diagram, preliminary hazard analysis, failure mode and effects analysis, etc., for the identification of material attributes and process parameters that may have a critical effect on critical quality attributes (CQAs) of the product (19).

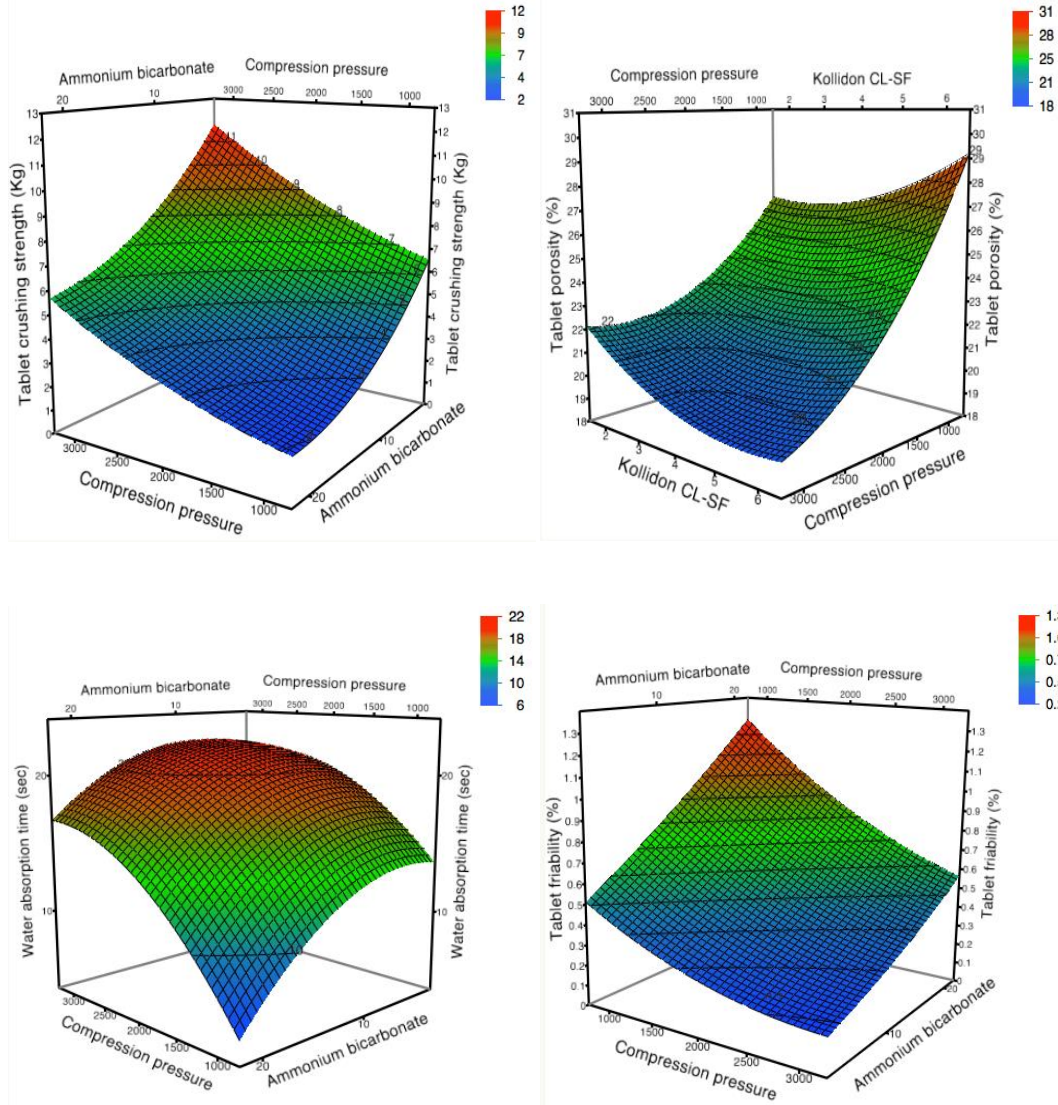


Figure 3: Response surface plot depicting the effect of independent variables on various CQAs of ODT. Adapted from Mishra and Rohera (2).

Although these tools can be helpful for the development and optimization purposes, major changes in the property of a system cannot be detected because of lack of resolution provided by these tools (15). Moreover, these tools are based on mere mathematical approximations or knowledge space and preliminary experiments that do not consider the geometrical or other physical aspects of the system which may lead to the failure of these strategic tools. Thus topological-based assessment is often necessary to take into account a critical behavior caused by geometrical phase transition, known as percolation event (15). One of such tools, that provide universal laws to determine geometrical and physical properties of a system, is percolation theory (20).

1.2. The Complexity of Pharmaceutical Powders

1.2.1. Powder: A 4th State of matter

Traditionally, solid, liquid and gas are the three states of matter in the universe. However, the classification of powders to any of these three states of matter is difficult. This can be attributed to the powders possessing deformation behavior such as solid, and flowable much like a liquid. Also to some extent, powders are compressible similar to gases. This leads to some of the scientists to classify powders as a fourth states of matter (21, 22). Moreover, it becomes more complex since formulation development of tablet involves compaction of multi-component powder system. In the present study, a systematic review of complex phenomenon of powder compression has been demonstrated systematically.

1.2.2 Phenomenon of Powder Compression

The process of powder compression into a tablet can be generally divided into four predominant stages which although occur sequential, however, in reality it occurs simultaneously. These are (1) rearrangement of powder particle, (2) plastic deformation and/or fragmentation, (3) elastic compact deformation, and (4) elastic recovery following unloading and tablet ejection (Figure 4).

Particle rearrangement

Immediately after pouring the powder into the die cavity, particle rearrangement occurs depending on the particles' size, shape, structure and density. Soon thereafter, the system reaches a state where its capacity to rearrange is saturated. This junction can be referred to as a constrained state. In addition, a small degree of fragmentation or deformation can occur during this initial stage of powder compression.

Plastic deformation/fragmentation

Upon reaching the constrained state with increase in compression pressure, further reduction in the porosity of the powder bed occurs as a result of a mechanical change in the structure of each of its composing particles. If the particles are plastic or elastic in nature, they will deform to accommodate the increasing applied load. If particles are brittle in nature, they will undergo fragmentation into smaller pieces which then displace the pores. Assuming the applied force is large enough, the particles can undergo one or all of these structural changes. It is during this transitional phase that bonding occurs between the contacting surfaces of the powder particles, either as in the case of deformation, by an

increased area of contact between particles or by an increase in the number of bonding sites as in the case of fragmentation.

Elastic recovery and ejection of tablet

Finally, at the maximum compression pressure, when the porosity is reduced to 5-10% of the product bed, i.e. when nearly all pores are eliminated, the powder will no longer be a system of distinct particles, but rather a single solid unit. Further compression of powder at this point will invariably be controlled by elastic deformation of this solid unit. Consequently, when the pressure is removed (unloading), the solid (tablet) begins to relax into its final dimensions, a process referred to as elastic recovery.

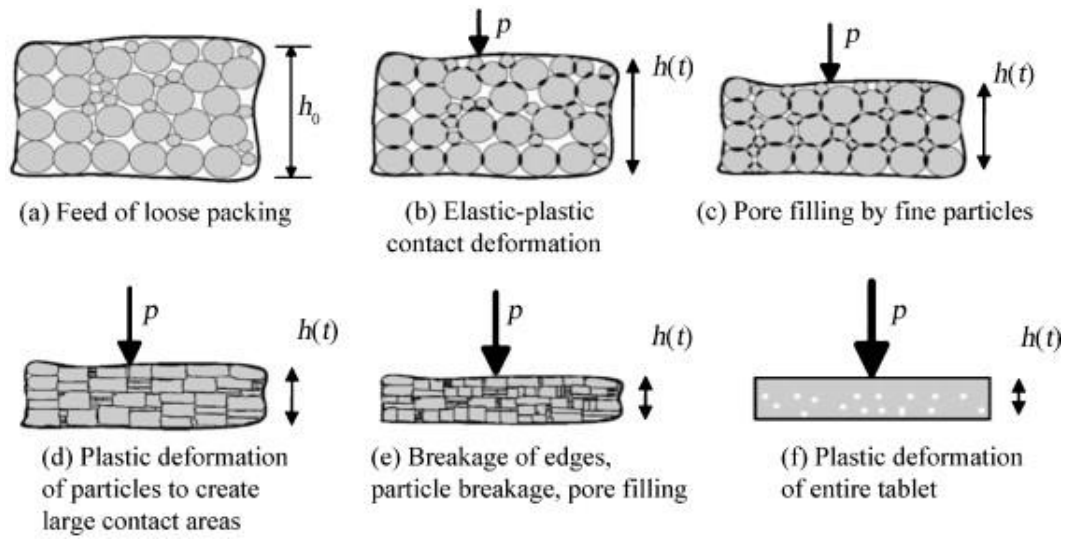


Figure 4: Schematic representation of Powder compression

1.3. Powder Properties and their characterization

Powders are studied from two viewpoints: physical characteristics and mechanical behavior. Physical characteristics involve particle attributes, such as chemical composition, shape, size distribution, particle density, etc. Mechanical behavior of powder specifically deals with the force-deformation or stress-strain behavior of the powder in bulk. The study of mechanical behavior of powder is important with respect to its handling, processing and packaging. Many constitutive models are reported to describe the stress-strain behavior of a powder (23). In powder technology, compression of powder is usually defined in terms of compressibility and compactibility.

1.3.1. Compressibility of powders

Compressibility can be defined as volume reduction or densification of powder bed under applied stress. Due to the importance of this process, several mathematical relationships have been proposed for modeling the relationship between the main macroscopic parameters, such as powder density or porosity, with the applied pressure. Assessment of deformation behavior and compressibility of powders is performed using a range of techniques (24). These techniques include measurement of changes in bed density or porosity during compression, effect of punch velocity on compression, strain-rate sensitivity index, stress-strain relaxation, various tablet indices, stress transmission during compression, work involved in compaction, compaction force versus time profiles, and elastic recovery during multiple compression. Traditionally, stress strain curve is typically used to access the deformation behavior of powder and thus its compressibility. Figure 5 is a typical stress-strain curve of a powder. The slope of the linear section of the curve is

used to calculate the elastic modulus or Young's modulus of a component whereas the compressive strength can be defined as the maximum stress before failure of the compact. Also stress-strain curve can be used to calculate the deformation behavior of the powder compacts (Figure 6). Thus ductility, elasticity and brittle properties of a powder can be easily determined by stress-strain curve (25).

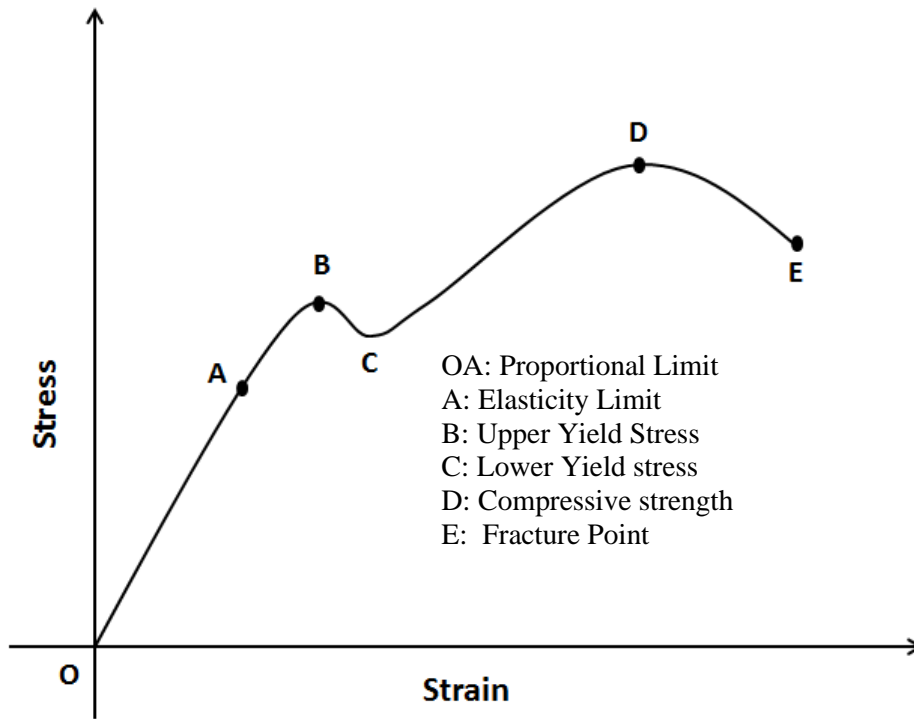


Figure 5: Typical stress-strain curve of a material

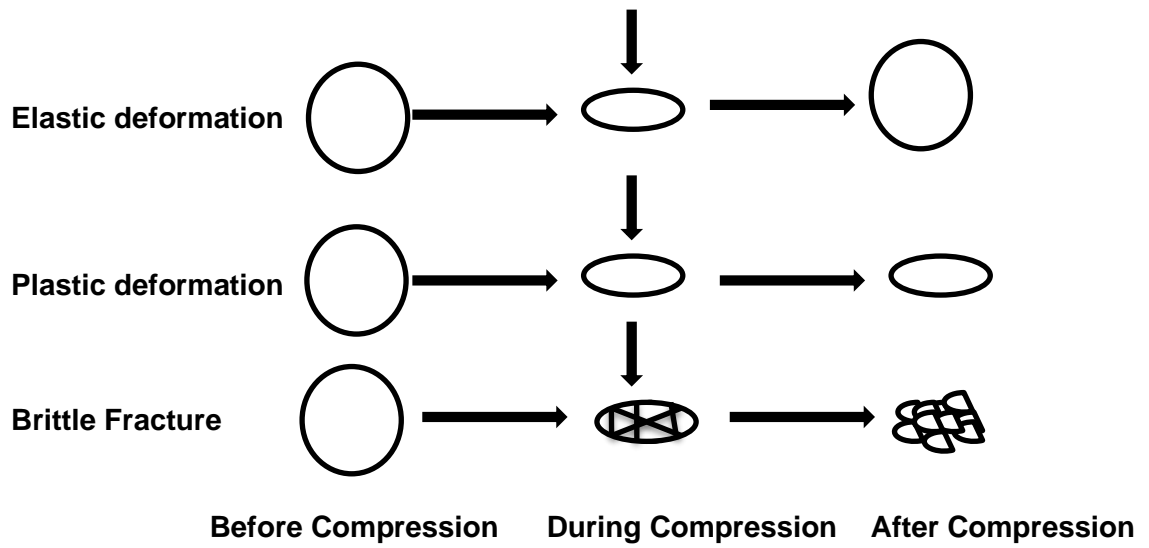


Figure 6: Deformation behavior of a solid under compression load

1.3.2 Compactibility of Powder

Compactibility of a powder material can be defined as its ability to form compact of adequate strength. While compressibility quantifies volume reduction of powder bed with increasing stress, it doesn't take into account subsequent mechanical strength or consolidation of material. Thus, ability of a powder material to form compact of adequate strength is of special interest to the tablet technologists. Similar to defining compressibility of powder material, numerous equations have been proposed to quantify the compactibility of material (26, 27). The compactibility of the powder constituent depends on the compaction conditions (compression pressure, speed), mechanical property, physical and chemical properties of the constituent powder, etc. In the case of some formulation excipients, the mechanical strength of the compact depends on physical properties, such as particle size, particle shape, free surface energy, etc, while mechanical strength of some excipients is independent of such properties. Similarly, certain external factors, such as moisture content, lubricants, etc, can affect the compactibility of some powders (28). The assessment of compactibility and mechanical strength is done by measurement of deformation hardness, compression force versus tablet strength, tensile strength, friability, indentation hardness, tableting indices and fracture mechanics. The process by which the mechanical strength of compact increases due to particle-particle interaction is called as mechanism of consolidation. Various mechanisms have been proposed to describe the process of consolidation, among which cold welding is the most widely accepted mechanism. Cold welding occurs due to strong attractive forces between the surface of two particles when close enough (van der Waals distance of less than 50 nm), resulting in stronger particle-particle bonding. Cold welding is also one of the major reasons for

increased mechanical strength of powder bed when subjected to rising compressive forces. On the macro scale, most of the pharmaceutical powder materials have an irregular shape, resulting in many points of contact in a bed of powder. Thus, even an application of small compression load to the powder bed is transmitted through the particle-particle contacts present in the powder bed. However, under higher compression load, this transmission may result in the generation of considerable frictional heat. If this heat is dissipated, the local rise in temperature could be sufficient to cause melting of the contact area of the particles, which would relieve the stress in that particular region. When the melt solidifies, fusion bonding occurs, which in turn results in an increase in the mechanical strength of the mass. In addition, the deformation effects may be accompanied by the breaking and formation of new bonds between the particles, which give rise to consolidation as new surfaces are pressed together. Another possible mechanism of powder consolidation is asperitic melting of the local surface of powder particles (29, 30). During compression, the powder compact typically undergoes a temperature increase usually between 4 and 30°, which depends on the friction effects, the specific material characteristics, the lubrication efficiency, the magnitude and rate of application of compression force, and the machine speed (30). As the tablet temperature rises, stress relaxation and plasticity increases while elastic recovery nature decreases and thus strong compacts are formed (31). Therefore, compression of material at elevated temperature with increase in ductility should result in stronger tablets (32). Asperitic melting is believed to play important role in consolidation only with relatively low melting point materials for which even very hard asperities are pushed into a more plastic material.

The bond formation between two particles is believed to involve more than one mechanism, which together contributes to the mechanical strength of the compacts. The phenomenon of bond formation is related to the porosity (ε) or relative density (ρ_r) of the compacts (Figure 7). Lower the porosity (higher the relative density) of the compacts, the more would be the particle-particle contacts and thus higher will be the bond formation.

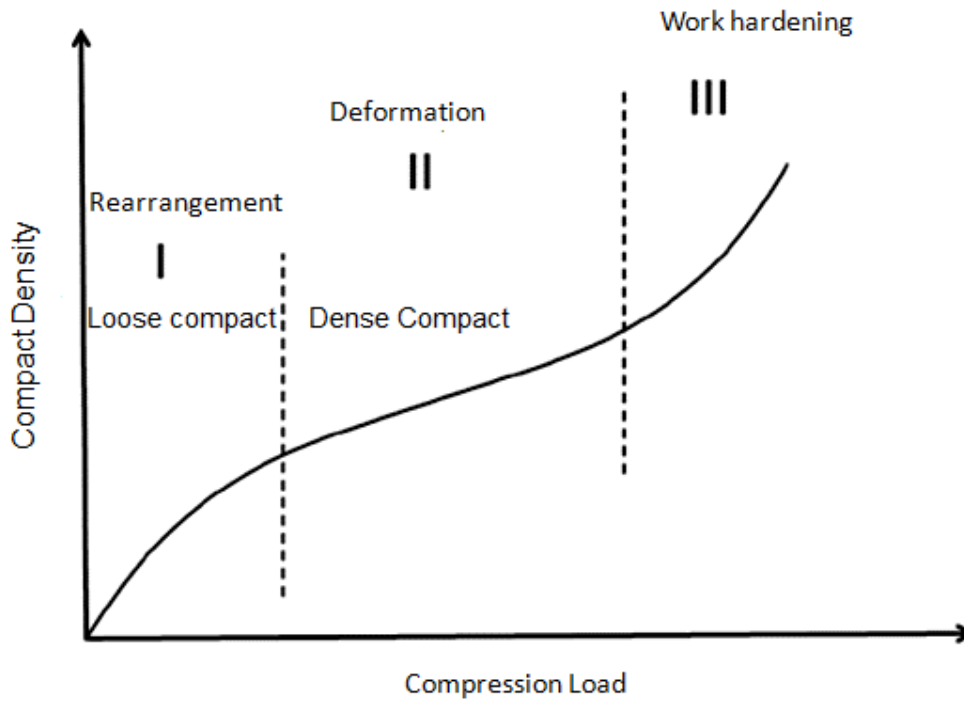


Figure 7: Transition of powder bed in a solid compact with respect to application of compression load

Depending on this principle, various mathematical models have been proposed to quantify the compactibility of materials for successful tablet formation. Every empirical model has a different hypothesis and involves the estimation of compactibility, which is a material dependent parameter. However, the compaction of powder bed and subsequent gain of strength is complex and involves multiple steps.

1.4. Compaction of Powder mixtures: Failure of Classical models

As dependence of the tensile strength of compacts of binary mixture correlates very well with the tensile strength of compacts of a multicomponent system, the elucidation of compaction behavior of multicomponent powder mixtures have been extensively illustrated using binary mixtures (16, 33). Thus, two individual powder components when combined together are expected to show properties representative of fraction of the specific properties of individual components. Based on this assumption, the mechanical properties, such as tensile strength, σ_{tm} , of compacts of the binary mixture of component A and B, can be expressed as follows:

$$\sigma_{tm} = X_A \sigma_{tA} + X_B \sigma_{tB} \quad (1)$$

Where X_A and X_B are the mass fraction of component A and B, respectively, and σ_{tA} and σ_{tB} are the tensile strength of compacts of component A and B, respectively. However, deviation of the tensile strength of compacts of binary mixtures from Equation 1 with complex non-linear relationships has been reported by many researchers (16, 34, 35). One of the possible drawbacks of the additive rule (Eq. 1) is the change in the deformation behavior of the components in the binary mixture when two components are blended

together. Moreover, this additive rule of the tensile strength of compacts of single components doesn't take into account of differences in consolidation natures, bonding propensity, attractive forces (cohesive and adhesive forces) of individual components. In addition to these complexities, factors such as powder flowability and post-compression changes, such as elastic recovery, are also pertinent parameters that exert a significant effect on the mechanical properties of binary mixtures (36). As a result, it is difficult for a simple mono-variate equation to describe the mechanical properties of the tablets of a multicomponent formulation. Thus in the present study, an attempt has been made to evaluate mechanical properties of the single components of dissimilar compression and compaction behavior and their binary mixtures by a topological tool such as percolation theory.

Percolation theory is a branch of probability theory dealing with the properties of random media. The idea was originally conceived to deal with crystals, mazes and random media, in general, by Broadbent and Hammersley (37). Since then it has gained tremendous attention in the field of petroleum engineering, hydrology, fractal mathematics, physics of magnetic induction and phase transitions (38). It is the simplest but not exactly solved model displaying a phase transition. Usually an insight into the percolation phenomenon facilitates understanding of many other physical systems (39).

1.5. Fundamentals of Percolation Theory

For adequate understanding of percolation theory, it is necessary to study the textbook authored by Aharony and Stauffer and the references cited in it (40). In the present thesis, fundamentals of percolation theory have been illustrated by one of the examples given by Berkowitz and Ewing through large array of squares (38). Assuming the lines intersecting as sites and the segments connecting them as bonds in Figure 8A, it can be seen that one bond is connected to six nearest neighboring bonds, while a site has only four nearest neighbor sites. Assuming that each site exists in two possible states, empty or open, the open sites can be denoted by presence of a large dot on the intersection with random probability and independent of its neighbors. Thus a bond can be assumed to exist between each pair of nearest neighboring sites in the lattice. If half the sites are open (Fig. 8B), it can be seen that they tend to group into clusters of many shapes and sizes. If the probability, p , of a site being open increases to 0.67 (Fig. 8C), change in the system property will be observed. Also, at some probability between 0.50 and 0.67, many of the sites connect each other forming one giant cluster which spans the whole array or lattice, both vertically and horizontally. The probability at which this happens (≈ 0.593 for the square lattice sites) is called the critical probability, p_c , also known as the percolation threshold. Thus below critical probability, p_c , only isolated cluster exists; however, at critical concentration, infinite cluster is formed spanning the whole lattice from right to left and top to bottom. Thus in two-dimensional square lattice, only one component can percolate the system.

In a three-dimensional lattice, two components can percolate the system at the same time (41) (Figure 9). This can be easily illustrated by a binary powder mixture supposedly

consisting of components A and B. In volumetric ratio (v/v), at low concentration of component A, isolated clusters of particles of component A are formed which exist within continuous phase of particles of component B. At critical concentration of component A (p_{ca}), it forms infinite cluster percolating through the three dimensional lattice. At p_{ca} , the particles of component B also form an infinite cluster spanning the three dimensional lattice. Thus it is evident that if particles of component A are increased at the expense of particles of component B, percolation threshold or critical concentration of particles of component B (p_{cb}) still exists. However, if the concentration of particles of component B is further reduced, it can only form an individual isolated cluster. Thus in three-dimensional lattice, a binary system shows two distinct percolation thresholds (p_{ca} and p_{cb}). Table 1 summarizes site and bond percolation thresholds for other ideal systems and lattices of 2- and 3-dimensions. As evident from Table 1, it can be observed that within a given dimension, the percolation threshold decreases with increasing number of nearest neighbors (42). Thus percolation threshold depends on the lattice types and dimensions of a system.

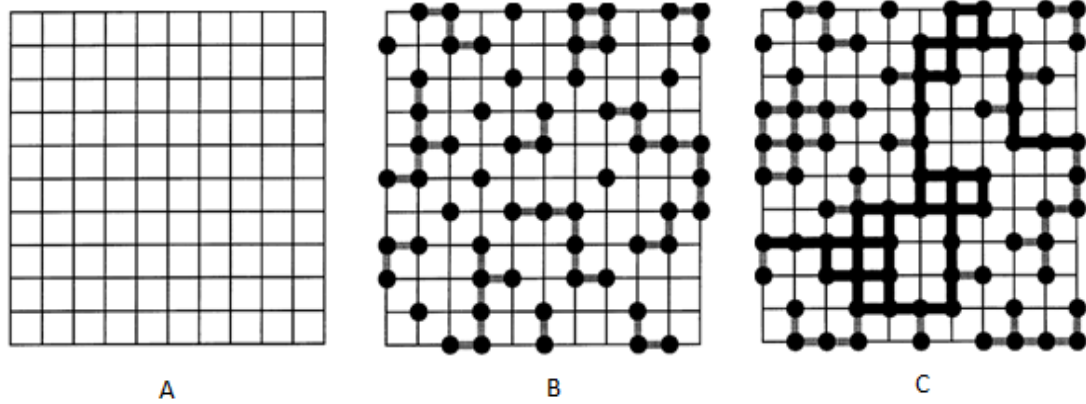


Figure 8: (A) Square lattice, (B) Square lattice with 50% open sites, (C) Square lattice with 67% open sites. In Fig. 8(c), infinite clusters are shown by dark bonds and isolated clusters are shown with light bonds. (20)

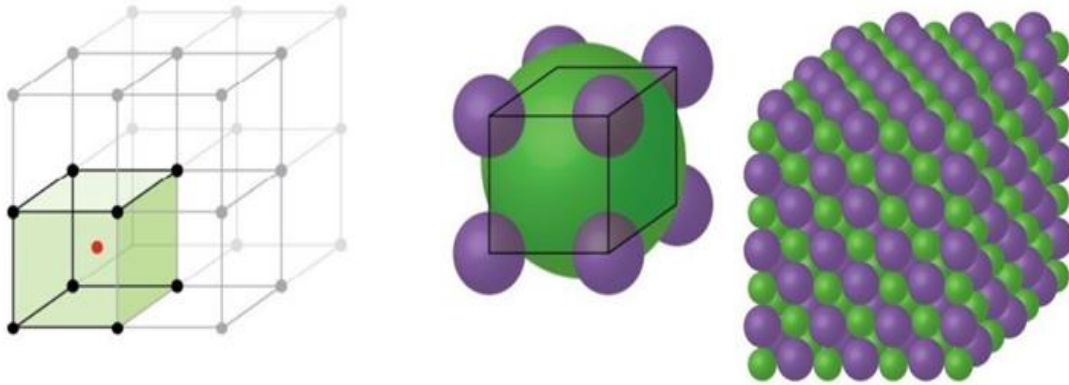


Figure 9: Body centered simple cubic structure. Indigo and green represents occupation of two components A and B in 3-dimensional structure.

Table 1: Values of bond and site percolation thresholds of ideal systems (Isichenko 1992)

Lattice	Dimensions	Bond percolation threshold, ρ_{cb}	Site percolation threshold, ρ_{cs}
Square	2	0.50	0.590 ± 0.010
Triangular	2	0.33	0.50 ± 0.005
Honeycomb	2	0.66	0.70 ± 0.01
Simple cubic	3	0.24	0.307 ± 0.010
Body-centered cubic	3	0.178 ± 0.005	0.243 ± 0.010
Face-centered cubic	3	0.119 ± 0.002	0.195 ± 0.005
Diamond	3	0.388 ± 0.05	0.425 ± 0.012

1.5.1. Theoretical Section

The classic percolation model assumes a lattice where the sites are either occupied with the probability, p , or remain unoccupied or empty with the counter probability, $1 - p$. At a defined probability, p_c , i.e. the percolation threshold, an infinite cluster is formed. In the vicinity of the percolation threshold, p_c , of the macroscopic cluster, property X obeys a power law relationship according to the following equation (43).

$$X \propto (p - p_c)^q \quad (2)$$

Based on this relationship, it can be understood that the key phenomenon of percolation theory is the existence of a percolation threshold, p_c , or the occupation probability. When the probability, p , is less than p_c ($p < p_c$), only finite clusters (singular or plural) exist. However, when probability, p , becomes larger than percolation threshold, p_c (i.e. $p > p_c$), an infinite cluster is formed that spans the entire lattice. From this threshold, p_c , the percolating cluster dominates the overall properties of the lattice (44). Although classical percolation theory originally dealt with the penetration of porous media by liquids, the statistical percolation models have been extensively applied in studying the electrical percolation phenomenon or conductivity of a binary mixture of a conductor and an insulator (45).

A representative example of such a binary mixture can be given in which two components of dissimilar properties are mixed together to give a mixture with tailored properties assuming that the hypothetical mixture consists of electrically conducting and insulating particles or electrically conductive particles incorporated in the matrix of

insulating particles. A two-dimensional representation of the binary mixture of a conductor and an insulator material has been shown in Figure 10A, assuming the black discs to be of conducting nature through which current can pass from one to the other on contact and white discs as non-conducting material or insulator (46). Further, a plot depicting the change in conductivity of the binary mixture as a function of the concentration of conductive material (tin, copper, and zinc) is shown in Figure 10B (47). When the conductivity of the binary mixture is plotted on a logarithmic scale, at a certain concentration of conductive material, a drastic increase in the conductivity of the binary mixture is observed (Figure 10B). Such a nonlinear curve can be explained as follows. At lower concentrations, the conductive material is distributed homogeneously in the volume of the insulating host material. At this concentration, there is no contact between adjacent conductive particles. However, with increasing concentration, agglomerates of conductive particles begin to form that start to develop contact with each other. At a certain concentration, the agglomerates reach a size in which all the vertices of conducting particles can touch each other. This results in the formation of the conducting phase network within the insulating material. Due to the formation of these conducting networks, binary mixture shows a sharp increase in the conductivity.

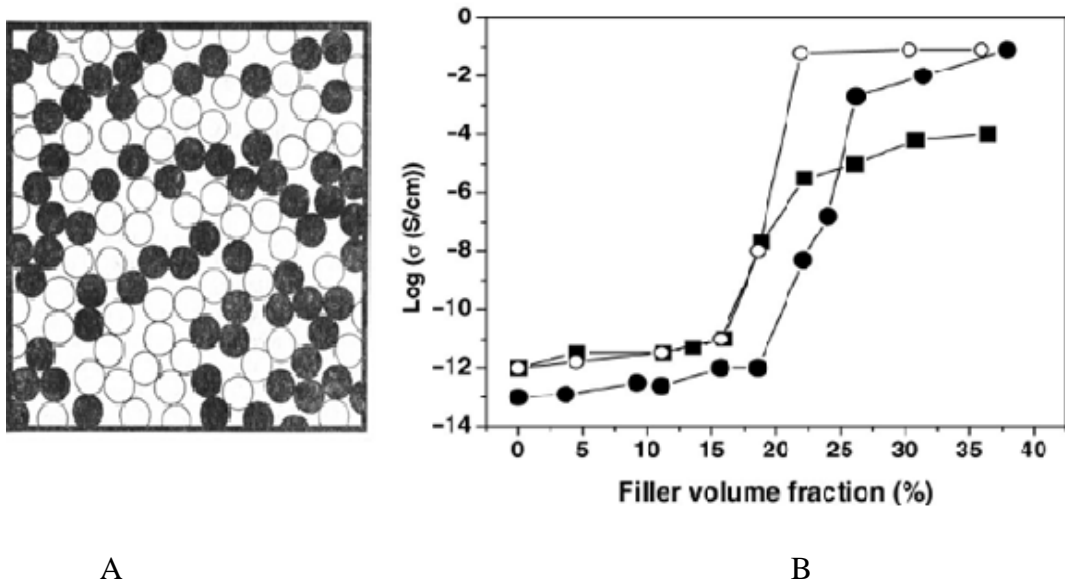


Figure 10: (A) Mixture of conductive and non-conductive grains assuming black discs of conductive and white discs of non-conductive nature. Adapted from (46).
 (B) Variation of electrical conductivity as a function of filler content of urea-formaldehyde embedded in cellulose composites. (○) Tin, (●) Copper, (■) Zinc. Adapted from (47).

1.5.2. Mathematical Aspects of Percolation Theory

Percolation model is a mathematical representation of the behavior of the system at critical concentration. Based on the above description and Figure 10B, it can be observed that the electrical conductivity of the binary mixture is not continuous and linear; rather it is discrete and nonlinear. There is a critical composition, also called as percolation threshold, at which electrical conduction is increased by several orders of magnitude leading the composite from an insulating range to semi-conductive and conductive ranges. To study the conductivity of the binary mixture, various percolation models have been proposed. Notable among them are Kirkpatrick's model, McLachlan's model, Mamunya's model, and Sigmoidal function model (48). These models are associated with an extended basic statistical percolation theory and make use of a nonlinear regression analysis to determine various model parameters and constants. Among these models, Kirkpatrick's model is the most widely used mathematical model to study the electrical conductivity of binary mixtures. Kirkpatrick model is based on the fundamental power law equation (Eq. 3) to predict the electrical conductivity based on the probability of contact between particles of filler within the composite (49).

$$\sigma_m = A(\phi - V_{bc})^b \quad (3)$$

Where σ_m is the conductivity of the composite of the binary mixture, A is the conductivity of the filler, ϕ is the volume fraction of filler, V_{bc} is the percolation threshold of filler, and b is the critical exponent which depends on the type of space dimension. The critical

exponent, b , is a characteristic value determined experimentally and usually shows universal value for a particular system and dimension.

1.5.3. Percolation Phenomenon in Powder Technology

Although percolation theory has been widely applied in other scientific fields since long, it was introduced in pharmaceuticals just three decades ago by Leuenberger *et al.* (50). Since then it has been applied in describing the formation of tablets, water uptake capacity and disintegration properties of disintegrants (51, 52). Later, Carabello *et al.* (53) explained the importance of drug and polymer percolation threshold on the release of drug from tablet matrices. However, its application still remains limited, possibly due to the complexity of the solid dosage forms and mathematical aspects of percolation theory.

The elucidation of processes underlying compression and consolidation of powders has been a challenge for a long time. It gets much more complex since theories proposed to explain the mechanical behavior of continuum bodies fail to satisfactorily explain the behavior of particulate bodies (54). The application of percolation theory in the present work is based on the critical observation of powder compression and compaction, and various stages involved in the formation of a tablet. During tableting process, at zero pressure, the die contains loosely packed powder particles or granules. At the onset of compression, particles within loosely packed bed undergo some rearrangement in their packing state reducing particle-particle contact distance (35). Further, with increasing compression load, depending on their properties, elastic/plastic deformation or fracture of particles occurs. Thus the process of tablet formation can be defined in two stages of relative densities. Initially, at low compression pressure, the transition of loosely packed

bed to loose compact occurs which is mechanically unstable. Further, with an increase in the compression pressure, the loose compact transitions to a dense compact which is mechanically stable. In terms of percolation phenomenon, the transition of loosely packed bed to a dense compact can be expressed as bond percolation threshold, ρ_{cb} , and site percolation threshold, ρ_{cs} , representing the formation of the loose and the dense compact, respectively (55).

As the pores and their network are one of the integral components of powder system, a powder mass of apparently single solid material can be called as a two-component system consisting of powder particles and pores. Thus compression and consolidation of powder particles highly depend on pores and its network. As network models and percolation theory are complementary to each other, the connection between the pore structure and the powder, and its behavior can be predicted by application of percolation theory (20). During compaction of powder, the bonding of the particles can be defined by bond percolation phenomenon. However, the pores undergo a phenomenon that can be best described as the site percolation phenomenon (56). Thus bond and site percolation phenomena can be envisaged in the compaction of particulate solids. From a mathematical point of view, this can be further explained by several characteristic functions, such as percolation probability, P (57). For loosely packed powder bed in the die, no or little bonding exists between the particles. Therefore, the value of percolation probability, P , equals to zero ($P = 0$). With the application of compression stress, the number of unoccupied sites is reduced until the formation of an infinite cluster. This can be described as a pure site percolation process in which the lattice sites are increasingly occupied until the tablet of finite dimensions is achieved. In the beginning, as the fine

powder particles are bonded by weak inter-particulate forces, a bond percolation throughout the powder bed can be expected as soon as these particles come in contact with each other (56). At this stage, the occupation or percolation probability, P , can be expressed by following equation (56, 57).

$$P \propto (\rho_r - \rho_c)^\beta \text{ at } \rho_r > \rho_c \quad (4)$$

Where ρ_r is the relative density of powder compact, ρ_c is the critical concentration or percolation threshold of pores, and β is critical index or exponent. Percolation threshold, ρ_c , can be defined as the stage where a stable compact is just formed. At this stage, the connecting bonds between the particles are such that a continuous network of bonds throughout the system of the particles results. This is also known as the pair-connectedness and depends on the relative positions of the particles and other parameters of the model, such as compact density. In case of tablets, positions of particles depend on the relative density of tablets.

The Kirkpatrick percolation model (Eq. 3) that explains conductivity of binary mixtures consisting of a good conducting material and an insulator has been extended and modified by Kuentz and Leuenberger (34) to apply it to assess the compactibility of binary mixtures of poor and well compactable materials. Since mechanical properties of powder material depends largely on the relative density of the compact, in terms of percolation theory, a tablet with a particular relative density, ρ_r , can be described by a lattice in which sites are randomly occupied by particles of well compactable or poorly compactable material with probability of ρ_r and $1 - \rho_r$, respectively. According to percolation theory,

the power law relationship for the mechanical strength of tablet close to the percolation threshold, ρ_c , can be expressed by the following equation.

$$M = S(\rho_r - \rho_c)^q \quad (5)$$

Where M is the mechanical strength of compact (tensile strength, compressive strength and elastic modulus) at a relative density, ρ_r , ρ_c is the percolation threshold, and q is the critical exponent that exhibits the change in tablet property, such as tensile strength, near percolation threshold. This equation defines the percolation threshold, ρ_c , as the critical relative density that marks the onset of tensile strength of compact of single powder component and critical volume fraction of each powder component in the binary mixture, and critical exponent, q, as the power of the mechanical strength curve (58).

1.6. Research Objectives

Among various properties, mechanical properties and drug release characteristics are the most important critical quality attributes (CQAs) of tablets. Among these CQAs, mechanical properties of tablets are the most difficult to characterize, establish and optimize. Although extensive research has been done to understand and define the mechanical properties of tablets with over 200 publications each year on compaction science, there is still some degree of confusion and disagreement regarding compression and consolidation of pharmaceutical powders. This uncertainty is due to the complexity of pharmaceutical powders and their heterogeneous properties. Thus the primary research objective of present thesis is to investigate and understand compaction behavior of pharmaceutical powders and their complex binary mixtures using percolation theory, a topological tool. The specific objectives of the studies are as follows:

1. To understand mechanics of tablet formation of single components and binary powder mixtures by classical models of powder compaction
2. To compare and evaluate superiority of percolation theory over classical theories to assess compaction behavior of powder and their binary mixtures
3. To assess compaction behavior of single component and binary mixtures of powders by a model based on fundamentals of percolation theory
4. To study and calculate percolation threshold or critical concentration of single component and binary powder mixtures of dissimilar deformation behavior (plastic, brittle, elastic deformation) to form mechanically stable compact

5. To study the significance of percolation theory in determining relationship between compressibility and compactibility of powder materials and their binary mixtures as well as bonding area and bonding strength of powder particles
6. To establish relationship between various mechanical properties of compacts to evaluate deformation and consolidation behavior of powders and their binary mixtures of dissimilar compaction behavior
7. To evaluate the effect of variables, such as morphology, particle size, crystallinity and tableting speed on compaction behavior of powders
8. To study uniaxial tableting process of powders in terms of percolation theory
9. To establish significance of percolation theory in current QbD paradigm for formulation development of tablet dosage form

2. Materials and Methods

2.1. Materials

Microcrystalline cellulose spheres (Vivapur[®] MCC Spheres 200) and sugar starch spheres (Nonpareil 101) were kind gifts from JRS Pharma (Patterson, NY) and Freund Corporation (Shinjuku-ku, Tokyo, Japan), respectively. Ibuprofen spheres and MCC Sanaq Burst[®] were kind gifts from Pharmatrans Sanaq AG (Basel, Switzerland). Carbamazepine, USP and potassium bromide were purchased from Alfa Aesar (Ward Hill, MA) and Merck KGaA (Darmstadt, Germany), respectively. Microcrystalline cellulose grades (Avicel[®] PH 101, 102, 105 and 200) and croscarmellose sodium, NF (AC-Di-Sol[®]) were kind gifts from FMC Biopolymer (Newark, DE) and crospovidone (Kollidon[®] CL-SF) was a kind gift from BASF (Ludwigshafen, Germany). Lactose monohydrate (Foremost Fast Flo[®] 316) was a kind gift from Foremost Farms (Baraboo, WI).

2.2. Methods

2.2.1. Physical Characterization of Powder Materials

Bulk and Tapped Densities

Bulk density of powder materials was determined by slowly sliding (to minimize the impact of falling particles) from the edge of a wide-mouth funnel a known quantity of pre-sieved powder material into a graduated cylinder and recording the occupied volume. From the mass and volume of the powder, the bulk density of the powder material was computed. Tapped density was determined by placing the same graduated cylinder on a Vankel Tap Density Tester (model 50-1200, Varian, Inc., Palo Alto, CA) which was

operated for a fixed number of taps to attain equilibrium in powder bed volume. From mass and tapped volume of the powder, the tapped density was computed.

Relative bulk density (ρ_b) and relative tapped density (ρ_t) of powder material was calculated from the Eqs. (6) and (7), respectively

$$\text{Relative bulk density } (\rho_b) = \frac{\text{Bulk density}}{\text{True density}} \quad (6)$$

$$\text{Relative Tapped density } (\rho_t) = \frac{\text{Tapped density}}{\text{True density}} \quad (7)$$

2.2.2. True Density

True density of the powder materials was determined using a gas pycnometer (AccuPyc[®] II 1340, Micromeritics Instruments Corp., Norcross, GA). The pycnometer allows non-destructive measurement of volume and density of powder and solid materials and uses gas displacement technique to determine the volume of the sample under test. An inert gas (helium) was used as the displacement medium. Pycnometer was calibrated with an iron sphere of known mass prior to each measurement. For the determination, a known weight of powder sample was transferred into an aluminum sample container of 3.5 cm³ volume, and helium gas was passed through the sample from the reservoir. The determinations were carried out at room temperature. The instrument automatically purges moisture and volatile materials from powder sample and repeats the analysis until successive measurements yield consistent results. The determination of sample density was repeated for up to 10 cycles. The average reading of 10 cycles was recorded as the true density of the material.

The true density of the binary mixture of component A and B in the binary mixture were calculated using Equation 8 (59)

$$\frac{1}{\rho_m} = \frac{m_A}{\rho_A} + \frac{m_B}{\rho_B} \quad (8)$$

Where ρ_m is the true density of the binary mixture, ρ_A and ρ_B are the true density of component A and B, respectively, determined using gas pycnometer, and m_A and m_B are the mass fractions of component A and B, respectively, in the binary mixture.

2.2.3. Compression of Powders and Evaluation of Tablet Properties

In the present study, due to limitation of maximum load capacity of tablet presses, spheres and powder materials were compressed using two different single punch presses. Although the process of compaction remains same, i.e uniaxial compression. Spheres (microcrystalline cellulose, sugar and ibuprofen) were compressed using a Carver laboratory press (model C, Fred S. Carver Inc., Menomonee Falls, WI) using a set of 9 mm, flat-faced tooling (Natoli Engineering Co. Inc., St. Charles, MO). Powder materials (carbamazepine, microcrystalline cellulose, croscovidone, croscarmellose sodium, lactose monohydrate, and MCC Sanaq Burst) were compressed using a set of 8 mm (0.315 inches), flat-faced tooling (Natoli Engineering Co. Inc., St. Charles, MO) using Instron Material Testing Machine (model 4502, Instron, Norwood, MA) equipped with a load cell of 10 kN. The cross-head speed of upper punch was set at 1 inch/min with automatic stop and return action, and dwell time was set at 0.01 min (0.6 sec). The powders were compressed using a range of compression loads to obtain compacts of a wide range of relative density (compact porosity). The die was externally lubricated using magnesium stearate

suspension (5% w/w in acetone) before each compression cycle. A minimum of six tablets was prepared at each compression pressure (n = 6).

To study universality of our study, microcrystalline cellulose (Avicel PH[®] 101) and dicalcium phosphate (Emcompress[®]) was compressed using Presster[®] (MCC Corporation, East Hanover, NJ) a tableting emulator simulating industrial scale rotary press Manesty (Betapress) and Fette (PT 2090 IC) at five different tableting speeds of 57600, 60000, 96000, 120600 and 162100 tablets per hour.

Binary mixtures of powder materials were prepared with varying weight fractions of the two components in ratios varying between 1:9 and 9:1. The powder blends were mixed using a Turbula[®] mixer (Glen Mills Inc., Clifton, NJ) for 10 minutes. The volume fraction of powder components A and B in the binary mixture was calculated using Eq. 9 and Eq. 10, respectively (59).

$$V_A = \frac{m_A \rho_m}{\rho_A} \quad (9)$$

$$V_B = \frac{m_B \rho_m}{\rho_B} \quad (10)$$

Where V_A and V_B are the volume fractions of components A and B, respectively, determined using gas pycnometer, m_A and m_B are the mass fractions of component A and B, respectively, in the binary mixture, ρ_A and ρ_B are the true density of components A and B, respectively, and ρ_m is the true density of the binary mixture.

2.2.4. Relative Density and Porosity

Relative density, ρ_r , of tablets compressed at various pressures were calculated from compact density data and true density of powder using following relationship (Eq. 11) (60).

$$\rho_r = \frac{\text{Compact density}}{\text{True density of the powder}} \quad (11)$$

The porosity of tablet, ε , was calculated using the following relationship:

$$\varepsilon = 1 - \rho_r \quad (12)$$

2.2.5. Radial Tensile Strength

Radial tensile strength, σ_t , of tablets was determined from tablet crushing strength and tablet dimension data using following equation (Eq. 13) (61).

$$\sigma_t = \frac{2F}{\pi \cdot d \cdot h} \quad (13)$$

Where F is the crushing strength (kg), d is diameter (mm), and h is thickness (mm) of the tablet. Crushing strength of tablets was determined using a Monsanto type tablet hardness tester (model PAH-01, Pharma Alliance Group, Valencia, CA). Tablet diameter and thickness were determined using a digital micrometer.

2.2.6. Young's or Elastic Modulus, E

Powder compacts of 8 mm, flat-faced tooling were prepared using Instron Physical Testing Instrument (model 4502) as described in compaction of powder section. Young's moduli, E, were determined by compression test using Instron Physical Testing Instrument (model 4467) equipped with 50 KN load cell at constant ramp rate of 0.009 mm/sec (Figure 11). The stress-strain curves were generated from load-displacement curve. A typical conversion of load displacement curve to stress-strain has been represented in Figure 12. Young's modulus, E, of powder material was determined from the average of five tablets (n=5)

2.2.7. Compressive strength of compact

Compressive strength, σ_{cs} , can be defined as the maximum stress a compact can take before undergoing permanent deformation. It can be measured as the first peak in the stress-strain curve. Like radial tensile strength, compressive strength also is one of the mechanical properties of a compact. The higher the value of compressive strength of a material, higher will be the compactibility of powder material.

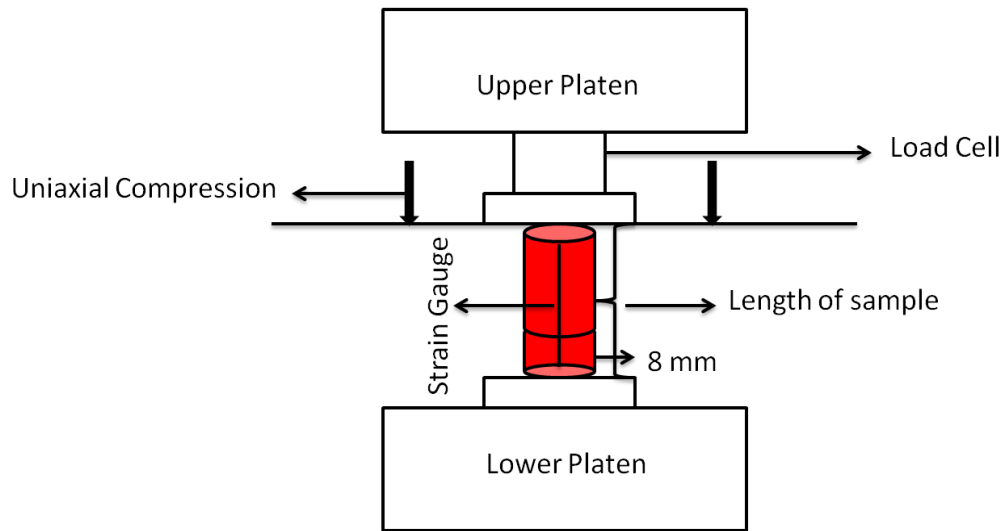


Figure 11: Schematic representation of uniaxial compression to generate stress-strain curve.

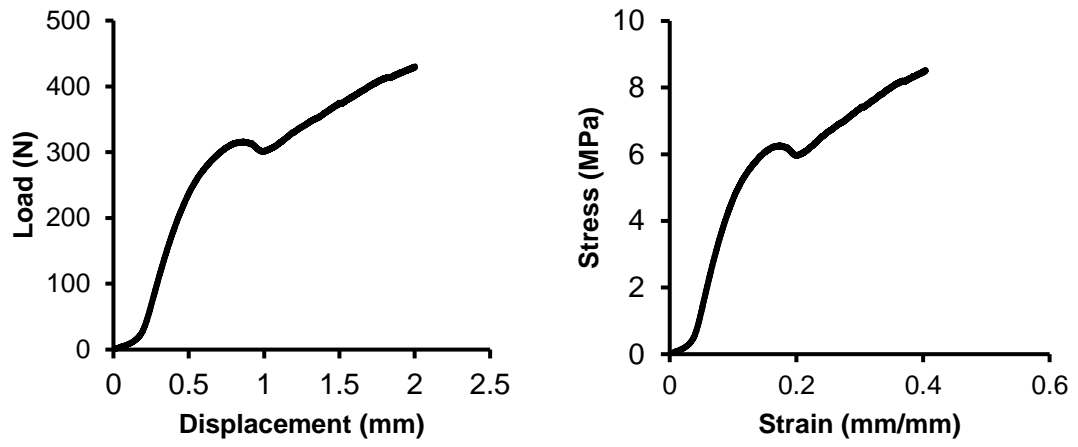


Figure 12: Schematic representation of load displacement and stress-strain curve

2.2.8. Compressibility of powder materials

Among various mathematical models to quantify compressibility of a powder, Heckel equation is still the most popular. In the present study, therefore, Heckel equation was used to quantify densification of powder material with increasing compression pressure. Heckel equation was developed on the line of first-order chemical reaction where reactant concentration is substituted by compact porosity and time by compression pressure. The rate of change of compact density with compression pressure is proportional to void volume or porosity according to the following relationship (62).

$$\frac{d\rho_r}{d\sigma_c} \propto (1 - \rho_r) \quad (14)$$

Integration of above equation yields following relationship.

$$\ln\left(\frac{1}{1-\rho_r}\right) = k \sigma_c + a \quad (15)$$

Where ρ_r and σ_c are relative density and compression stress, respectively, k and a are constants derived from the slope and intercept of the plot, respectively. The Heckel plot is divided into two linear segments representing loose and dense compact, i.e. compact formed at low and intermediate pressure, respectively (Figure 7). The linear segments with highest R^2 values were selected based on the best fit method. Regression analysis was performed to obtain slopes and intercepts of both linear segments of the plot. Further, to interpret the deformation behavior of material, the value of mean yield pressure, P_y , was calculated from the reciprocal of slope, k , of the plot. Since initial segment of Heckel plot usually represents particle rearrangement, and the subsequent segment is indicative of

deformation behavior, value of mean yield pressure, P_y , was computed from the second segment of Heckel plot at intermediate pressure (dense compacts) (63).

Modified Heckel equation

In the differential form, Heckel equation (Eq. 15) can be written in the form of Eq. 16

$$\frac{d\rho_r}{d\sigma_c} = \chi_p(1 - \rho_r) \quad (16)$$

Here σ_c , ρ_r is compression load and relative density of compact, respectively, χ_p represents compressibility parameter or pressures susceptibility of powder material. Kuentz and Leuenberger further modified Eq. 16 to define the compressibility of powder more accurately which is popularly called as modified Heckel equation by taking account of pressure susceptibility given in Eq. 17 (64).

$$\chi_p = \frac{C}{\rho_r - \rho_c} = \frac{C}{\varepsilon_c - \varepsilon} \quad (17)$$

Where χ_p represents compressibility parameter or pressures susceptibility of the powder material, ρ_r , ε is relative density and porosity of compact, respectively, and ρ_c and ε_c is critical relative density and critical porosity of powder compact at which first mechanical stable compact is formed.

By combing Eq. 16 and Eq. 17, a relationship in the differential form can be given in the form of Eq. 18

$$-\frac{1}{\varepsilon} \frac{d\rho_r}{d\sigma_c} = C \frac{1}{\varepsilon_c - \varepsilon} \quad (18)$$

After separating each variable, Eq. 18 can be written as -

$$-\frac{\varepsilon_c - \varepsilon}{\varepsilon} d\varepsilon = C d\sigma_c \quad (19)$$

Assuming at negligible compression pressure, $\sigma_c = 0$, integration of Eq. 19 can be performed from the critical porosity, ε_c .

$$\int_{\varepsilon_c}^{\varepsilon} \frac{\varepsilon_c - \varepsilon}{\varepsilon} d\varepsilon = C \int_0^{\sigma_c} d\sigma_c \quad (20)$$

Solving and rearranging Eq. 20 yields Eq. 21.

$$\varepsilon - \varepsilon_c + [\ln(\varepsilon_c) - \ln(\varepsilon)] = \varepsilon - \varepsilon_c + \ln\left(\frac{\varepsilon_c}{\varepsilon}\right) = C\sigma_c \quad (21)$$

By further rearrangement, modified Heckle equation (Eq. 22) in terms of porosity of compact with respect to compression pressure can be achieved.

$$\sigma_c = \frac{1}{C} \left[\varepsilon - \varepsilon_c - \varepsilon_c \ln\left(\frac{\varepsilon}{\varepsilon_c}\right) \right] \quad (22)$$

Here C represents compressibility parameters of powder material and ρ_c is the percolation threshold defining critical porosity at which pressure susceptibility of powder materials changes.

Further, based on the relationship between porosity of the compact, ε , and relative density, ρ_r , modified Heckle equation in terms of relative density can be given as.

$$\sigma_c = \frac{1}{C} \left[\rho_c - \rho_r - (1 - \rho_c) \ln\left(\frac{1 - \rho_r}{1 - \rho_c}\right) \right] \quad (23)$$

2.2.9. Compactibility of powder materials

Leuenberger Equation

Leuenberger equation is one of the widely accepted model to quantify compactibility of a powder material (24). It was initially developed to access the deformation hardness of powder material with increasing compression load, but was subsequently also used to describe tensile strength and other compactibility parameters (65). This equation is based on the assumption that the cross-sectional area, A , of a cylindrical tablet contains N_+ number of bonding contact points and N_- number of non-bonding contact points. Based on this assumption, a relatively simple equation was derived that can be written as follows (24).

$$A = N_0 a = (N_+ + N_-) a \quad (24)$$

Where, N_0 is total number of contact points in the cylindrical tablet of cross sectional area, A , N_+ and N_- are bonding and non-bonding contact points, respectively, and a is unit area per contact bonding point.

Since only bonding contact points, N_+ , contribute in the compact hardness and non-bonding points, N_- , play a passive role, compact hardness, P , is postulated to be proportional to the number of bonding contact points, N_+ , as represented in Eq. 25.

$$P = \lambda N_+ = \lambda (N_0 - N_-) \quad (25)$$

Where λ is proportionality factor. Further, by assuming relative decrease in the number of non-bonding contact points, $\frac{dN_-}{N_-}$, being directly proportional to the externally

applied compression force, σ_c , and change in relative density, $d\rho_r$, of the compact, following differential equation is obtained:

$$\frac{dN_-}{N_-} = -\gamma \sigma_c d\rho_r \quad (26)$$

By incorporating limiting condition that at relative density, $\rho_r = 0$, only non-bonding contact points exist in the absence of any external stress, i.e. $N_0 = N_-$, following equation can be derived by integration:

$$N_- = N_0 e^{-\gamma \sigma_c \rho_r} \quad (27)$$

With further mathematical treatment and algebraic rearrangement considering powder technology rules, Leuenberger equation is obtained (Eq. 28) (66). The original equation, which was developed in terms of deformation hardness, P , of the compacts, was successfully applied to tensile strength of compacts by substituting deformation hardness, P , with tensile strength, σ_t , and maximum deformation hardness, P_{\max} , with maximum tensile strength, $\sigma_{t\max}$.

$$\sigma_t = \sigma_0 (1 - e^{-\gamma \sigma_c \rho_r}) \quad (28)$$

Where σ_t is the tensile strength, σ_0 is maximum tensile strength at relative density, $\rho_r \rightarrow 1$, and compression load, $\sigma_c \rightarrow \infty$, and γ is compression susceptibility defining deformation behavior of powder material. These two parameters, i.e., $\sigma_{t\max}$ and γ , help in assessing bonding behavior of particles and characterizing deformation behavior of material under pressure (35).

Ryshkewitch-Duckworth Equation

The Ryshkewitch-Duckworth equation is another classical model widely used to assess the compactibility of powder material. It was first proposed by Ryshkewitch in 1953 while studying the tensile strength of porous sintered alumina and zirconia (67). The model was based on the assumption that logarithm of tensile strength is inversely proportional to the porosity of compact. A modification of the proposed model by Duckworth yielded the following relationship which is popularly called as Ryshkewitch-Duckworth equation (Eq. 29) (36).

$$\sigma_t = \sigma_0 \exp (- b\varepsilon) \quad (29)$$

Where σ_t is tensile strength of the compact, σ_{tmax} , is compactibility or tensile strength at zero porosity, b is bonding capacity of powder material, and ε is porosity of the compact.

Prediction of compactibility of binary mixtures

Wu *et al.* (59) suggested that in a binary mixture, the compactibility of individual component follows linear mixing rule assuming no change in volume fraction of the constituent powders occurs during the tableting of binary mixtures. Based on this assumption, it was proposed that the compactibility of binary mixtures is additive and can be calculated using Eq. 30.

$$\sigma_{0m} = \sigma_{0A}V_A + \sigma_{0B}V_B \quad (30)$$

Where σ_{0m} , is the compactibility of a binary mixture or tensile strength of binary mixture at zero porosity, v_A and v_B are the volume fractions of component A and B,

respectively, σ_{0A} and σ_{0B} are the tensile strength at zero porosity or compactibility of components A and B, respectively, calculated using Eq. 29. Similarly, a power mixing rule to define compactibility of the binary mixture can be represented as follows:

$$\sigma_{0m} = \sigma_{0A}^{v_A} * \sigma_{0B}^{v_B} \quad (31)$$

To evaluate the correlation between the predicted value of compactibility by linear and power mixing rule (Eqs. 30 and 31), the tensile strength at zero porosity, σ_{0m} , of a binary mixture of component A and component B at each volume fraction was calculated using Ryshkewitch-Duckworth model (Eq. 29).

2.3. Estimation of Young's modulus/Elastic modulus at zero porosity

Sprigg's equation

In 1961, RM Spriggs proposed that similar to calculating tensile at zero porosity by plotting logarithm of tensile strength as a function of porosity, elastic modulus too can be calculated using same assumption. From then, it is popularly called as Sprigg's equation (Eq. 32) to define elastic modulus or Young's modulus, E_0 of a porous compact.

$$E = E_0 \exp (- b\varepsilon) \quad (32)$$

Where E is Young's or Elastic modulus of the compact, E_0 is elastic modulus at zero porosity, b is empirical constant, and ε is porosity of the compact.

2.3.1. Estimation of bond and site percolation threshold

Tablet density as a function of compression pressure data were plotted according to Heckel equation (Eq. 15). Linear regression analysis was performed to obtain values of

the slope and intercept of both linear segments of Heckel plot, i.e. at low and intermediate compression pressures. The values of bond and site percolation thresholds (ρ_{cb} and ρ_{cs}) of powder material were calculated from the intercepts of segments representing loose and dense compacts, respectively, according to the methodology proposed by Leuenberger and Leu (55, 68).

2.3.2. Percolation Model

It is well documented that tensile strength of a compact depends on its relative density or porosity. However, relative density usually fails to determine the compactibility of pharmaceutical powder materials due to the difference in deformation behavior and sensitivity of powders to the compression pressure. Kuentz and Leuenberger (69) introduced the concept of normalized relative density in the line of effective medium approximations to establish a relationship between tensile strength, σ_t , and the normalized relative density of compact. The concept of effective medium approximation (EMA) was first proposed by Bruggeman for the studies of macroscopically inhomogeneous media that was further generalized by numerous researchers to treat a variety of problem phenomenon (70). It has been widely used in the study of percolation phenomena in electrical conductivity, dielectric function, elastic modulus, etc. The EMA is the theoretical aspect based on the theoretical approximation of individual component additive in the composite system as the precise calculation is not possible (71). As described earlier, pharmaceutical powders are inhomogeneous and heterogeneous, thus studying their mechanical properties by EMA is very useful. The use of EMA in pharmaceuticals has been successfully applied to study percolation phenomenon in the tensile strength of pharmaceutical powders by linear and exponential approximations (72).

In the present study, normalization of relative density was used to study the compactibility of single powder materials and their binary mixtures as follows:

The relationship between relative density and porosity can be given as follows:

$$\rho_r = 1 - \varepsilon \quad (33)$$

where ρ_r is the relative density and ε is the porosity of compact.

At a certain porosity of compact, particles of components begin to percolate or span the entire lattice of compacts called as a critical porosity (ε_c). This is similar to the probability of bonding or network of contacts required to increase the coherence of compacts. Thus it becomes necessary to consider reduced porosity or normalization of porosity considering critical porosity of compacts. Kuentz and Leuenberger defined this normalization as follows (69):

$$\varepsilon_{\text{nor}} = \frac{\varepsilon}{\varepsilon_c} \quad (34)$$

Here, ε_{nor} is normalized porosity, and ε and ε_c is porosity and critical porosity of the compact, respectively. The, reduced or normalized relative density (ρ_{nor}) based on Eq. 34 can be given as follows:

$$\rho_{\text{nor}} = 1 - \varepsilon_{\text{nor}} \quad (35)$$

Further, Eq. 35 can be rewritten as Eq. 36.

$$\rho_{\text{nor}} = 1 - \frac{\varepsilon}{\varepsilon_c} \quad (36)$$

The mathematical rearrangement based on the relationship between relative density, ρ_r , and porosity, ε , in the above equation (Eq. 33), Eq. 36 can be modified in the form of Eq. 37.

$$\rho_{\text{nor}} = 1 - \frac{1-\rho_r}{1-\rho_c} \quad (37)$$

Further, rearrangement of Eq. 38 can be represented mathematically as follows:

$$\rho_{\text{nor}} = \frac{\rho_r - \rho_c}{1 - \rho_c} \quad (38)$$

To define compactibility or tensile strength of compact at zero porosity, σ_0 , the change in tensile strength of binary mixtures with respect to normalized relative density can be represented as follows (73).

$$\sigma_t \propto \sigma_0 \rho_{\text{nor}}^q \quad (39)$$

Where σ_t is the tensile strength of compacts of the binary mixture, σ_0 is the tensile strength of compact at zero porosity, ρ_{nor} is the normalized relative density, and q is the critical exponent.

Thus combining Eqs. 38 and 39, at $\rho_r > \rho_c$, power law relationship describing tensile strength at zero porosity can be given as follows:

$$\sigma_t = \sigma_0 \left(\frac{\rho_r - \rho_c}{1 - \rho_c} \right)^q \quad (40)$$

where, σ_t is the tensile strength of compact, σ_0 is the tensile strength of compact at zero porosity, ρ_r is the relative density of the compact, ρ_c is percolation threshold, and q is the critical exponent.

Similar to the above discussed theory to define tensile strength using normalized relative density of compact, elastic modulus (E_0) as well as compressive strength at zero porosity (σ_{cs0}) can also be calculated considering normalized relative density of compact using Eq. 41 and 42, respectively

$$E = E_0 \left(\frac{\rho_r - \rho_c}{1 - \rho_c} \right)^q \quad (41)$$

$$\sigma_{cs} = \sigma_{cs0} \left(\frac{\rho_r - \rho_c}{1 - \rho_c} \right)^q \quad (42)$$

The normalization of the relative density of compact can be done by substituting the value of the percolation threshold directly into Eq. 40 (74). Also, the relative density of compact can also be normalized using the relative tapped density of powder as well as bond percolation threshold determined from the initial section of Heckel plot (Eq. 15). Holman and Leuenberger (56) reported that relative tapped density can be used as percolation threshold for normalization of the relative density of compact in Eq. 40. As bond percolation threshold, ρ_{cb} , theoretically equals to relative tapped density, ρ_t , of powder material ($\rho_{cb} \cong \rho_t$), in the present study, bond percolation threshold, ρ_{cb} , determined from the intercept of Heckel plot representing region of loose compacts was used as percolation threshold for normalization of relative density of compact in power law equation (Eq. 40) (55, 68). One of the advantages of using this approach is the elimination of flip-flop effect between adjusting functions, q and ρ_c , of power law equation.

2.3.3. Universality of critical exponent, q

Geometry of the system cannot be separated from physical properties. For instance, the physical properties of a crystal are determined by the geometry of its lattice. Similarly,

the "geometry of disorder" determines a number of properties of a system in the vicinity of a critical point (75).

As it has been already discussed in introduction section, percolation theory is based on the probability, p , of occupation of sites and formation of clusters. Thus property of system depends on the number of clusters, n_s . For $p \gg p_c$, there is an infinite clusters with strength P (fraction of sites belonging to the infinite clusters). At $p \ll p_c$, the remaining cluster of size, s , corresponds to the Eq. 43

$$\sum n_s S = p \quad (43)$$

Thus for $p > p_c$, we have infinite cluster with the strength, P , and the remaining sum of finite cluster of size, S , which defines together the occupation probability as follows.

$$P + \sum n_s S = p \quad (44)$$

Thus it can be shown that close to the percolation threshold, the fraction P can be written as follows:

$$P = (p - p_c)^\beta \text{ at } p > p_c \quad (45)$$

Here, p_c is the critical concentration or percolation threshold of pores, and β is critical index or exponent. Thus in the context of percolation theory, a percolation transition is characterized by a set of universal critical exponents which describe the fractal properties of the percolating medium at large scales and sufficiently close to the transition. The exponents are universal in the sense that they only depend on the type of percolation model and on the space dimension. They are expected not to depend on microscopic details, e.g. the lattice structure, or whether site or bond percolation is

considered. Percolating systems have a parameter, p , which controls the occupancy of sites or bonds in the system. At a critical value, p_c , the mean cluster size goes to infinity and the percolation transition takes place. As one approaches critical value, p_c , various quantities either diverge or go to a constant value by a power law in $(p-p_c)$, and the exponent of that power law is the critical exponent (76). While the exponent of that power law is generally the same on both sides of the threshold, the coefficient or "amplitude" is generally different leading to a universal amplitude ratio. The most interesting feature is that owing to the large size of the blocks, the geometry is virtually independent of the atomic structure of the material and thus possesses properties common to a number of quite dissimilar systems; hence, the universality of the physical properties that we find in the neighborhood of critical points. This type of relation between physics and geometry can be traced in percolation theory. Percolation theory is formulated in terms of simple geometric images, such as wire nets, spheres or crystal lattices. Percolation theory, as a theory of critical phenomena, is not yet a mathematically rigorous science. A large number of important propositions have not yet been proved, and certain questions remained answered. Thus in the present thesis, attempt has been made to evaluate critical exponent, q , and its possible universality in defining mechanical properties of a compact (tensile strength, compressive strength and Young's modulus) using power law equation.

As discussed earlier, based on fundamentals of percolation theory, the critical exponents should depend only on the dimensionality of the system studied and not on the details of the microstructure, i.e. of the lattice chosen. On the other hand, the second parameter of percolation theory, i.e. the percolation threshold, p_c , is directly related to the microstructure. Thus a change in the particle size and size distribution of a system studied

can affect the percolation threshold. Additionally, it should be kept in mind, that the critical exponent, q , and the percolation threshold, ρ_c , are correlated. Thus it is often necessary that one of the parameters is already known. For this reason, the universality of critical exponent, q , is an important feature of percolation theory.

2.3.4. Critical exponent for powder compression

The universal exponent q is linked to the geometrical compression process, i.e. to type of percolation (directed, purely correlated, mixed) of the particles and on the type of “reaction” of the material of the particles involved. In case of tableting, powder undergoes uniaxial compaction process especially during when single punch tablet press is used. Uniaxial die compaction is compaction process of a powder within a die cavity by action of an upper punch at a constant velocity, while the lower punch does not move within the mechanical assembly (Figure 13). The uniaxial compression process is kind of two stage process, i.e. z -direction initially and radial direction as a follow-up. During compression, the number of sites to be occupied is constantly reduced. According to the principle of uniaxial compression, the mean particle particle separation distance is reduced more in the z -direction than in the lateral directions. Thus, it can be assumed that in the beginning, a 1-dimensional bond percolation is responsible for stress transmission. After the rearrangement of the particles, an important buildup of stress occurs as particles can no longer be displaced easily. This situation is typical for a site percolation process. The stress transmission is mainly in the lateral direction. Thus, the original 3-dimensional problem can be split into a 1-dimensional and, subsequently, 2- dimensional percolation phenomenon.

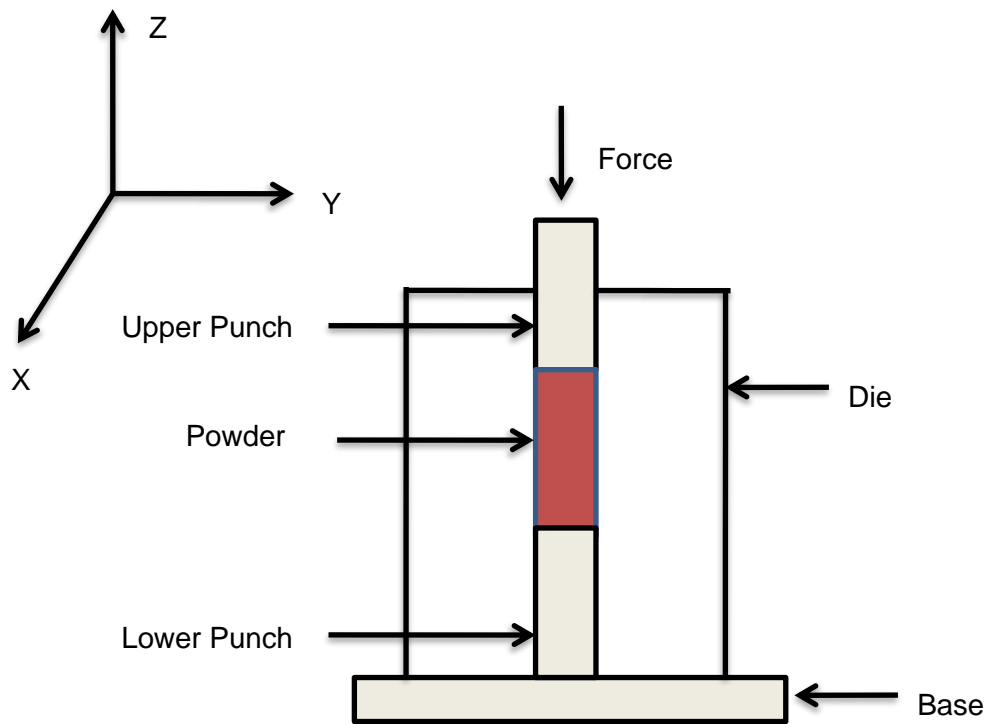


Figure 13: A schematic representation of powder compaction by uniaxial compression

Table 2: Values of critical exponent of lattice in various dimensions

Properties	Exponent	Values of critical exponent, q		
		d = 2	d = 3	Bethe
Strength, P	β	5/36	0.41	1
Backbone of P	β_{BB}	0.48	1.05	2
Mean cluster size, S	$-\gamma$	-43/18	-1.80	-1
Correlation length, ξ	$-v$	-4/3	-0.88	-1/2
Conductivity, g_e	μ	1.3	2.0	3
Elastic modulus, E	f	3.96	3.75	4
Fractal dimension (FD)		91/48	2.52	4

*d = dimension

2.3.5. Approximation to Bethe Lattice assuming the value of $q=1$

The Bethe approximation is one of the common practices in percolation models (77). The approximations for ferromagnetism by Peierls (78) and for anti-ferromagnetism by Ziman (79) have been reported earlier. A recent review on the Bethe and other approximations give a clear insight of their significance including in the lattice gas problem (80). A Bethe lattice is a perpetual branching network that lacks any reconnections. Figure 14 is a typical example of Bethe lattice with coordination number, $z = 3$. It is also called as Cayley tree and has only one possible path connecting any two sites making them much more amenable to mathematical treatment. Due to this convenience, much of the mathematical treatment of percolation theory was originally developed and studied on Cayley tree (38). Leuenberger *et al.* (55) established a relationship between compression susceptibility, γ , of powder material and slope value, k , of the Heckel equation by substituting exponential terms of Eq. 5 with the terms of Heckel equation (Eq. 15). Further, to interpret compactibility of the material, maximum tensile strength, σ_{max} , of the compact can be computed from the power law equation (68). This approach although is simple and can be explained, it fails to calculate accurately the compactibility of powder materials owing to the simple approximation to effective medium. Thus the study was further shifted to find more accurate value of critical exponent, q , by closer outlook of tableting process of powder compaction.

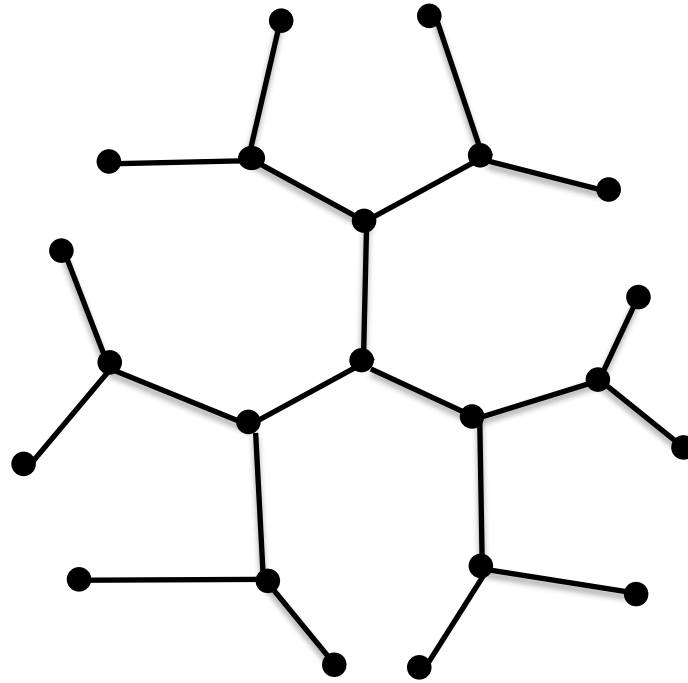


Figure 14: A typical example of small Bethe lattice with coordination number, $Z = 3$.

2.3.6. Assuming the value of critical exponent based on mechanical lattices

To study mechanical strength in a percolation model, brittle beams can be imagined in a lattice, or also springs that undergo brittle fracture if their elastic limit is exceeded. In case of the Young's modulus, a lattice can be imagined in which elastic springs represent the occupied sites whereas for tensile strength a brittle beam can be imagined in a lattice. Guyon et al. (81) proposed a theoretical value for the strength or fracture exponent, $\tau = 2.7$ for tensile strength and $f = 3.96$ for Young's modulus. However, it was theoretically shown that the occurrence of bond-bending forces, i.e. torque, leads to a significantly higher elastic exponent than expected. An experimental value of critical exponent, $f = 4.0$ was found by Kuentz and Leuenberger for modified Young's modulus of different grades of microcrystalline cellulose (MCC). Whereas the tensile strength of MCC tablets when tested on a diametrical compression test yielded an experimental value of $\tau_f = 3.2 \pm 0.01$ which was slightly higher than the expected values of 2.7. These authors attributed this deviation to the anisomorphous shape of the particles, anisotropy of the compact as well as the broad distribution of macroscopic properties causing deviation of the measured values of critical exponent from the theoretical value of the critical exponent of 2.70. Van Veen *et al.* (73) too have reported the value of the critical exponent, q , for sodium chloride and pregelatinized starch as 2.45 and 2.92, respectively. In the present study too attempt was made to study the critical exponent for single component powder materials and its binary mixture.

2.3.7. Correlated Percolation Phenomenon

Standard percolation usually deals with the problem when the constitutive elements of the clusters are randomly distributed. However, correlations cannot always be neglected. In this case, correlated percolation is the appropriate theory to study such systems. The primary substance particles represent a disordered system of powder or granules, i.e. processed powder, which contain the right amount of API and excipients (diluent, disintegrant, binder, lubricant, etc). A disordered particulate system consists of solid particles but often behaves differently, more like a liquid or gas, and should probably be described as a fourth state of matter (22). The characterization of a disordered particulate system is still a challenge (82) since a long range order is missing and the local structure can often be only approximated with an estimated physical coordination number, z (83). Since the first use of percolation theory, it has always been assumed that there is no correlation or existences of dependence between segments in particularly defined systems. However, given the nature of disordered systems, it can be argued if the physical phenomenon of a system depends only upon the random probability. Thus some kind of correlation, finite or infinite, exists in such system. It has been earlier discussed how powder is 4th states of matter. In addition to that, pharmaceutical powders possess more disorderness due to the process of synthesis as well as multi-functionality. Moreover, transition of a powder bed into a tablet involves a number of steps and mechanisms. It commences with the application of compaction force to a powder bed followed by interparticular bonding by various mechanisms and deformations, i.e. elastic, plastic and fragmentation. Particles pass through one or several of these deformation phases during a compression process. These are more often concurrent than sequential as a single particle

is likely to pass through multiple deformation cycles. Due to overlapping processes, the dominating volume reduction mechanism for most pharmaceutical materials are complex and often cannot be simply characterized as either elastic, plastic or fragmenting. Thus it can be hypothesized that with such kind of disordered nature of pharmaceutical powders, correlation phenomenon does exist. Thus it becomes necessary to study the powder compaction in the light of correlated percolation phenomenon.

Correlated percolation models are systems where sites in a lattice are occupied randomly by a given species, and then species are removed (bootstrap percolation) or added (diffusion percolation) according to the site's environment. As described earlier, a powder component consists of solid particles along with pores. Thus essentially even a single component powder can be called as binary system consisting of powder particle and pores. With the application of stress, the pores are dissipated and powder particles occupy the spaces. Thus a correlated diffusion based percolation phenomenon can be envisaged in powder compaction.

During tableting process, pores dissipates from powders. Since the pores are randomly distributed, the process of occupation of the void space is governed by a stochastic process similar to heat diffusion. On the other hand, the stress between the upper and lower punch is only transmitted if the particles touch each other to form a connective path between the punches, which is true in radial direction. In other words, the formation of a compact is the result of the percolation of particles (50, 84). Since the die wall pressure is directly correlated to the punch pressure in z direction of the uniaxial compression, the tableting process corresponds to a diffusive correlated percolation. The percolation threshold for a 3-D correlated percolation is $\rho_c = 0.634$ for a coordination number $z = 6$ and

$\rho_c = 0.366$ for $z = 12$ and its critical exponent, q , for the correlated percolation is equal to 2.0 (85, 86). In this context, it has to be kept in mind, that the critical exponent is universal, i.e. an invariant, however, the value of the percolation threshold depends on the material, the particle size, its size distribution and crystalline structure leading to a more or less well-defined coordination number, z , in the tableting process (44, 87). Thus, the basic percolation equation for a powder bed to be compressed to achieve a compact of the relative density, ρ_r , is as follows: $\sigma_t = S(\rho_r - \rho_c)^q$ with σ_t = tensile strength of the tablet being related to the force to break a tablet, S = scaling parameter, ρ_r = solid fraction, ρ_c = critical solid fraction or percolation threshold, and $q = 2$ as a critical exponent in 3-D. The value of critical exponent, $q = 2$ being a universal value governs all diffusional processes such as heat diffusion or drug dissolution (88, 89). It is important to realize that in a process far-from-equilibrium, the time plays an essential role being hidden in the variable, z , of the uniaxial tableting process since the tableting speed defines the time and the position of the punch.

2.3.8. Statistical Evaluation and Nonlinear Regression Analysis

As a researcher, it is important to determine the relationship between the dependent variable, y , and independent variable, x , from an experimental data set. This is called regression analysis which is represented by a simple relationship, $y = f(x)$, where f is the function that may include one or more parameters to describe the relationship between x and y (90). The function, f , is then used to predict the value of unknown variable y' at the desired value x' . Thus, the extent to which the predicted values match with the experimentally observed values (goodness of fit) depends on the efficiency and accuracy of the function, f . Several computer programs are commercially available to perform the

regression analysis. If the relationship, $y = f(x)$, is linear, then the analysis is called linear regression analysis which can be performed using simple computer programs like Microsoft[®] Office Excel (91). However, if the relationship, $y = f(x)$, is nonlinear, Microsoft[®] Excel can still be used along with other sophisticated software like OriginPro[®], SigmaPlot[®], Minitab[®], Prism[®] etc. Nonlinear regression analysis or curve fitting is an iterative process that converges to find the best possible solution. The analysis is based on initial estimates of parameters to see how well the nonlinear model fits. This iteration continues until the differences between the residual sums of squares between the observed and the predicted values no longer decrease significantly (92). Thus unlike linear regression, nonlinear regression analysis of a data set cannot be performed directly unless the researcher has some experience with the mathematical model in order to set the initial parameters.

Various physical phenomena follow nonlinear behavior, of which powder compaction is widely studied across various disciplines like chemical, mechanical, material and pharmaceutical sciences. Owing to the importance of this process, various nonlinear regression models have been proposed in the literature. The suitability of a nonlinear model to define powder compaction depends on the values of fitting parameters, e.g. compressibility and compactibility values, and the resulting statistical parameters, such as correlation coefficient (R), coefficient of determination (R^2), adjusted as well as predicted R^2 values, residual sum of squares (RSS), root mean square error (RMSE), coefficient of variation (CV) and standard error-of-fit (SE) (93). The definitions of these statistical parameters along with their desirability have been summarized in Table 3.

All physical parameters and constants in this study were calculated at 95% confidence interval using OriginPro[®] (OriginLab Corporation, Northampton, MA). The maximum number of iterations was set to 400 for the analysis and Lavenberg Marquardt algorithm was used for iteration. The parameter's confidence interval computation was done using asymptotic symmetry-based method. A typical example of detailed analysis of nonlinear regression analysis of microcrystalline cellulose using percolation model (Eq. 40) has been given in appendix.

Table 3: Various statistical parameters that describe a nonlinear regression analysis

Statistical parameters	Definitions	Desirability
Coefficient of determination, R^2	Proportion of the variance in the dependent variable that is predictable from the independent variable(s)	Close to 1
Adjusted R^2 values	R^2 values adjusted for the number of predictors in the model	Close to 1
Residual sum of squares (RSS)	Sum of the squares of residuals (difference between predicted and experimental results) ²	Small or close to 0
Root Mean Square Error (RMSE)	Root mean square of the error or the Standard Deviation of the model; equal to the square root of reduced χ^2	Small or close to 0
Confidence Interval (CI)	Lower and upper limit interval between fitted parameter	Narrow
Standard error-of-fit	Precision of the fitted parameter or standard deviation of the fitted value at 95% confidence interval	Small or close to 0
Coefficient of variation (CV)	Ratio of standard error of fit to the estimated parameters at 95% confidence interval	Small or close to 0

3. Results and Discussion

3.1 Chapter I: Compaction Behavior of Single Component Powders and Understanding Mechanics of Tablet Formation by Classical Models And Percolation Theory

The present section is based on the following hypotheses

1. The bond and site percolation phenomena play an important role in the compression and consolidation of a powder material with bond percolation threshold being as the lower threshold corresponding to the relative tapped density ($\rho_{cb} \cong \rho_t$) of the material and site percolation threshold as higher threshold ($\rho_{cs} > \rho_t$) corresponding to the formation of a mechanically stable compact.
2. Comparative evaluation of bond and site percolation thresholds of a powder material can be a predictive tool for the evaluation of its deformation behavior under compression pressure.
3. Percolation model (Eq. 40), considering percolation phenomenon in powder compaction, can be a better tool to predict compactibility of powder materials compared to the classical models of powder compaction.
4. Fundamental understanding of bond and site percolation thresholds of individual components in a multicomponent powder system can help in improving the compaction properties of a poorly compactable material, e.g. a drug, in the powder blend.

To study the validity of above-stated hypotheses and to further comparatively evaluate percolation phenomenon with classical concepts of powder compaction, four materials of different deformation properties were used; carbamazepine was used as a model, poorly-compactable material and microcrystalline cellulose, croscarmellose sodium, and crospovidone were used as representative well compactable materials. Among the three well compactable materials used, microcrystalline cellulose is one of the widely used tablet diluents and has been studied extensively for its compression and compaction properties. One of the reasons for the selection of crospovidone and croscarmellose sodium, that are popular tablet disintegrants, for this study was the availability of limited information about their compression and consolidation behavior as well as their role in enhancing bonding of particles during compression even in small quantity. Further to validate the accuracy of fourth hypothesis, three sets of binary mixtures, i.e. carbamazepine with microcrystalline cellulose, carbamazepine with croscarmellose sodium and carbamazepine with crospovidone, with increasing volumetric ratio (v/v) of carbamazepine in the blend were prepared at the relative density above site percolation threshold, ρ_{cs} , of carbamazepine.

3.1.1 Compressibility and Compression Behavior of Powder Materials

The compressibility of powder materials was determined from compression constants derived from the Heckel plots (Figure 15). The slope values and intercepts of two linear segments of compression data with highest values of coefficient of determination, R^2 , representative of loose and dense powder compacts were determined (55, 68). The values of bond and site percolation thresholds were determined from intercepts of linear segments of plot representing loose and dense compacts formed at low

and intermediate compression pressure, respectively (55, 68). Further, to assess the deformation behavior of powder material, the value of mean yield pressure, P_y , was calculated from the slope value of linear segment representing dense compacts (63). These values are summarized in Table 4. As evident (Table 4), values of bond percolation threshold, ρ_{cb} , of powder materials correspond to their relative tapped density, ρ_t , except in the case of crospovidone while values of site percolation threshold, ρ_{cs} , are higher than relative tapped density, ρ_t , of powder materials and are close to the values of site percolation threshold of various lattices in two dimensions (Table 5). These results suggest the formation of an initial weak bond between particles in the vicinity of bond percolation threshold, ρ_{cb} , at lower compression pressure (powder bed \rightarrow loose compact). With an increase in the compression pressure, the bonding between particles becomes coherent and stronger due to the progressive occupation of sites forming a dense and stable compact at site percolation threshold, ρ_{cs} (loose compact \rightarrow dense compact) (55). This confirms the validity of our first hypothesis that physical transition of powder bed from loose compact to dense compact involves bond and site percolation phenomena.

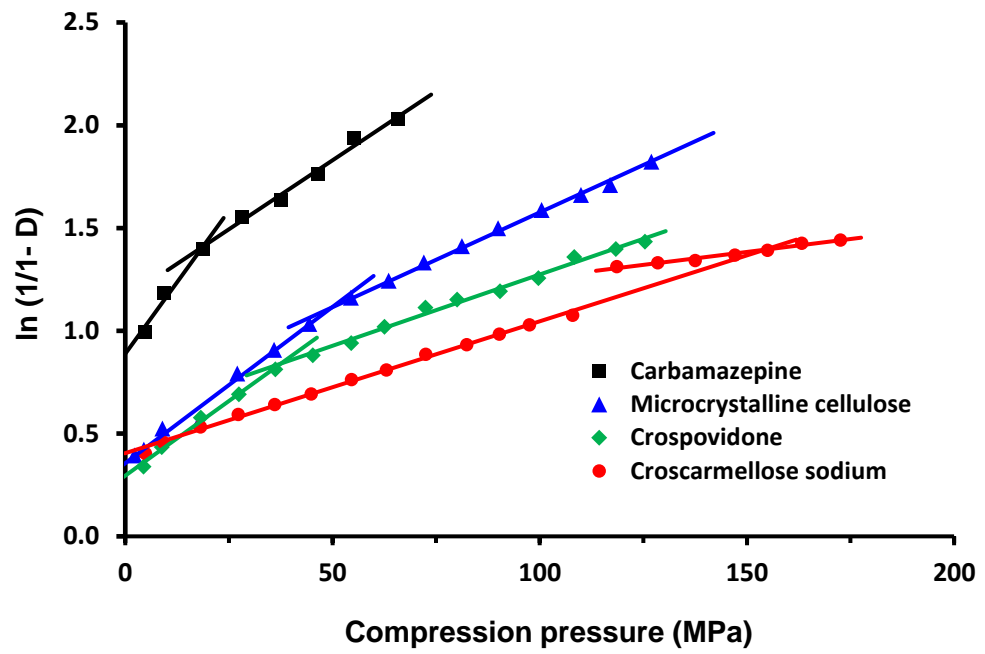


Figure 15: Heckel plot of carbamazepine, microcrystalline cellulose, crospovidone and croscarmellose sodium (Eq. 15)

Table 4: Values of bond and site percolation thresholds estimated using Heckel equation

(Eq. 15).

Materials	Loose compacts		Dense compacts		Mean yield Pressure, P_y (MPa)
	Bond percolation threshold (ρ_{cb})	R^2 value	Site percolation threshold (ρ_{cs})	R^2 value	
Carbamazepine	0.588	0.9746	0.685	0.9806	74.63
Microcrystalline cellulose	0.299	0.9924	0.480	0.9965	108.69
Crospovidone	0.244	0.9935	0.440	0.9901	144.09
Croscarmellose sodium	0.334	0.9962	0.634	0.9787	396.82

The value of mean yield pressure, P_y , of carbamazepine (74.63 ± 6.13 MPa) calculated from the slope value of linear segment of Heckel plot representing dense compact was found to be lowest amongst the four powder materials indicating higher plasticity followed by microcrystalline cellulose (108.69 MPa), crospovidone (144.09 MPa) and croscarmellose sodium (396.82 MPa) (Table 4). Since slope value, k , in Heckel plot depends on both fragmentation as well as elastic and plastic deformation of the material, it often yields false value of mean yield pressure (94). Thus, the value of mean yield pressure, P_y , can be deceptive in characterizing deformation or compression behavior of a powder material. The limitations of Heckel equation in interpreting compression behavior of a powder material and various reasons for these limitations have been reported in detail by Sonnergaard (95). In the present study, therefore, an attempt was made to determine deformation behavior of materials by critical evaluation of values of their bond and site percolation thresholds. The difference in bond and site percolation thresholds of materials with dissimilar deformation characteristics have also been reported by Leuenberger *et al.* (51, 55, 68).

Table 4 shows a significant difference between the values of bond and site percolation thresholds of powder materials determined from their loose and dense compacts, respectively. It can also be observed that significant difference in percolation thresholds exists among the four materials in the formation of loose (mechanically unstable) and dense (stable) compacts (Table 4). For instance, the value of bond percolation threshold was lowest for crospovidone ($\rho_{cb} = 0.244$) indicating the rapid transition of powder material to loose compact as compared to microcrystalline cellulose, croscarmellose sodium, and carbamazepine. This indicates higher compression

susceptibility of crospovidone as compared to the other three powder materials. A similar difference in site percolation threshold, ρ_{cs} , of crospovidone with microcrystalline cellulose, croscarmellose sodium, and carbamazepine was observed with its value being lowest for crospovidone ($\rho_{cs} = 0.440$). These results suggest that crospovidone forms stable compact even at lower relative density followed by microcrystalline cellulose, croscarmellose sodium, and carbamazepine. This can be attributed to the higher plasticity of crospovidone as compared to other three materials that leads to the rapid transition of crospovidone powder bed to a stable compact (96). The higher plasticity and excellent binding capability of crospovidone have also been reported in our previous study (2). Moreover, the lower values of bond and site percolation thresholds of microcrystalline cellulose also confirm its rapid transition from powder bed to loose and dense compact indicating its high compression susceptibility. The plastic deformation as dominant compression behavior of microcrystalline cellulose is well documented. Additionally, the calculated values of bond and site percolation thresholds of microcrystalline cellulose are in close agreement with those reported by Leuenberger *et al.* (55, 68). This confirms the validity of approach and hypothesis of our present study. Based on the similar assessment, the higher values of bond and site percolation thresholds of croscarmellose sodium and carbamazepine confirm their poor compressibility. Li *et al.* (97) also have reported fragmentation as predominant compression behavior of croscarmellose sodium confirming its brittle nature. Also, Nokhodchi *et al.* (98) have reported poor compressibility of carbamazepine. Hence it can be concluded that comparative evaluation of bond and site percolation thresholds of powder materials can be a better approach for the evaluation of their compression behavior as compared to the use of mean yield pressure, P_y , values

derived from Heckel plot. Moreover, the conclusion derived by critical evaluation of bond and site percolation thresholds of powder materials in the present study is consistent with the deformation behavior of all four powder materials reported in the literature (55, 96-98). This assessment confirms the validity of our second hypothesis of characterizing compressibility of powder materials by application of percolation phenomena.

Table 5: Physical properties of powder materials

Materials	True density (g/cc)	Bulk density (g/cc)	Tapped density (g/cc)	Relative bulk density, ρ_b	Relative tapped density, ρ_t
Carbamazepine	1.3380	0.438	0.824	0.327	0.615
Microcrystalline cellulose	1.5803	0.347	0.494	0.220	0.313
Crospovidone	1.2640	0.143	0.243	0.113	0.192
Croscarmellose sodium	1.6304	0.385	0.607	0.236	0.372

3.1.2. Compactibility of Powder Materials

The compactibility or tensile strength, σ_0 , at zero compact porosity and other model parameters along with the coefficient of determination, R^2 , values calculated using Leuenberger equation (Eq. 28), Ryshkewitch-Duckworth equation (Eq. 29) and percolation model (Eq. 40) are summarized in Table 6. Although the compactibility or tensile strength, σ_{tmax} , at zero compact porosity obtained from the three equations for all four materials vary, carbamazepine demonstrated the lowest compactibility among all the materials confirming its poor compactibility (Table 6).

The compression susceptibility of the powder materials assessed using Leuenberger equation (Figure 16) exhibited microcrystalline cellulose to have the highest compression susceptibility of all materials due to its high plasticity, and croscarmellose sodium yielded the highest value of tensile strength, σ_{tmax} , at zero porosity or $\rho_r \rightarrow 1$ followed by microcrystalline cellulose indicating high compactibility while crospovidone and carbamazepine exhibited relatively low compactibility (Table 6). Similarly, croscarmellose sodium demonstrated the highest compactibility or tensile strength, σ_{tmax} , at zero porosity determined by Ryshkewitch-Duckworth equation (Figure 17), followed by crospovidone, microcrystalline cellulose, and carbamazepine (Table 6). Whereas, tensile strength, σ_0 , at zero porosity determined using percolation model (Eq. 40) by plotting tensile strength vs. normalized relative density of compact (Figure 18) demonstrated croscarmellose sodium to have the highest compactibility followed by crospovidone, microcrystalline cellulose, and carbamazepine (Table 6). A comparative evaluation of the three models to assess compactibility of the powder materials demonstrates percolation model (Eq. 40) to yield results with higher values of coefficient of determination ($R^2 = 0.9861 \pm 0.015$) with lower

standard deviation compared to Ryshkewitch-Duckworth equation (Eq. 29) ($R^2 = 0.9708 \pm 0.021$) and Leuenberger equation (Eq. 28) ($R^2 = 0.9432 \pm 0.066$) (Figure 19).

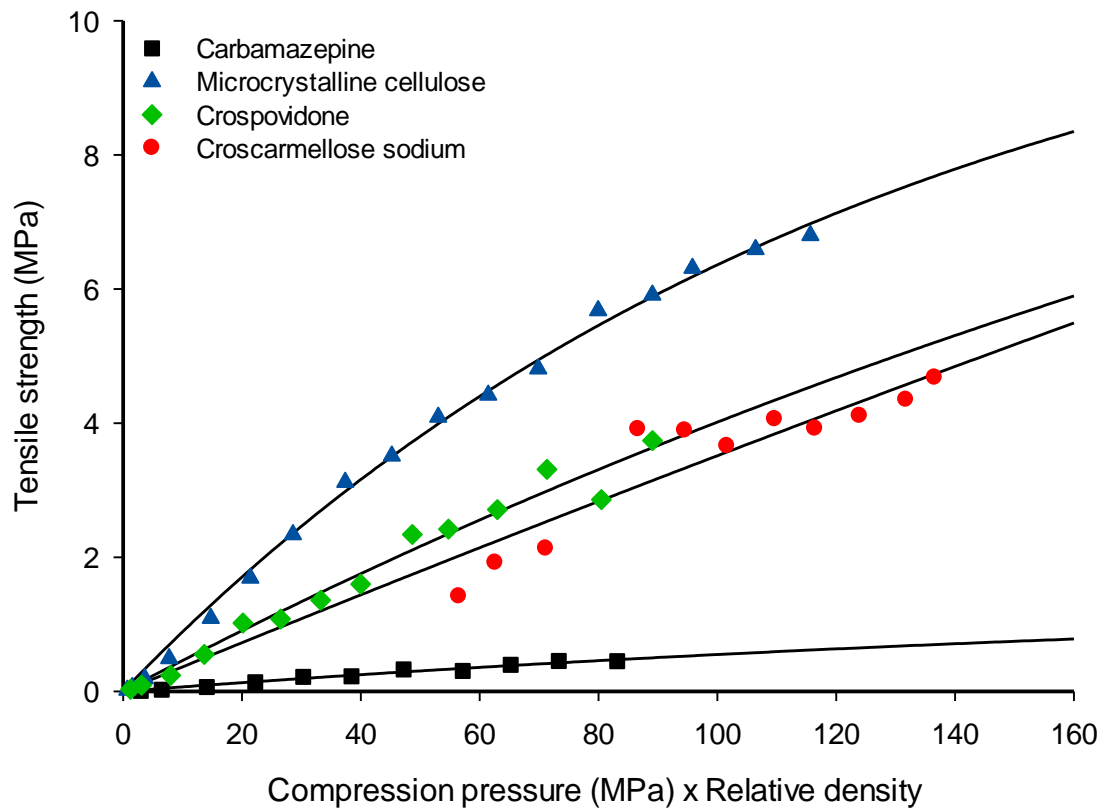


Figure 16: Plot of tensile strength vs. product of compression load and relative density of compacts according to Leuenberger equation (Eq. 28)

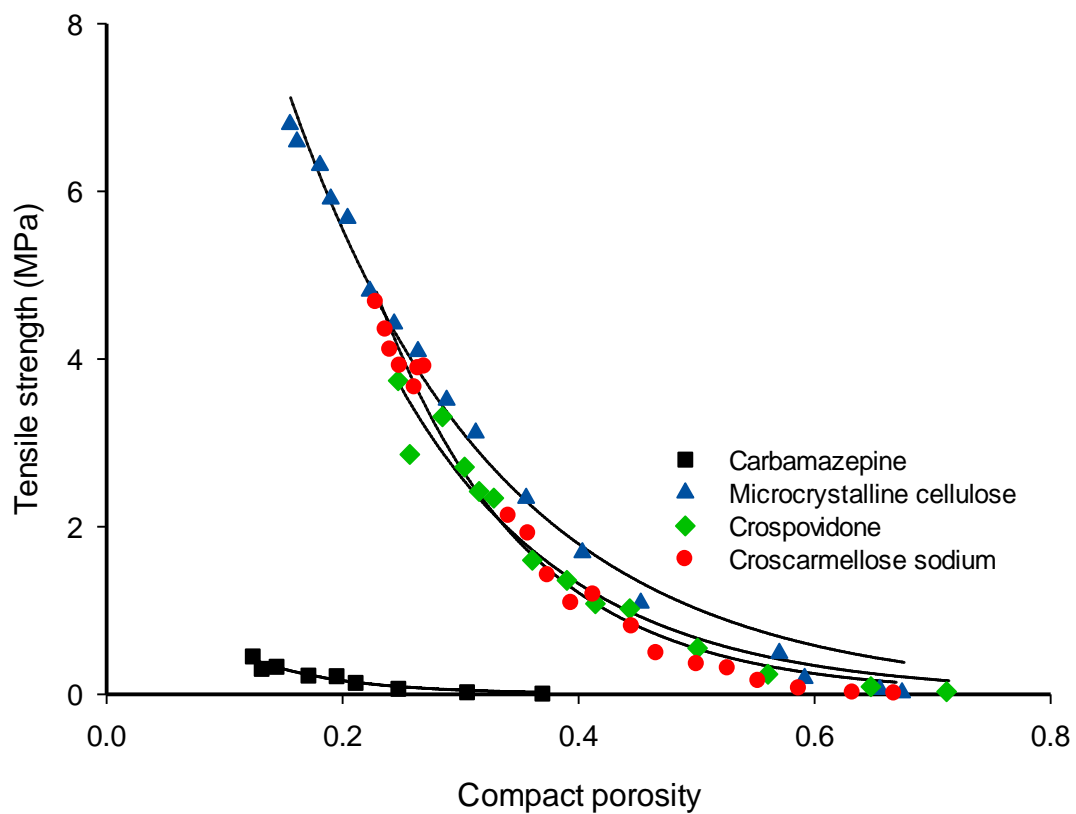


Figure 17: Plot of tensile strength vs. porosity of compacts according to Ryshkewitch

Duckworth equation (Eq. 29)

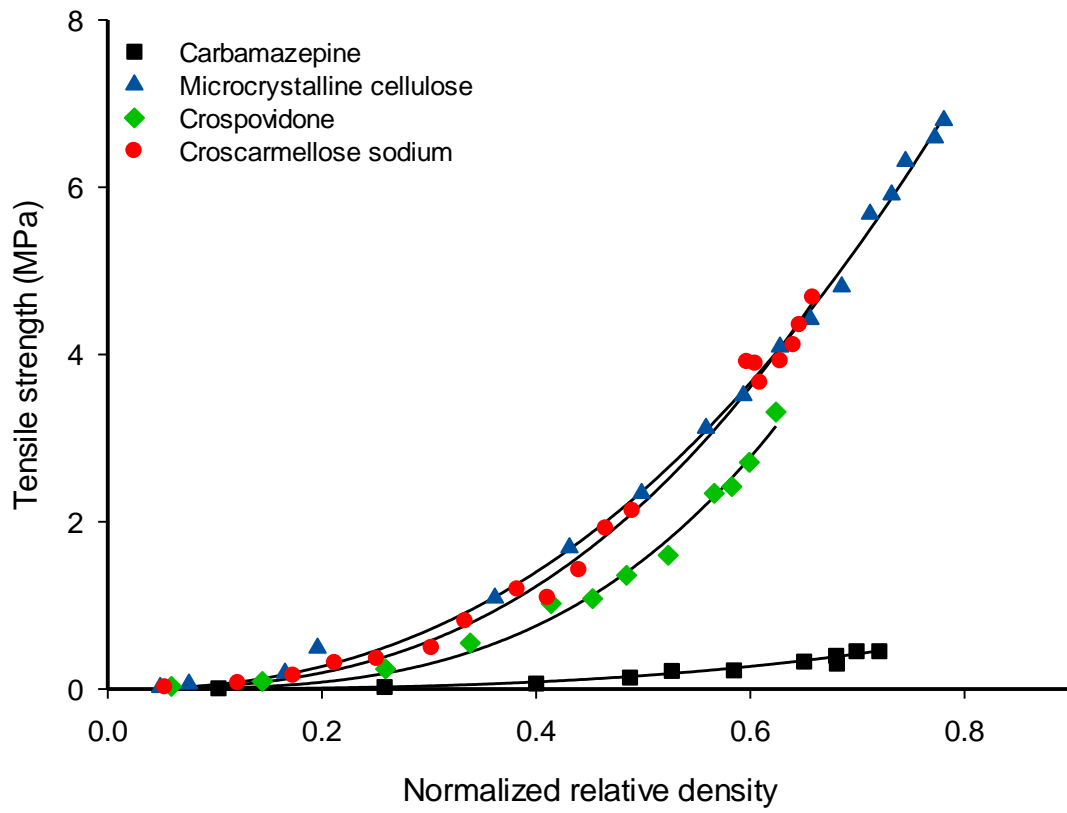


Figure 18: Plot of tensile strength vs. normalized relative density of compacts according to Percolation model (Eq. 40).

Table 6: Values of compactibility parameters determined using Leuenberger equation (Eq. 28), Ryshkewitch Duckworth equation (Eq. 29) and Percolation model (Eq. 40).

Material	Leuenberger Equation (Eq. 28)			Ryshkewitch Duckworth Equation (Eq. 29)			Power Law Equation (Eq. 40)		
	Tensile strength at zero porosity, σ_0 , (MPa)	Compression susceptibility, $\gamma \times 10^{-3}$ (MPa ⁻¹)	R ²	Tensile strength at zero porosity, σ_0 , (MPa)	Bonding propensity, b	R ²	Tensile strength at zero porosity, σ_0 , (MPa)	Critical exponent, q	R ²
Carbamazepine	1.55	4.4	0.9522	1.94	12.54	0.9454	1.18	2.96	0.9633
Microcrystalline cellulose	11.60	7.9	0.9971	17.17	5.67	0.9901	12.26	2.33	0.9979
Crospovidone	7.39	3.1	0.9759	19.93	6.81	0.9614	14.25	3.20	0.9900
Croscarmellose sodium	47.02	0.8	0.8478	30.20	8.06	0.9865	15.96	2.65	0.9933

Another model parameter of interest in Ryshkewitch-Duckworth equation which has widely been studied and reported is bonding capacity, b , of powder materials. Bonding capacity, b , can be defined as the bonding property or consolidation behavior of primary particles of the powder material. Thus a higher value of bonding capacity, b , suggests stronger bonding of primary particles (99). Of the four powder materials used in the present study, carbamazepine demonstrated highest bonding capacity, b , followed by croscarmellose sodium, crospovidone and microcrystalline cellulose (Table 6). From these results, one will assume that carbamazepine that has the highest value of bonding capacity, b , would be a highly compactible material. In contrast, carbamazepine demonstrated the lowest compactibility ($\sigma_0 = 1.94$ MPa) of all materials (Table 6). A similar contrast between bonding capacity and compactibility of powder materials was reported by Zuurman *et al.* (100) who studied the effect of magnesium stearate on materials with varying consolidation properties using Ryshkewitch-Duckworth equation. Thus the values of bonding capacity, b , calculated using Ryshkewitch-Duckworth equation may not provide correct assessment of the consolidation behavior of powder materials. In addition, the values of compactibility parameters determined by Ryshkewitch-Duckworth equation were relatively higher compared to those yielded by percolation model (Table 6). Patel and Bansal (99) too obtained higher values of compactibility of powder materials from Ryshkewitch-Duckworth equation compared to the power law equation. This may be attributed to the assumption of the first-order relationship between tensile strength and compact porosity by Ryshkewitch-Duckworth equation resulting in an overestimation of compactibility of powder materials when extrapolating the data to zero porosity (Table 6).

However, percolation model (Eq. 40) does not suffer from this mathematical limitation of overestimation since it uses lower threshold or bond percolation threshold, ρ_{cb} , for normalization of the relative density of the compact, and therefore can calculate the compactibility of powder material with better accuracy (54). Thus, based on the above results, it can be concluded that percolation model (Eq. 40) is a better model to determine the compactibility parameter of powder materials that yields results with higher R^2 values compared to Ryshkewitch-Duckworth and Leuenberger models. This confirms the validity of our third hypothesis of the present study.

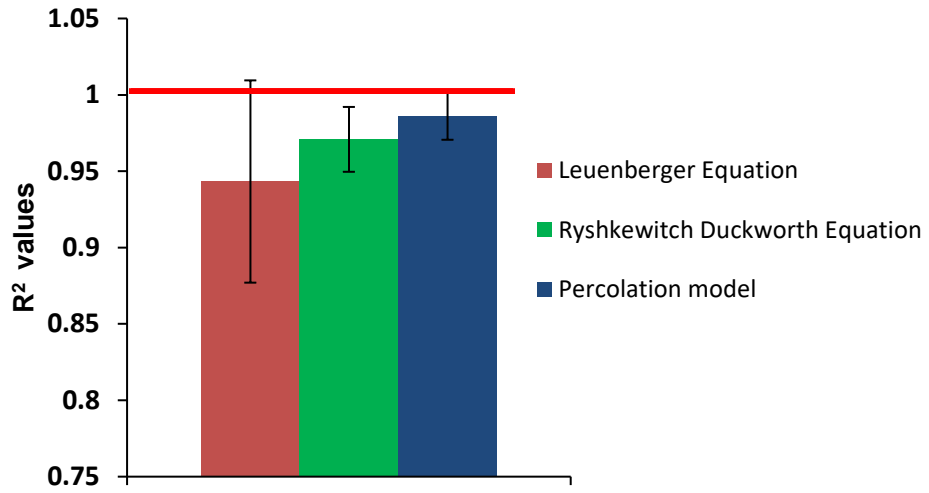


Figure 19: R^2 values along with standard deviation determined by Leuenberger equation (Eq. 28), Ryshkewitch Duckworth equation (Eq. 29) and percolation model (Eq. 40). The red line indicates reference line of $R^2 = 1$

One of the important aspects of percolation theory is the determination of the value of critical exponent, q . The critical exponent in power law equation is assumed to be universal and depends on Euclidean or fractal dimensions (43). The determination of value of critical exponent, q , to assess powder compaction has been topic of interest in percolation theory since its introduction in pharmaceutical development (58). Kuentz and Leuenberger (58) suggested that the value of critical exponent correlating tensile strength with relative density of the compact should be close to the theoretical value of 2.70. However, Kuentz and Leuenberger (58) experimentally found average value of the critical exponent, q , using the power-law equation for various grades of microcrystalline cellulose to be 3.2 ± 0.1 which was higher than the theoretically predicted value of 2.70 (58). The authors attributed this deviation to the anisomorphous shape of the particles, anisotropy of the compact as well as the broad distribution of macroscopic properties causing deviation of the measured values of critical exponent from the theoretical value of the critical exponent of 2.70. Van Veen *et al.* (73) too have reported the value of the critical exponent, q , for sodium chloride and pregelatinized starch as 2.45 and 2.92, respectively. In the present study, the value of the critical exponent, q , for all four powder materials using percolation model (Eq. 40) was found to be as low as 2.33 for microcrystalline cellulose and as high as 3.20 for crospovidone (Table 6). Thus, values of the calculated critical exponent, q , obtained for the four powder materials studied were very close to the values reported in the literature (58, 73). This confirms the application and validity of power-law equation (Eq. 40) to determine compactibility of powder materials and value of the critical

exponent, q , to assess the curvature of the plot of tensile strength as a function of relative density of the compact.

3.1.3. Compactibility of Binary Mixtures

In the present study, of the four investigated materials, carbamazepine yielded the highest value of site percolation threshold (Table 4). Even at a high relative density (>0.85), carbamazepine yielded compacts of low mechanical strength (~ 0.45 MPa) (Figures 20 - 22) that leads to the conclusion that it is a poorly compactable material. The poor compactibility of carbamazepine has also been reported by Nakhodchi *et al.* (98). In the present study, another hypothesis was to improve compactibility of poorly compactable material by combining with it a well compactable material in accordance with percolation phenomenon. Therefore, to validate this hypothesis, three sets of binary mixtures were prepared consisting of poorly compactable material, i.e. carbamazepine, with well compactable materials, i.e. microcrystalline cellulose, crospovidone and croscarmellose sodium. Since these binary mixtures were composed of powder components of dissimilar deformation characteristics, two different segments each dominated by properties of individual powder component in the binary mixture can be anticipated. The tensile strength data of compacts of various volumetric fractions (v/v) of carbamazepine with microcrystalline cellulose, croscarmellose sodium and crospovidone have been plotted in Figures 20 - 22.

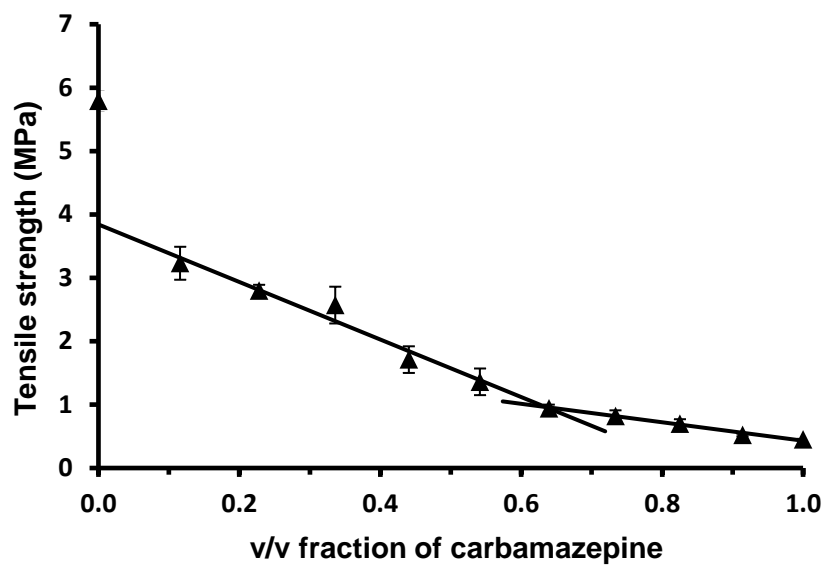


Figure 20: Tensile strength of compacts of carbamazepine and microcrystalline cellulose binary mixtures with increasing volume fraction of carbamazepine

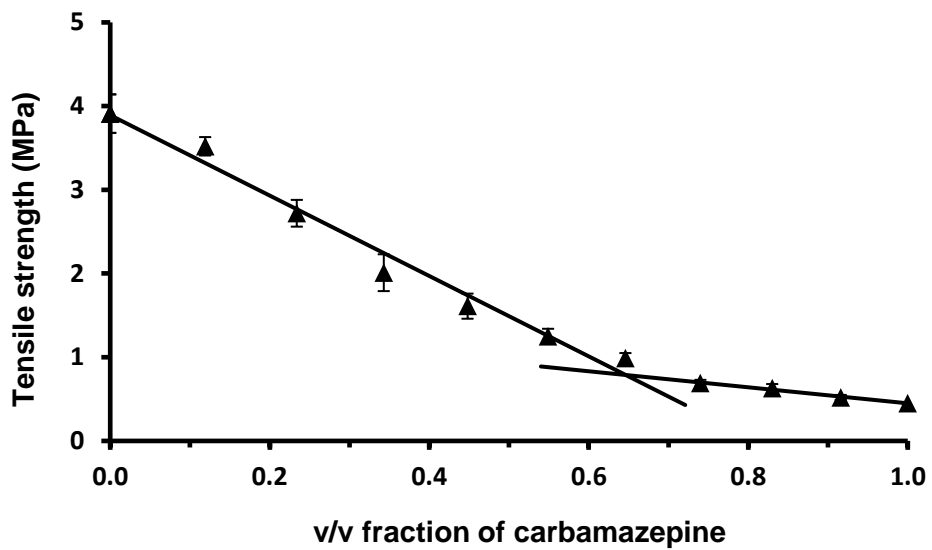


Figure 21: Tensile strength of compacts of carbamazepine and croscarmellose sodium binary mixtures with increasing volume fraction of carbamazepine

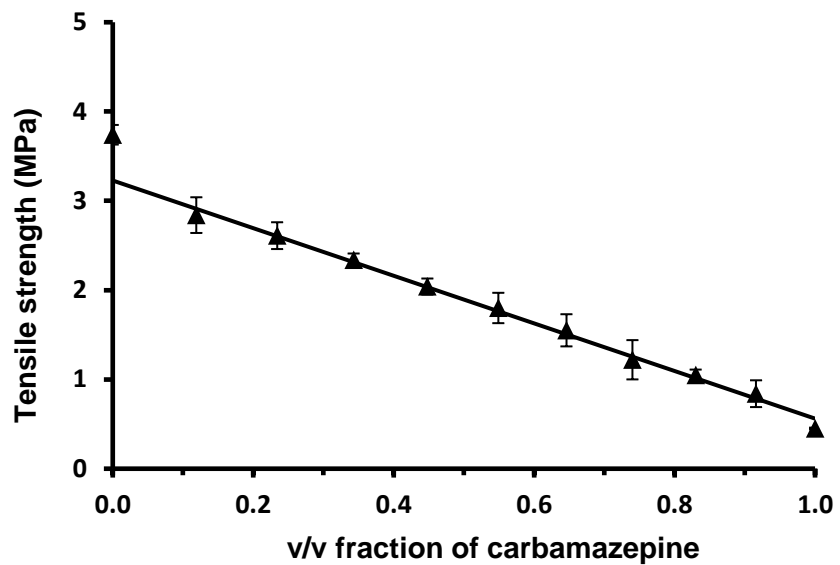


Figure 22: Tensile strength of compacts of carbamazepine and crosprovidone binary mixtures with increasing volume fraction of carbamazepine

It can be observed that there is an increase in the tensile strength of compacts of binary mixtures with increasing volumetric ratio of microcrystalline cellulose, crospovidone and croscarmellose sodium in the powder blend. However, the volumetric ratio at which these three well compactable powder materials start to dominate the tensile strength of the compacts in the binary mixture differs from one material to another. For example, in binary mixtures of carbamazepine and microcrystalline cellulose, two distinct linear segments can be seen (Figure 20). The first linear segment (1.0 - 0.64 v/v carbamazepine) is where tensile strength of the compacts is apparently, and almost entirely, dominated by carbamazepine exhibiting low tensile strength; the second linear segment (0.36 -1.0 v/v microcrystalline cellulose) shows rapid increase in tensile strength of compacts indicating progressive dominance of microcrystalline cellulose resulting in higher tensile strength of the compacts. These two linear segments of dominating fractions of carbamazepine and microcrystalline cellulose in the binary mixture can be explained on the basis of fundamentals of percolation phenomenon. At a higher proportion of carbamazepine ($v > 0.64$ v/v) in the powder blend, microcrystalline cellulose particles exist as isolated clusters. However, with an increase in the proportion of microcrystalline cellulose, at a critical concentration ($v \cong 0.36$ v/v), an infinite cluster of microcrystalline cellulose particles begins to form that spans the entire system. Above this critical concentration, the compactibility of binary mixture is dominated by an infinite cluster of microcrystalline cellulose particles. Assuming that in the binary mixtures of carbamazepine and microcrystalline cellulose, the contribution of carbamazepine to the mechanical strength of the compacts is negligible, carbamazepine particles can be

hypothesized as pore components present in the continuous phase of microcrystalline cellulose (34). As discussed in the earlier section, bond percolation threshold of a powder material characterizes the threshold of particles when in contact with each other; with an increase in compression pressure, an infinite cluster of particles is formed. Thus, the dominant volumetric fraction of microcrystalline cellulose can be compared with its bond percolation threshold, ρ_{cb} , above which microcrystalline cellulose particles develop contact with each other. Although, at the dominant volumetric fraction of microcrystalline cellulose, isolated clusters of carbamazepine still exist in the binary system. With further increase in the proportion of microcrystalline cellulose in the binary mixture, an infinite cluster of microcrystalline cellulose particles is formed and clusters of carbamazepine particles decline. This can be expected at the site percolation threshold of microcrystalline cellulose, ρ_{cs} , where maximum sites in the binary system are occupied by microcrystalline cellulose particles at the expense of carbamazepine particles (41). As seen in Figure 20, the proportion of dominating volumetric fraction of microcrystalline cellulose (~ 0.36 v/v) in the binary mixture is in close agreement with the value of bond percolation threshold of microcrystalline cellulose calculated using Heckel equation ($\rho_{cb} = 0.299$) (Table 4). Mohammed *et al.* (101) too have reported that at or above 0.39 v/v fraction, microcrystalline cellulose dominated the tensile strength of binary mixtures consisting of paracetamol and microcrystalline cellulose. Similarly, two linear segments can also be observed in binary mixtures of carbamazepine and croscarmellose sodium where croscarmellose sodium starts dominating tensile strength of compacts at and above approximately 0.35 v/v fraction (Figure 21) that is close to its calculated bond percolation

threshold ($\rho_{cb} = 0.334$) (Table 4). This confirms the validity of our fourth hypothesis that understanding of bond and site percolation thresholds of individual powder components in a binary and multicomponent system can help in improving the compaction properties of powder blend consisting of a poorly compactable drug by using an appropriate proportion of a well compactable excipient. Additionally, prior knowledge of percolation threshold of excipients can also be helpful in estimating the dilution capacity of excipients and their dominating behavior in binary and multicomponent mixtures for the development of robust directly compressible tablet formulations (34). In contrast, a linear increase in tensile strength of compacts with decreasing volumetric ratio of carbamazepine was observed in case of binary mixtures of carbamazepine with crospovidone (Figure 22) making it difficult to interpret the critical volumetric fraction of crospovidone in the binary mixture. This could possibly be due to lower bond and site percolation thresholds of crospovidone (Table 4) due to which it spans the binary mixture lattice even at low concentration thereby making it difficult to obtain two distinct linear segments of compactibility in the binary mixture where one component dominates the other.

3.1.4. Chapter Summary

The compression and compaction of powder materials is a complex phenomenon that is influenced by many factors, especially their physiochemical and mechanical properties. The process becomes even more complex when two or more powders, especially of dissimilar deformation behavior, are blended in the formulation which is almost always the case in tablet dosage formulations. It is therefore difficult to assess the

compression and compaction phenomenon of powder materials by a single approach or a mathematical relationship. In the present study, the fundamentals of percolation phenomenon were applied to understand the compression and compaction behavior of pharmaceutical powders and their blends. Four hypotheses to study and apply fundamentals of percolation phenomenon to understand compression and compaction behavior of pharmaceutical powders are proposed that are successfully validated in the present study. Based on these hypotheses, it was observed that transition of powder bed to mechanically stable compact involves bond and site percolation phenomena depending on the existence of an isolated and infinite cluster of powder material. It was also observed that the comparative evaluation of values of bond and site percolation thresholds of powder materials was helpful in the interpretation of their compression characteristics or deformation behavior. Further, it was found that power law equation considering the normalized relative density of compact was able to determine the compactibility and consolidation behavior of powder materials with higher R^2 values compared to the classical theories of powder compaction. The value of critical exponent, q , defining power law relationship between tensile strength and normalized relative density of compact was found to range between 2.33 and 3.20 for the four powder materials. Based on the compaction study of three sets of binary mixtures of carbamazepine with microcrystalline cellulose, croscarmellose sodium and crospovidone, it was also observed that understanding of percolation phenomenon can be helpful in determining the behavior of individual component in binary and multicomponent powder mixtures, suggesting its relevance for the selection of type and amount of excipient needed for successful formulation

development of tablet dosage forms. Thus it can be concluded that comprehensive application of percolation phenomenon in the study of compaction behavior of pharmaceutical powders is helpful in understanding the complexity of disordered pharmaceutical powders and their multicomponent mixtures.

3.2. Chapter II: Compaction Behavior of Disordered Binary Powder Mixtures

Till now, the application of percolation theory has been limited to the estimation of percolation threshold of various powder materials in pharmaceutical formulations. In the present study, the application of percolation theory is extended further to determine the compactibility of individual components and complex binary mixtures. To determine the compactibility of individual components and their binary mixtures, a normalized relative density concept was used based on the study of Holman and Leuenberger (21). This normalization of relative density is based on the concept of effective medium approximation discussed in the methodology section. One of the reasons to use the concept of normalized relative density and the effective medium approximation is that although the classical theories are able to estimate the compactibility of single components, they largely fail to estimate the compactibility of mixtures of two or more components. As the successful implementation of quality by design (QbD) tools depends largely on the understanding of material properties, an early understanding of these complex mixtures can be helpful in establishing a robust design space. For this purpose, an attempt has been made to understand and evaluate compaction behavior of single-components powders and their binary mixtures using percolation model. An attempt has also been made to assess the compactibility of the binary mixture with increasing volume fraction of well compactable material (microcrystalline cellulose and crospovidone) in the binary mixture. To assess the performance and efficiency of percolation model (Eq. 40) over the established classical theories, Ryshkewitch-Duckworth model (Eq. 29) as well as its derived linear (Eq. 30) and power mixing rule (Eq. 31) were used.

3.2.1 Percolation threshold and compactibility of single components

In order to study the relationship between tensile strength and relative density of the compacts of single powder components, the power law equation (Eq. 5) was used. The computations were performed by assuming two different values of the critical exponent, q ; in the first case, the value of q was > 0 , and in the second case, the value was fixed at 2.7. The calculated values of percolation model parameters have been summarized in Table 7.

The computations based on assuming the value of the critical exponent, $q > 0$, yielded a large difference in the value of percolation threshold, ρ_c , among the single powder components, i.e. carbamazepine, microcrystalline cellulose and crospovidone. Also, the values of the critical exponent, q , with a large error of fit was found particularly for carbamazepine ($q = 3.55$). Kuentz and Leuenberger too have reported the value of the critical exponent, q , for microcrystalline cellulose to be 3.2 ± 0.1 which is higher than the value theoretically predicted by Guyon *et al.* of 2.7 (58). However, in the present study, it was found that calculated value of critical exponent, q , for microcrystalline cellulose (2.79) was much closer to the theoretically predicted value of 2.7 with an excellent fit ($R^2 = 0.9982$); the value of critical exponent, q , for crospovidone was found to be (2.20).

Table 7: Percolation model parameters of the single components determined by assuming $q > 0$ and $q = 2.7$ using Eq. 5.

Material	Values of parameters obtained assuming value of $q > 0$						Values of parameters obtained assuming value of $q = 2.7$				
	S	q	ρ_c	R^2	Adj. R^2	RSS	S	ρ_c	R^2	Adj. R^2	RSS
Carbamazepine	19.69	3.55	0.539	0.9550	0.9422	0.001	13.94	0.606	0.9548	0.9491	0.009
Microcrystalline cellulose	25.21	2.79	0.216	0.9982	0.9979	0.171	25.85	0.232	0.9982	0.9980	0.171
Crospovidone	23.32	2.21	0.317	0.9747	0.9707	0.589	21.98	0.244	0.9750	0.9727	0.583

In the second case, assuming the value of the critical exponent, $q = 2.7$, the tensile strength vs. relative density relationship yielded almost similar value of R^2 values. Thus, based on higher Adj. R^2 values and the lower residual sum of squares (RSS) values, it can be observed that assumption of the value of the critical exponent, $q = 2.7$ is a better approach in determining the relationship between tensile strength vs. relative density of the compact using power law equation (Eq. 5). This is due to the absence of a possible flip-flop effect between the value of percolation threshold, ρ_c , and that of the critical exponent, q , when the value of critical exponent was assumed constant ($q = 2.7$) in the second case. As the better value of goodness of fit with the lower error was obtained with the value of $q = 2.7$, this value was used for subsequent computations to determine compactibility parameter or tensile strength, σ_0 , of the single powder components at zero porosity using Eq. 40. In our previous study, we reported that the value of the percolation threshold, ρ_c , can be used to characterize the compaction behavior of powder materials (74). It was observed that lower the value of percolation threshold, ρ_c , lower would be the relative density required to form a mechanically stable compact. In Table 7, it can be seen that carbamazepine shows the highest value of percolation threshold ($\rho_c = 0.606$) among the three powder materials studied while microcrystalline cellulose and crospovidone show lower and almost similar values of percolation threshold. Thus based on percolation threshold values, it can be inferred that carbamazepine is poorly compactable material compared to microcrystalline cellulose and crospovidone. This observation is in line with that reported in the literature. Moreover, the value of percolation threshold, ρ_c , obtained for microcrystalline cellulose ($\rho_c = 0.232$) by assuming the value of $q = 2.7$, was similar to the threshold values reported by Kuentz and Leuenberger ($\rho_c = 0.211$) that was calculated

by inverse exponent plot for tensile strength vs. relative density data (34). This confirms the validity of our approach in the present study.

Further, compactibility parameter or tensile strength at zero porosity, σ_0 , for the three powder materials was calculated using percolation model (Eq. 40) assuming the value of $q = 2.7$ (Figure 23). In addition, the values of compactibility parameter of powder materials were also calculated using Ryshkewitch-Duckworth model (Eq. 29) (Figure 24). The values of compactibility parameter of powder materials calculated by both the models have been summarized in Table 8. By percolation model (Eq. 40), it was found that carbamazepine has lowest compactibility ($\sigma_0 = 1.13$ MPa) followed by crospovidone ($\sigma_0 = 10.26$) and microcrystalline cellulose ($\sigma_0 = 12.66$). Similarly, values of compactibility parameter, σ_0 , yielded by Ryshkewitch-Duckworth model also confirm carbamazepine having poor compactibility ($\sigma_0 = 1.94$) followed by microcrystalline cellulose ($\sigma_0 = 17.17$) and crospovidone ($\sigma_0 = 19.93$). A comparative evaluation of both the models reveals that values of compactibility parameter, σ_0 , computed using Ryshkewitch-Duckworth model (Eq. 29) shows higher values of the compactibility parameter compared to the percolation model (Eq. 40). Patel and Bansal (99) too have reported higher values of compactibility parameter of powder materials from Ryshkewitch-Duckworth equation compared to the power law equation. This may be attributed to the assumption of the first-order relationship between tensile strength and compact porosity by Ryshkewitch-Duckworth equation resulting in an overestimation of the values of compactibility parameter of powder materials when extrapolating the tensile strength of the compacts at zero porosity (Table 8). However, percolation model (Eq. 40) does not suffer from this mathematical overestimation since the relative density values of compacts were normalized. A

comparative evaluation of the two models reveals a better fit by percolation model (Eq. 40) with higher R^2 and adj. R^2 values and the lower values of the residual sum of squares (RSS) compared with the Ryshkewitch-Duckworth model (Table 8). This confirms that compaction behavior of powder materials can be illustrated much better by percolation model (Eq. 40) with higher accuracy and goodness of fit.

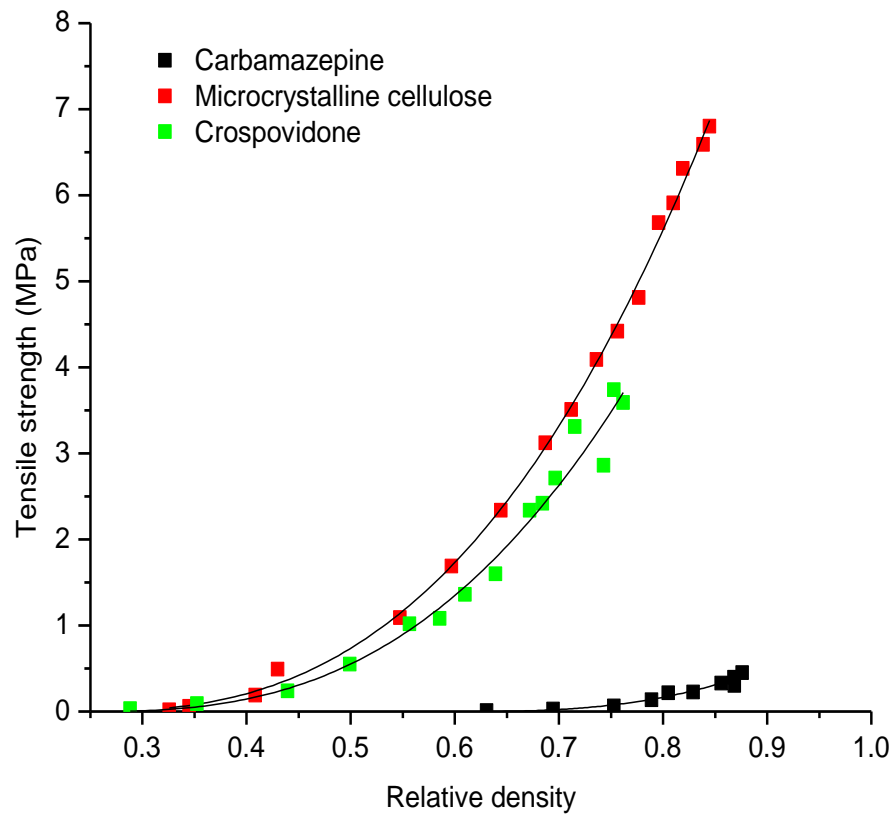


Figure 23: Compactibility of carbamazepine, microcrystalline cellulose and crospovidone using percolation model (Eq. 40)

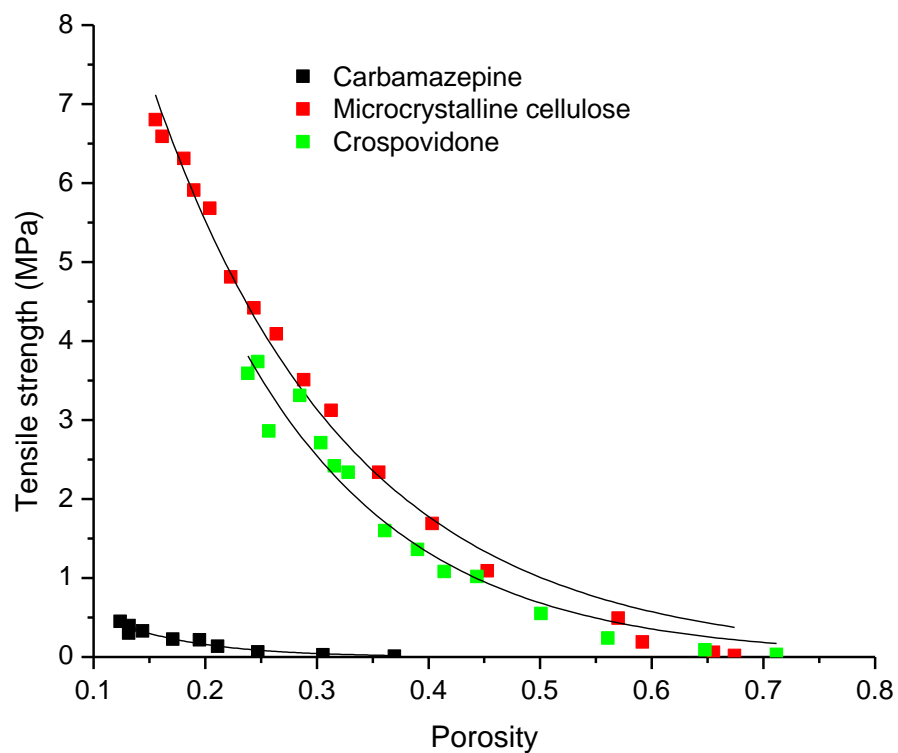


Figure 24: Plot of tensile strength of compacts as a function of compact porosity for determination of compactibility parameter of carbamazepine, microcrystalline cellulose and crospovidone according to Ryshkewitch-Duckworth model (Eq. 29)

Table 8: Values of parameters of single component powders determined using percolation model (Eq. 40) and Ryshkewitch-Duckworth model (Eq. 29).

Material	Percolation model (Eq. 40)					Ryshkewitch-Duckworth model (Eq. 29)				
	σ_0	ρ_c	R^2	Adj. R^2	RSS	σ_0	b	R^2	Adj. R^2	RSS
Carbamazepine	1.13	0.606	0.9548	0.9491	0.009	1.94	12.54	0.9454	0.9463	0.010
Microcrystalline cellulose	12.66	0.232	0.9982	0.9980	0.171	17.17	5.67	0.9901	0.9894	0.947
Crospovidone	10.26	0.244	0.9750	0.9727	0.583	19.93	6.81	0.9614	0.9611	0.840

3.2.2. Percolation threshold of binary mixtures

As discussed in the previous section, calculation of percolation threshold, ρ_c , by assuming the value of the critical exponent, $q = 2.7$, was found to be a better approach, therefore percolation threshold, ρ_c , of binary mixtures was computed using Eq. 40 assuming the value of $q = 2.7$. The results of computation of percolation threshold, ρ_{cm} , of both the binary mixtures, i.e. carbamazepine-microcrystalline cellulose and carbamazepine-crospovidone, with increasing mass fraction of well compactable material along with the R^2 values have been summarized in Table 9. An excellent fit with a higher coefficient of determination ($R^2 > 0.99$) was obtained by percolation model (Eq. 40). From Table 9, it can be observed that with increasing mass fraction of well compactable material in the binary mixture, there was a decrease in the value of percolation threshold, ρ_c , for both binary mixtures. For instance, the percolation threshold of a binary mixture of carbamazepine and microcrystalline cellulose, at a concentration of 10% w/w of microcrystalline cellulose, the percolation threshold was the highest ($\rho_{cm} = 0.640$) (Table 9). With an increase in the concentration of microcrystalline cellulose in the powder blend, the effect of poor compaction properties of carbamazepine starts to diminish due to the formation of clusters of microcrystalline cellulose, and percolation threshold lowers and shifts towards the value of microcrystalline cellulose. As the concentration of microcrystalline cellulose in the powder blend increases, the compaction property of the powder blend is increasingly dominated by microcrystalline cellulose. A similar behavior was in the case of binary mixtures of carbamazepine and crospovidone. To illustrate this hypothesis, the values of percolation threshold, ρ_c , of both sets of binary mixtures calculated using Eq. 40 are plotted against volume fraction of well compactable material

(Figs. 25A and 25B). As seen in Figures 25A and 25B, a linear relationship is observed between the percolation threshold, ρ_{cm} , of the binary mixture with increasing volume fraction of microcrystalline cellulose or crospovidone in the binary mixture. This relationship between the percolation threshold of binary mixtures, ρ_{cm} , and volume fraction of well compactable material in the powder blend can be represented by the following equation:

$$\rho_{cm} = \rho_{cA}V_A + \rho_{cB}V_B \quad (46)$$

Where ρ_{cm} is the percolation threshold of the binary mixture; v_A and v_B are the volume fraction of component A (microcrystalline cellulose or crospovidone) and component B (carbamazepine), ρ_{cA} , and ρ_{cB} are the percolation threshold of component A (microcrystalline cellulose or crospovidone) and component B (carbamazepine) in the binary mixture, respectively. Kuentz and Leuenberger too have reported a similar linear relationship for binary mixtures of paracetamol and microcrystalline cellulose (60). However, the authors reported a lower range of validity of a linear relationship (up to 30% of microcrystalline cellulose). In the present study, Eq. 14 was found to be valid for all mass fractions of microcrystalline cellulose or crospovidone in the binary mixtures. Also, the R^2 values obtained for the plot of percolation threshold vs. v/v fraction were 0.9884 and 0.9844 for carbamazepine-microcrystalline cellulose and carbamazepine-crospovidone binary mixtures, respectively (Figs. 25A and 25B). An excellent linearity between percolation threshold, ρ_{cm} , vs. volume fraction of the well compactable material, i.e. microcrystalline cellulose and crospovidone, in the binary mixtures suggests that these materials systematically overtake the mechanical strength of compacts of a binary system. Further, based on the established linear relationship (Eq. 46), percolation threshold of

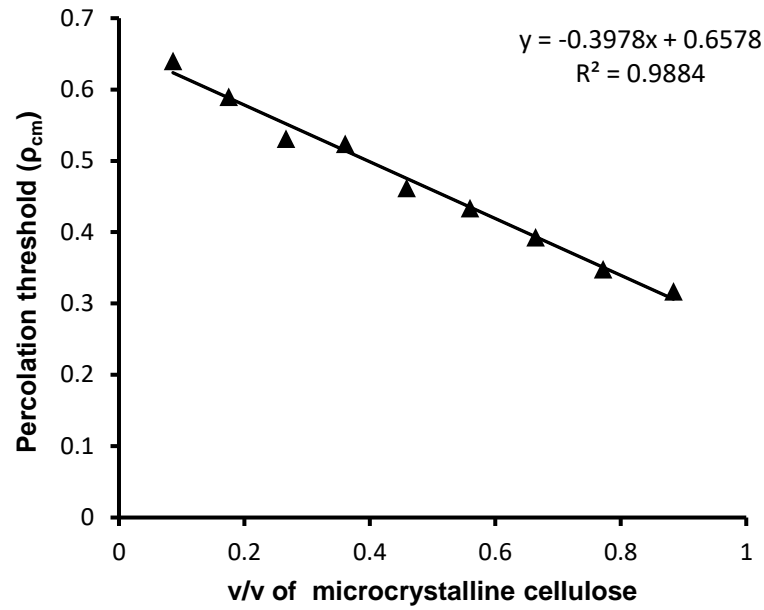
single component at a volume fraction of 1 (100% w/w) can also be predicted. As tablet formulation constitute of drug and excipients in different volume fractions, knowledge of individual percolation threshold of single-component powder materials can be helpful in predicting the threshold of powder mixtures from Eq. 46. This will help in a better design of tablet formulation and thus concentration of drug or excipient in the vicinity of percolation threshold can be avoided. This will be helpful in the robust formulation development of tablet dosage forms. The values of percolation threshold of carbamazepine and microcrystalline cellulose using Eq. 46 were found to be 0.657 and 0.260, respectively. This is in close agreement with the value of percolation threshold calculated using power law equation for individual components assuming the value of the critical exponent, $q = 2.7$ (Table 8); the calculated values of percolation threshold for carbamazepine and crospovidone from carbamazepine-crospovidone binary mixtures were found to be 0.602 and 0.199, respectively. An interesting observation worth highlighting over here is the difference in the predicted value of the percolation threshold of carbamazepine in both the binary mixtures. This could be attributed to the difference in the particle size and true density of microcrystalline cellulose and crospovidone (Table 5). However, given the complexity of powder systems, the predicted value of the percolation threshold is satisfactory and is closer to the values of percolation threshold calculated using Eq. 5.

Table 9: Values of compactibility parameter and percolation threshold of binary mixtures determined using percolation model

(Eq. 40) assuming the value of the critical exponent, $q = 2.7$.

Carbamazepine and Microcrystalline cellulose				Carbamazepine and Crospovidone			
Microcrystalline cellulose (% w/w)	σ_{0m}	ρ_{cm}	R^2	Crospovidone (% w/w)	σ_{0m}	ρ_{cm}	R^2
10	2.10	0.640	0.9982	10	1.33	0.543	0.9647
20	2.19	0.590	0.9953	20	1.77	0.522	0.9845
30	3.00	0.531	0.9901	30	2.74	0.469	0.9847
40	3.37	0.524	0.9986	40	3.89	0.446	0.9959
50	4.37	0.462	0.9956	50	4.13	0.363	0.9895
60	5.67	0.434	0.9989	60	5.06	0.336	0.9852
70	7.79	0.393	0.9981	70	7.34	0.359	0.9948
80	9.01	0.348	0.9966	80	7.84	0.288	0.9845
90	10.39	0.317	0.9994	90	8.43	0.228	0.9967

(A)



(B)

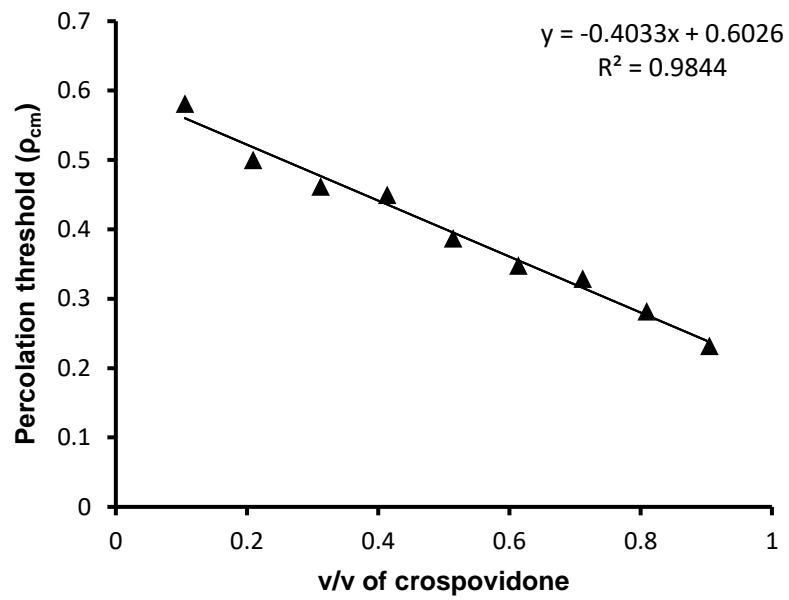


Figure 25: Relationship between estimated percolation thresholds (ρ_{cm}) with increasing volume fraction of well compactable material in binary mixtures (A) v/v of microcrystalline cellulose, (B) v/v of crospovidone.

3.2.3. Compactibility of binary mixtures

Percolation model

In the past several decades, many mathematical models have been proposed to analyze compressibility and compactibility of powders. While these models have worked well with single powder components, a model to assess the compactibility of binary mixtures has been challenging. Various reasons for the failure of a model that works very well for the single powder components but fails in the case of binary mixtures are discussed in detail in the introductory section. In the present study, after successfully analyzing the compactibility of single powder components, i.e. carbamazepine, microcrystalline cellulose and crospovidone, the percolation model was used to assess compactibility of the more complex binary disordered mixtures. The values of maximum tensile strength, σ_0 , computed using the concept of normalized relative density and assuming the value of critical exponent, $q = 2.7$ along with the R^2 values are summarized in Table 9. As expected, the compactibility of both sets of binary mixtures, i.e. carbamazepine-microcrystalline cellulose and carbamazepine-crospovidone, was observed to increase with an increase in the volume fraction of well compactable component, i.e. microcrystalline cellulose and crospovidone, due to dominance of poor compaction properties of carbamazepine by compaction properties of well compactible material, microcrystalline cellulose and crospovidone. To establish a relationship between compactibility of the binary mixture at each volume fraction, compactibility parameter or maximum tensile strength at zero porosity, σ_0 , vs. v/v fraction of well compactable material, i.e. microcrystalline cellulose and crospovidone, are plotted (Figure 26A and 26B). From Figure 26A and 26B, a linear relationship can be observed between compactibility parameter or maximum tensile

strength at zero porosity, σ_0 , vs. volume fraction of well compactable materials with R^2 value of 0.9609 and 0.9655 for microcrystalline cellulose and crospovidone, respectively. Thus an excellent linear fit between the compactibility parameter of binary mixture vs. volume fraction of powder component can be established in the present study. It is worth mentioning over here since a binary mixture of powder with different deformation behavior usually shows nonlinear relationships (16). However, with the application of percolation model (Eq. 40), the compactibility of binary mixtures at each volume fraction can be assessed more accurately from a simple linear relationship. Thus it can be concluded that the percolation model can simplify the study of compaction behavior of binary powder mixtures. Moreover, it can also be observed that no significant change in the compactibility of a binary mixture of carbamazepine and microcrystalline cellulose occurs until volume fraction, v , of microcrystalline cellulose in the binary mixture is equal to 0.266, i.e. 30% w/w of microcrystalline cellulose (Figure 26A). This volume fraction is close to value of percolation threshold, ρ_c , of microcrystalline cellulose ($\rho_c = 0.232$) determined using from Eq. 4 assuming the value of critical exponent, $q = 2.7$ (Table 7). Therefore, it can be called as a critical volume fraction of microcrystalline cellulose in the binary mixture for direct compression of carbamazepine and microcrystalline cellulose. Kuentz and Leuenberger have termed this as dilution potential or capacity of microcrystalline cellulose to form a stable compact for a binary mixture of paracetamol and microcrystalline cellulose (34). The dilution capacity of a tablet excipient can be called as the fraction of excipient at which it starts dominating the overall properties of the compact (34). Similarly, in the case of binary mixture of carbamazepine and crospovidone, the change in the compactibility of the

binary mixture occurs at a volume fraction of 0.209 that is closer to the calculated percolation threshold of crosopovidone ($\rho_c = 0.244$) (Figure 26B).

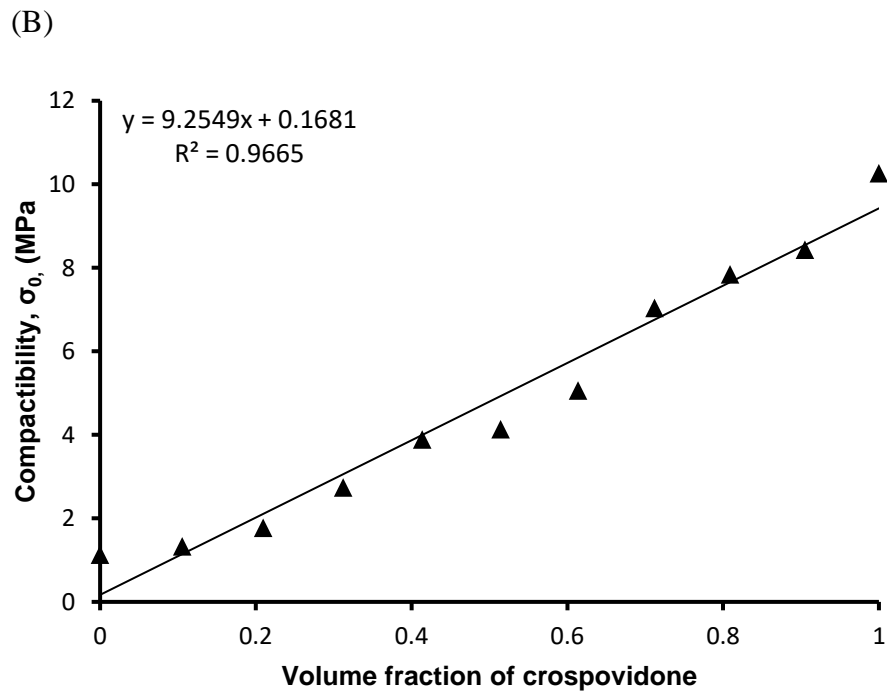
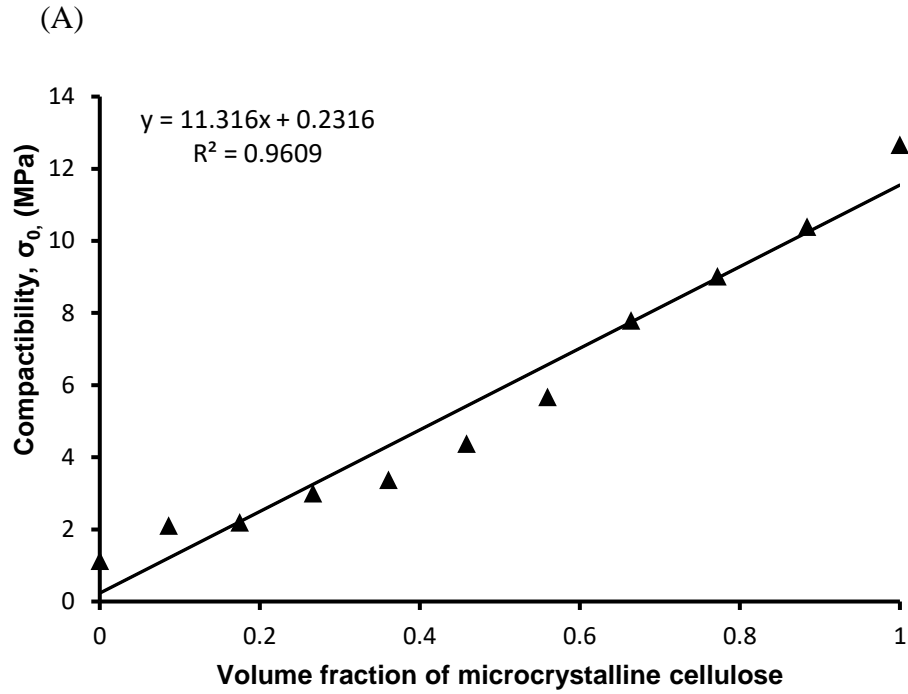


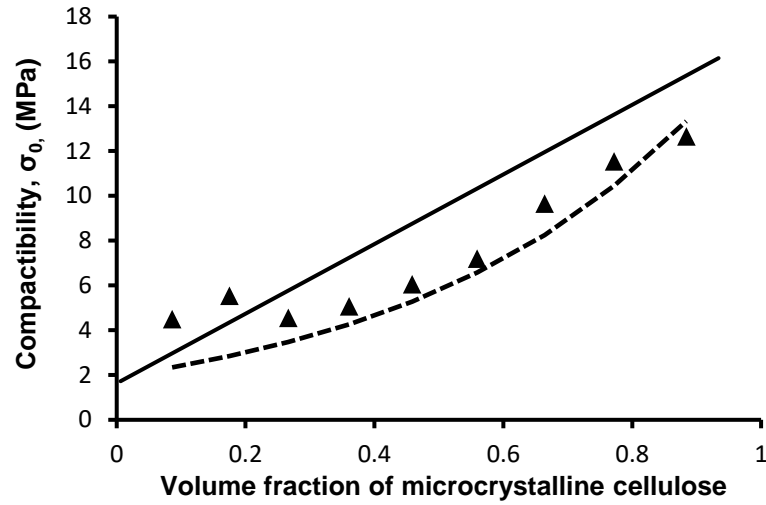
Figure 26: Maximum tensile strength at zero porosity or compactibility of binary mixture at each volume fraction of well compactable material as per Eq. 40. (A) v/v of microcrystalline cellulose, (B) v/v of crospovidone

Ryshkewitch-Duckworth model

The values of compactibility parameter or maximum tensile strength at zero porosity, σ_0 , of single-component powder materials computed using Ryshkewitch-Duckworth model (Eq. 29) are summarized in Table 8 along with the bonding propensity, b , of each powder material. Although bonding propensity, b , represents bonding properties of primary particles, its application to assess the mechanical properties of powder material has been largely unsuccessful, probably due to limitations of the exponential model. Therefore, the present study was focused largely on the determination of compactibility of powder material or maximum tensile strength at zero porosity, σ_0 , using Eq. 29 and its significance. Based on the compactibility parameter of single powder components (Table 8), an attempt was made to predict the compactibility, σ_{0m} , of binary mixtures using linear mixing model (Eq. 30) and power mixing model (Eq. 31) (59, 99). A comparative evaluation was performed between the compactibility parameters of the binary mixtures determined using Ryshkewitch-Duckworth model (Eq. 29), linear mixing model (Eq. 30) and power mixing model (Eq. 31). Figure 27A and 27B demonstrate that the values of compactibility parameter computed using Eq. 29 have a poor relationship with the volume fraction of well compactable material in the binary mixture. Moreover, a significant difference with poor correlation coefficient exists between the values of compactibility parameter computed using Eq. 29 and those obtained by using linear mixing model (Eq. 30) and power mixing model (Eq. 31) for both sets of binary mixtures, i.e. carbamazepine-microcrystalline cellulose and carbamazepine-crospovidone. A comparison of values of compactibility parameter calculated using Ryshkewitch-Duckworth model (Eq. 29) with those obtained by using linear mixing model (Eq. 30) and power mixing model (Eq. 31)

reveals that in the case of binary mixtures of carbamazepine-microcrystalline cellulose, the values of compactibility parameter have good correlation with that obtained from power mixing model ($R^2 = 0.9550$). Similar correlation between the values of compactibility parameter obtained using Ryshkewitch-Duckworth model and power mixing model has been reported by other authors too (33, 36, 99). However, in the case of binary mixtures of carbamazepine and crospovidone, a poor correlation was found between the values of compactibility parameter obtained using Ryshkewitch-Duckworth model and two mixing models (Fig. 27B). Thus, from the present study, it can be concluded that the classical compaction models, such as Ryshkewitch-Duckworth model (Eq. 29), and derived mixing models, such as linear and power mixing models, have limited application that depends on the types of powders as well as the experimental parameters (compression pressure, compact porosity) used (33). However, percolation model is more suitable for the assessment of compactibility of pharmaceutical powders and their mixtures and thus has wider application in pharmaceutical powder technology.

(A)



(B)

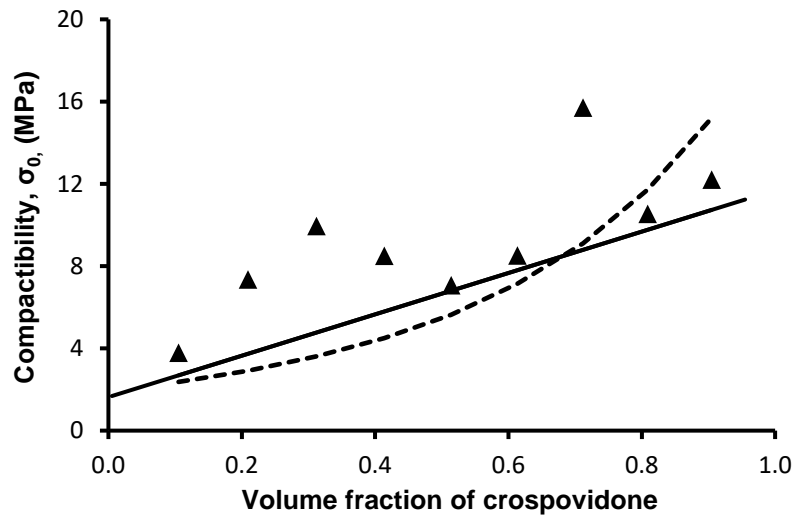


Figure 27: Plot of maximum tensile strength of compacts as a function of volume fraction of well compactible component in the binary mixture according to Ryshkewitch-Duckworth model (Eq. 29). The solid line represents compactivity parameter of binary mixture according to linear mixing model (Eq. 30) and dotted line represents compactivity parameter according to power mixing model (Eq. 31).

The failure of classical models, such as Ryshkewitch-Duckworth model, to assess the compactibility of binary mixtures may also be attributed to the failure of consideration of physical interaction between the powders in the binary mixture and thus neglecting the importance of interaction effect. In a simple binary mixture of two powder components, say A and B, three types of interactions are possible at almost every volume fraction. These can be given as A-A only, B-B only and A-B interaction. The magnitude of these three types of interactions largely depends on the volume fraction of the two components, i.e. A and B. The kind of interaction that dominates the system is affected by variables, such as mechanical properties of powder components, pressure used to make tablets, compact porosity etc., that determine bonding affinity and contacts between powder particles. Since the magnitude of interaction between particles varies with a change in the compression pressure and volume fraction of powders, it is difficult to assess the type of interaction. Thus to study the overall interaction effect, compactibility parameter or tensile strength at zero porosity, σ_0 , was used. Mathematically, the total mechanical strength of compacts of binary mixtures depends on the statistical weight of each powder component in the binary mixture that can be represented as follows (102).

$$\sigma_{0AB} = \sigma_0 v_A + \sigma_0 v_B + v_A * v_B * I \quad (47)$$

Where σ_{0AB} is compactibility parameter or tensile strength at zero porosity of binary mixture of component A and B, v_A and v_B are volume fraction of component A and B, σ_{0A} and σ_{0B} are the compactibility parameter or tensile strength at zero porosity of individual component A and B, and I is an interaction parameter that determines the magnitude of interaction or adhesive forces between component A and B. The deviation of the compactibility parameter of binary mixtures from Eq. 47 with complex nonlinear

relationship has been reported by many authors (34). In the present study also, the linear mixing rule derived from Ryshkewitch-Duckworth fails to assess the compactibility of binary mixtures accurately. One of the possible drawbacks of this additive rule is its failure to take into account the change in the deformation behavior of the binary mixture when two powder components are mixed together. Moreover, this additive rule doesn't take into account of differences in consolidation behavior, bonding propensity, attractive forces (cohesive and adhesive forces) of the constituent powder materials. In addition to these complexities factors, such as powder flowability and post-compression changes, e.g. elastic recovery, are also pertinent factors that exert significant effect on the mechanical properties of binary mixtures (36). Moreover, classical models fail to consider the adhesive forces between component A and B defined by interaction term, I , in Eq. 47. As a result, it is difficult for a simple mono-variate mathematical relationship to determine the mechanical properties of the compacts of disordered powder components. However, percolation model can be helpful in taking into account the interaction between powder components. Assuming a binary mixture of powder components A and B in a three-dimensional lattice, the particles of both powder components can percolate the system at the same time (41). This can be easily illustrated by a binary powder mixture consisting of components A (a well compactable material) and B (a poorly compactable material). At lower concentration of component A in the mixture, isolated clusters of its particles are formed which exist within a continuous phase of particles of component B. At a critical concentration of component A, it forms an infinite cluster percolating through the three-dimensional lattice. However, at the same time, the particles of component B also form an infinite cluster spanning the three-dimensional lattice. Evidently, if the particles of component A are

increased at the expense of particles of component B, percolation threshold or critical concentration of particles of component B still exists. This is in line with the interaction parameters A-A, B-B, and A-B defined in Eq. 47. If the ratio of particles of component B in the mixture is further reduced, it can form only an individual isolated cluster or multiple small clusters, and at this stage, only component A controls the mechanical properties of the powder mixture, such as compressibility and compactibility. Thus percolation model can systematically take into account level of interaction between powders of component A and B. The sequential interaction of particles of component A (a well compactable material) and B (a poorly compactable material) can also be visualized from Figures 26 and 27 of percolation threshold as well as compactibility of binary mixtures at each volume fraction of well compactable material (microcrystalline cellulose and crospovidone). A linear relationship between the percolation threshold and compactibility parameter of binary mixtures with the volume fraction of well compactable material demonstrates a systematic shift in the interaction of particles in binary mixtures (Figures 25-26)

3.2.4. Significance of Percolation model and its application in QbD

The formation of a tablet from a powder or powder blend is a complex and dynamic process. The mechanical properties of a single-component powder material when compressed into a tablet can be easily characterized using various mathematical models proposed in the literature. However, when two powders of different deformation behavior are mixed together, the assessment of compaction behavior becomes difficult. Along with the compression load applied and other material properties, the percolation threshold, ρ_c , is an important parameter that affects the compaction behavior of powder materials (14). Thus percolation threshold, ρ_c , is a critical material attribute (CMA) of powder materials

along with other micromeritics properties of powders and should be considered for the formulation development of solid dosage form. In the present study, the percolation model was able to successfully assess the percolation threshold and compactibility parameter of single-component powder materials as well as their binary mixtures. The knowledge of percolation threshold of single-component powder materials can be helpful in predicting the threshold of binary mixtures thus helpful in a better design of tablet formulation. Moreover, the linear relationship observed between compactibility parameter and volume fraction of well compactable material (microcrystalline cellulose and crospovidone) in the mixture (Figure 27A and 27B) can also be used to predict the compactibility parameter of each component in the binary mixture at any volume fraction. A typical tablet formulation is composed of multiple ingredients, among them drug and diluent form a major part (~90%) of the tablet formulation. During the early stage of drug development, where the amount of drug available is low and experimental determination of its mechanical behavior with diluents is limited, one can use Eq. 40 to predict the compactibility of drug and diluents. If the compactibility parameter of drug and diluent is known, one can easily predict the compactibility parameter of their mixtures at desired volume or weight fractions. Thus it can be used as material-sparing technique for the selection of the amount of excipients needed for the development of tablet formulation with desired CQAs. Moreover, since tablet formulations are multicomponent mixtures of powders with large differences in particle size, density, crystalline nature etc., it would be beneficial to use a single mathematical model to determine the mechanical properties of the tablet formulation. Earlier studies have reported that the compactibility of multicomponent mixtures can be determined using classical theories, such as Ryshkewitch-Duckworth

equation and derived mixing model (33, 36, 99). However, it is complex and time and material consuming since one should have prior knowledge of the compactibility parameter or tensile strength at zero porosity and other parameters of single-component powder materials to successfully assess the mechanical properties of binary mixtures. From the present study, it is clear that these mixing models are often specific to the type of powder materials used and may not have a universal application. However, from the present study, it can be concluded that the percolation model (Eq. 40) can serve as a single approach with a universal application to determine the compactibility parameter of powder materials as well as their binary mixtures. Thus in the current quality by design (QbD) approach, the percolation model can be used to successfully understand the compaction behavior of powder materials and the establishment of robust design space for the development of tablet formulation.

3.2.5. Chapter Summary

The present study is an attempt to understand the significance of percolation model in solid dosage forms. Although introduced in powder technology three decades ago, its application still remains limited. From the above studies, it can be concluded that percolation theory is a better tool than much established classical theories, such as Ryshkewitch-Duckworth model and its derived linear and power mixing models to assess compaction behavior of powder materials. The percolation threshold and compactibility parameter of binary mixtures show a linear relationship with increasing volume fraction of well compactable material in the powder blend. Thus percolation theory in combination with the concept of normalized relative density provides an idea of critical relative density and critical volume fraction of components which can be further explored to determine the

dilution capacity of pharmaceutical excipients. This can avoid long trial and error experimentation to obtain the desired mechanical properties of compacts. Moreover, it was found that the complex interaction between the drug and excipient particles in the binary mixture can be simplified and understood by application of percolation model. Thus percolation theory can serve as a single effective tool to understand the complexity of solid dosage forms and can be effectively used in the current quality by design (QbD) practice to establish robust design space.

3.3. Chapter III: Relationship between Mechanical Properties and Anisotropy of compact

Successful formation of tablet requires an understanding and analysis of fundamental steps involved in the compaction process. In pharmaceuticals, the quantitative definition of mechanical properties of tablets is usually assessed by determination of its tensile strength. Although, usually an indicator of mechanical properties of final compacts, tensile strength of compacts fails to give complete evaluation of material properties of powder materials (96). Thus in the present study, to understand powder densification and compaction behavior, analysis of Young's modulus, E , compressive strength, σ_c , in combination with tensile strength, σ_t , of two commonly used tablet diluents of dissimilar deformation behavior, i.e. microcrystalline cellulose (Avicel[®] PH 102) and lactose (FastFlo[®] 316) were determined.

Microcrystalline cellulose and lactose were compressed at several compression pressures to achieve wide range of compact porosities to study Young's modulus, compressive strength and tensile strength of compacts. Young's modulus, also known as elastic modulus, E , is a measure of the stiffness of a solid material defining relationship between stress (force per unit area) and strain (proportional deformation) in a material. Compressive strength of a material is peak value of uniaxial compressive stress-strain curve when the material fails completely (103). The advantage of Young's modulus and compressive strength over tensile strength is that it provides information about mechanical properties of compact under constant deformation rate. The experimental set up for determining elastic modulus, compressive strength and tensile strength of compact has been described in detail in methodology section.

3.3.1. Effect of Compression load on Elastic modulus, Compressive strength and Tensile strength

In tableting process, compression load is most critical process parameter that determines the final property of compact including the tableability, elastic modulus as well as other mechanical properties (2). In the present study too attempt was made to study the effect of compression load on mechanical properties of compact, such as elastic modulus, E , compressive strength, σ_{cs} , tensile strength, σ_t . It was found that with an increase in the compression load an increase in elastic modulus, compressive strength and tensile strength occurred in both materials, i.e. microcrystalline cellulose and lactose monohydrate (Figure 28-30). Due to increase in compression load, the particles come closer due to dissipation of pores and thus strengthen of particles occur which leads to increase in elastic modulus, compressive strength and tensile strength. Moreover, a linear relationship between elastic modulus and compression load can be observed in case of microcrystalline cellulose with correlation coefficient, R^2 values of 0.9944 (Figure 28). Similarly, a linear relationship can also be observed in case of lactose monohydrate too, however, the R^2 value was found to be relatively low ($R^2 = 0.9550$) (Figure 28).

The effect of increase in compression load was also studied on compressive strength as well as tensile strength of the compactss. From Figure 29A and 29B it can be observed that with an increase in compression pressure, increase in compressive strength as well as tensile strength occurred. However, microcrystalline cellulose exhibited higher compressive strength as well as tensile strength compared to lactose monohydrate owing to its higher compactible.

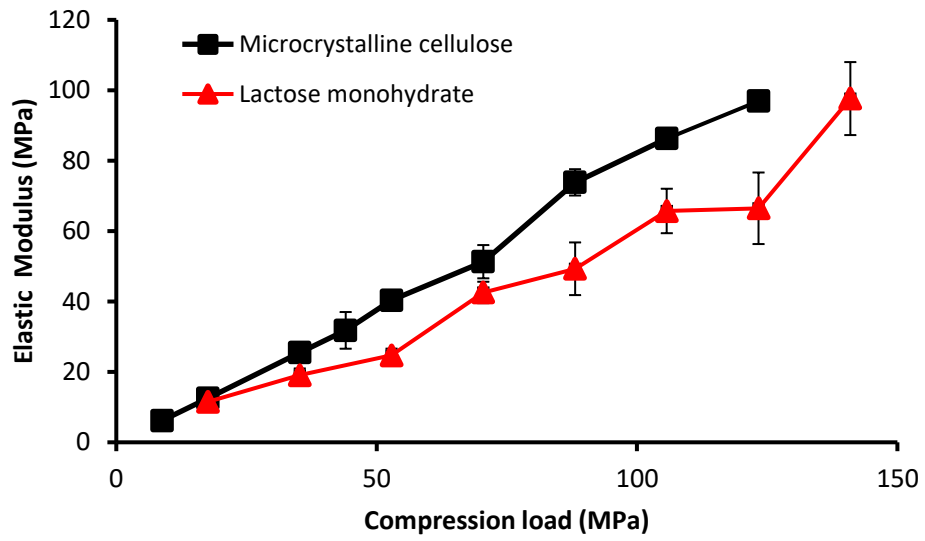
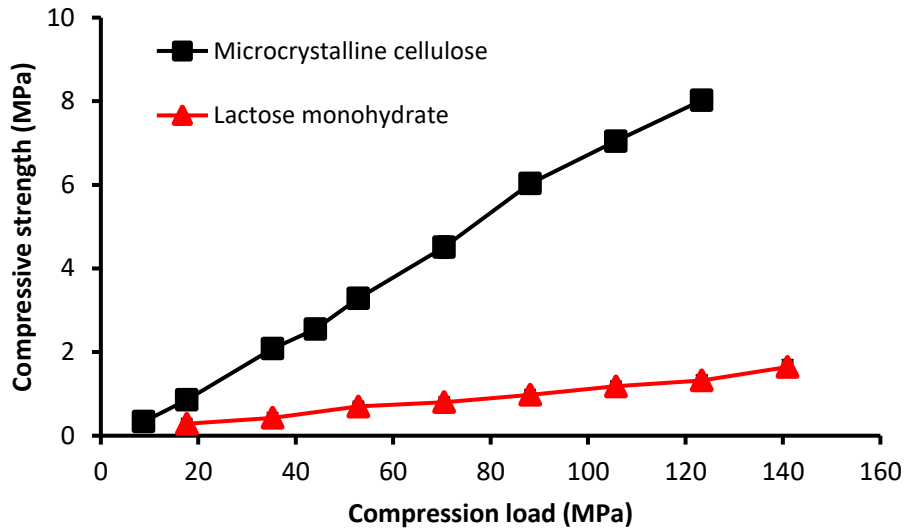


Figure 28: Effect of increasing compression load on elastic modulus of microcrystalline cellulose and lactose monohydrate

(A)



(B)

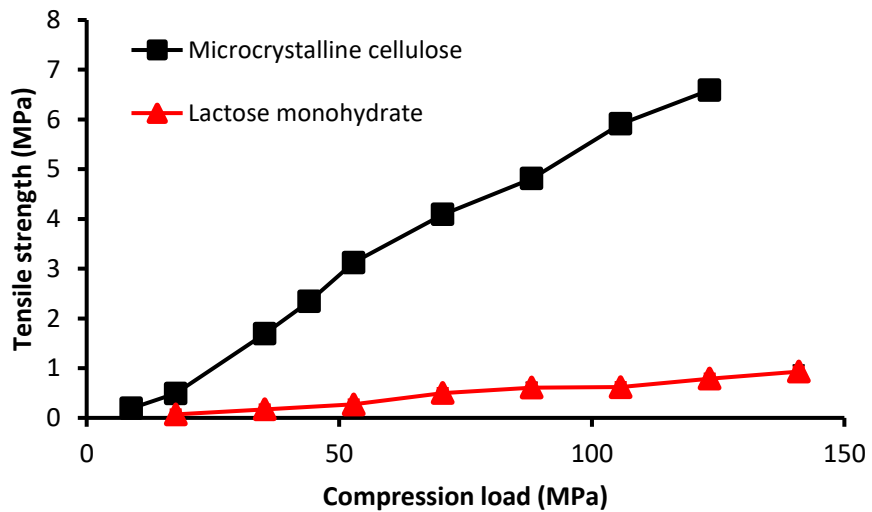


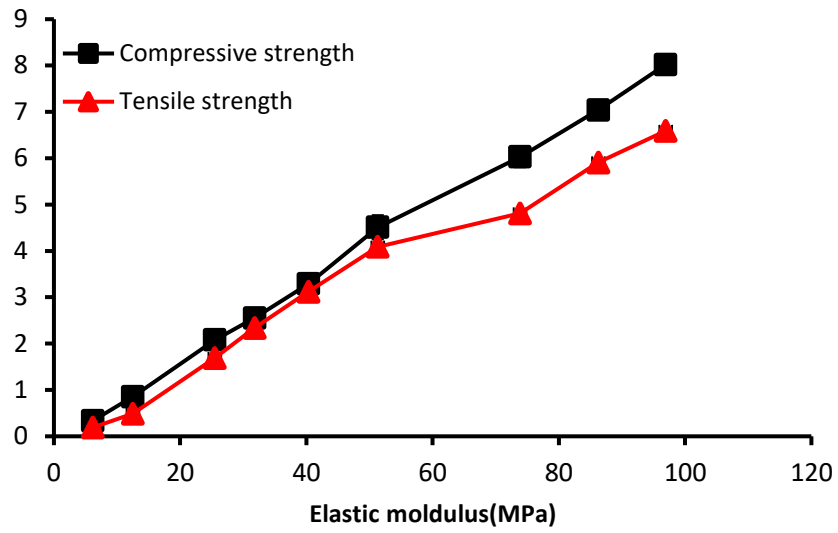
Figure 29: Effect of increasing compression load on mechanical strength of microcrystalline cellulose and lactose monohydrate. (A) Effect on compressive strength. (B) Effect on tensile strength

3.3.2. Establishing a relationship between mechanical properties

During the initial stage of formulation development of the product, not enough material is available to test all kinds of mechanical properties of compact. Thus all type of mechanical characterization is not possible in initial formulation development stage. Since complete understanding of mechanical properties for the development a robust tablet formulation is essential, an approach should be made to predict the mechanical property of materials from a single test (104). One of the most common practices of evaluating a mechanical property of a compact is its tensile strength. Since evaluation of other mechanical properties, such as Young's modulus, needs sophisticated material testing instrument, relatively simple experimental set up of analyzing tensile strength makes it more popular to analyze the mechanical properties of compacts (99). In the present study, three distinct mechanical properties of a compact (elastic modulus, compressive strength, tensile strength) of two different powder materials with dissimilar deformation behavior was studied. An attempt was made to correlate these mechanical properties of compacts in order to understand their relationship.

Figure 30A and 30B represents the relationship between elastic modulus with compressive strength and tensile strength of microcrystalline cellulose and lactose monohydrate. It was observed that there was a systematic increase in both compressive strength and tensile strength with increase in elastic moduli of powder materials. Thus one can predict elastic modulus from a simple experimental setup of tensile strength. Additionally, in the present study, since only two kinds of powders material with extremely dissimilar deformation behavior were used, this hypothesis can be applied to other kinds of powder materials too.

(A)



(B)

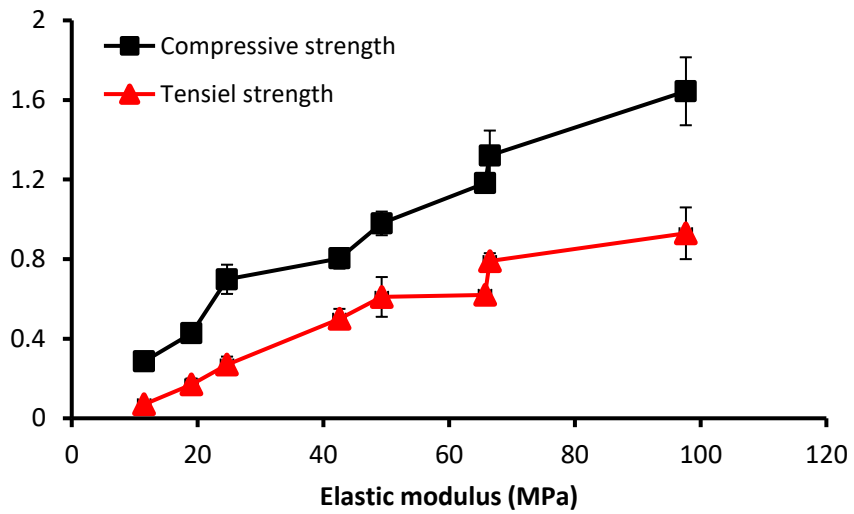
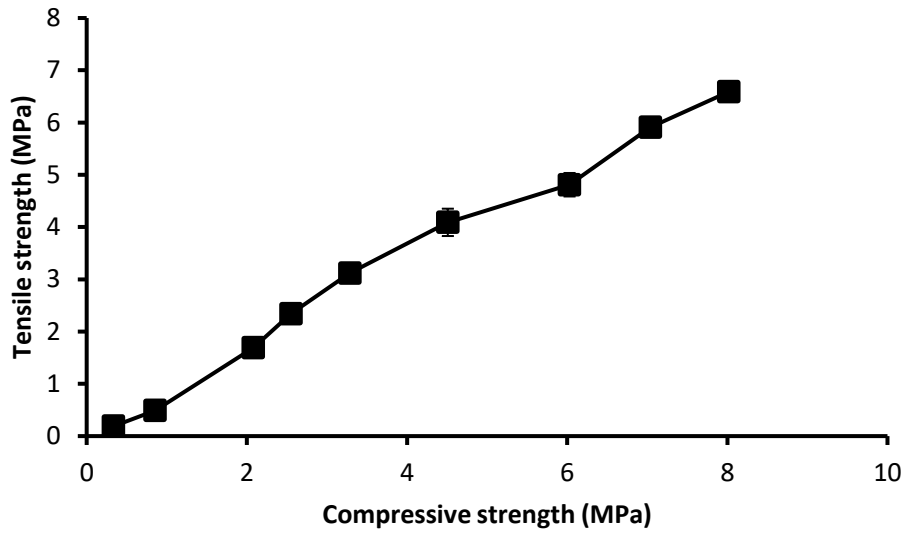


Figure 30: Relationship between elastic modulus with compressive strength and tensile strength (A) microcrystalline cellulose, (B) lactose monohydrate

One of the interesting aspects of the present study was two different types of compact strength, compressive strength as well as tensile strength of powder compact. As discussed in the methodology section, compressive strength was evaluated from stress-strain curve at the point where the axial failure of the tablets occurs whereas tensile strength of the tablets is radial failure of tablet. Thus a correlation between these two parameters can precisely define the overall mechanical strength of a tablet. Figure 31A and 31B illustrate the relationship between compressive strength and tensile strength for both microcrystalline cellulose and lactose monohydrate. It can be observed that microcrystalline cellulose shows higher degree of linear relationship between compressive strength and tensile strength whereas in case of lactose monohydrate, a poor correlation exists between compressive strength and tensile strength. This could be attributed to the anisotropy of lactose monohydrate since it undergoes fragmentation. Other authors too have reported the anisotropy of lactose monohydrate as well as other brittle material, i.e. dicalcium phosphate (104, 105). The fragmentation of brittle particles causes more anisotropy due to dissimilarity in particle sizes under load whereas in case of microcrystalline cellulose, particles undergo plastic deformation thus anisotropy is less.

(A)



(B)

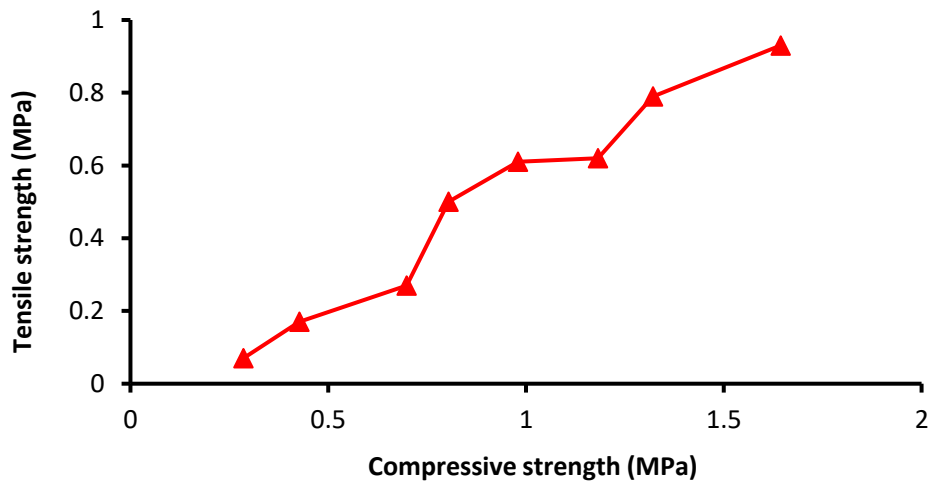


Figure 31: Relationship between compressive strength and tensile strength. (A) microcrystalline cellulose, (B) lactose monohydrate

3.3.3. Elastic modulus at zero porosity

Elastic deformation of the powder compact is a critical step involved in successful tableting. Thus tremendous effort has been dedicated to improve the understanding of interrelations between porosity, elasticity and strength of pharmaceutical tablets. Elasticity has been assessed either as fundamental material property referring to elastic modulus at zero porosity, E_0 , or as property of compacted material or radial recovery to a certain compaction state or porosity (106). Elastic modulus at zero porosity, E_0 , is indirectly determined for powders by extrapolation since the powder compact cannot be compressed at zero porosity. Furthermore, the size of the particles and their deformational behavior (elastic or plastic deformation and fragmentation) may affect both the size and the shape of pores in the compact. Various predictive equations have been proposed relating elastic deformation with porosity and different techniques (compressive or bending) have been applied for the determination of elastic deformation (107). The equations are either empirical or based on fundamental fluid mechanics but their applicability is restricted over a narrow, typically low, porosity range (108, 109). Thus, the adequacy of Young's modulus prediction is limited since the conditions of testing are not ideal (105).

In compressive tests, the loading and the measurement of deformation are unidirectional and therefore non-isotropic, while bending tests include application of both compressive and tensile stress (25, 106). In the present study, Young's modulus at zero porosity, E_0 , was computed using Sprigg's equation (Figure 32). The values of elastic modulus at zero porosity, E_0 , of single-component powder materials computed using Sprigg's model (Eq. 32) are summarized in Table 10 along with empirical constant, b , of each powder material. It can be observed that lactose monohydrate shows higher E_0 values

($E_0 = 604.97$ MPa) compared to microcrystalline cellulose ($E_0 = 251.27$ MPa) due to its fragmentative nature under pressure. Lactose monohydrate undergoes brittle fragmentation, thus particle breaks and form new binding strength whereas microcrystalline cellulose undergoes plastic deformation (110). It should be noted over here that the E_0 values determined in the present study are smaller compared to the values reported in the literature for both lactose monohydrate and microcrystalline cellulose. This is possibly due to the difference in the methodology applied. In the case of four-point or three-point bend test, the application of compressive load on the compact is usually determined by placing the sample on a rig, thus the compaction forces acting on the sample is different than the flat platen methodology applied in this study (104). Moreover, the shape and the size of the sample compact also plays an important role. For instance Sun *et al* reported the elastic modulus at zero porosity of microcrystalline cellulose ($E_0 = 5.1 \pm 0.2$ GPa) by using rectangular compact of 16.6×9.6 mm dimension (104). Whereas Rowe *et al.* reported the E_0 value of 9.19 GPa for microcrystalline cellulose when tested using four point beam bending test using load rate of 0.5 mm/min (25). Thus difference in the value of Young's modulus reported in the literature can be observed due to difference in the methodology studies. Thus it is advisable to select the methodology and evaluate the resultant elastic modulus data and its application carefully.

Another parameter of interest in Sprigg's model is empirical constant, b , which is related to the geometry of pore. It has been reported that values of $b = 2.7$ indicates spherical pores whereas value more than 4.4 indicates pores in the compact being oblate in shape (105). In the present study, the empirical constant, b , calculated by Sprigg's model was found to be 5.76 and 12.21 for microcrystalline cellulose and lactose monohydrate,

respectively. Although the value of b is higher than 4.4 indicating oblate shape of the pores, lactose monohydrate shows the value almost two times larger than microcrystalline cellulose (Table 10). The lower value of b of microcrystalline cellulose can be attributed to extensive elasto-plastic deformation followed by a significant degree of axial (visco-elastic) post compression recovery. A smaller degree of elastic recovery of the individual particles of microcrystalline cellulose may result in regaining the initial sphericity or shape isotropy of pores after the decompression, resulting in lower values of b . Whereas, in the case of lactose monohydrate the higher values of b could be due to the irregular shape of fragmented particles and inter-particle pores. Additionally, the change in the particle size caused by the brittle fracture upon compaction of lactose monohydrate also contributes to higher values of b . Thus it can be hypothesized that lactose monohydrate may contain interconnected pores as a result of the collapse of particle structures upon fragmentation. Similar higher values of empirical constant, b , for brittle materials have been reported by other authors too (25, 72, 104-106).

Percolation model

Leuneberger reported theoretical value of critical exponent, $q = 3.9$ for evaluation of the relationship between apparent Young's (elastic) modulus, E , vs. relative density, ρ_r (111). It was found that due to the absence of a possible flip-flop effect between the value of percolation threshold, ρ_c , and that of the critical exponent, q , the power law equation can predict the percolation threshold efficiently. Thus in the present study the elastic modulus at zero porosity, E_0 , of both the powder materials was computed using percolation model (Eq. 41) assuming value of critical exponent, $q = 3.9$ (Figure 33). The value of E_0 and percolation threshold, ρ_c , along with statistical fit has been summarized in Table 10.

As anticipated, lactose monohydrate shows higher value of elastic modulus ($E_0 = 335.30$ MPa) compared to microcrystalline cellulose ($E_0 = 197.40$ MPa) due to its brittle nature. A comparative evaluation of both the models reveals that values of elastic modulus, E_0 , computed using Sprigg's model (Eq. 32) shows higher values of E_0 compared to the percolation model (Eq. 41). This may be attributed to the assumption of the first-order relationship between elastic modulus and compact porosity by Spriggs equation resulting in higher values when extrapolating the data to zero porosity (108). Further, a comparative evaluation of the statistical fit between two models reveals a better fit by Sprigg's model (Eq. 32) with higher R^2 and adj. R^2 values and the lower values of the residual sum of squares (RSS) compared with the Percolation model (Table 10). This confirms that elastic deformation behavior of powder materials can be illustrated much better by exponential approximation of Sprigg's model (Eq. 32) with higher accuracy and goodness of fit.

Table 10: Values of parameters of single component powders determined using percolation model (Eq. 41) and Sprigg's model (Eq. 32).

Material	Percolation model (Eq. 41)					Sprigg's model (Eq. 32)				
	E_0	ρ_c	R^2	Adj. R^2	RSS	E_0	b	R^2	Adj. R^2	RSS
Microcrystalline cellulose	197.40	0.033	0.9883	0.9866	97.84	251.27	5.76	0.9930	0.9920	58.36
Lactose monohydrate	335.30	0.463	0.9452	0.9360	321.10	604.97	12.21	0.9581	0.9511	245.36

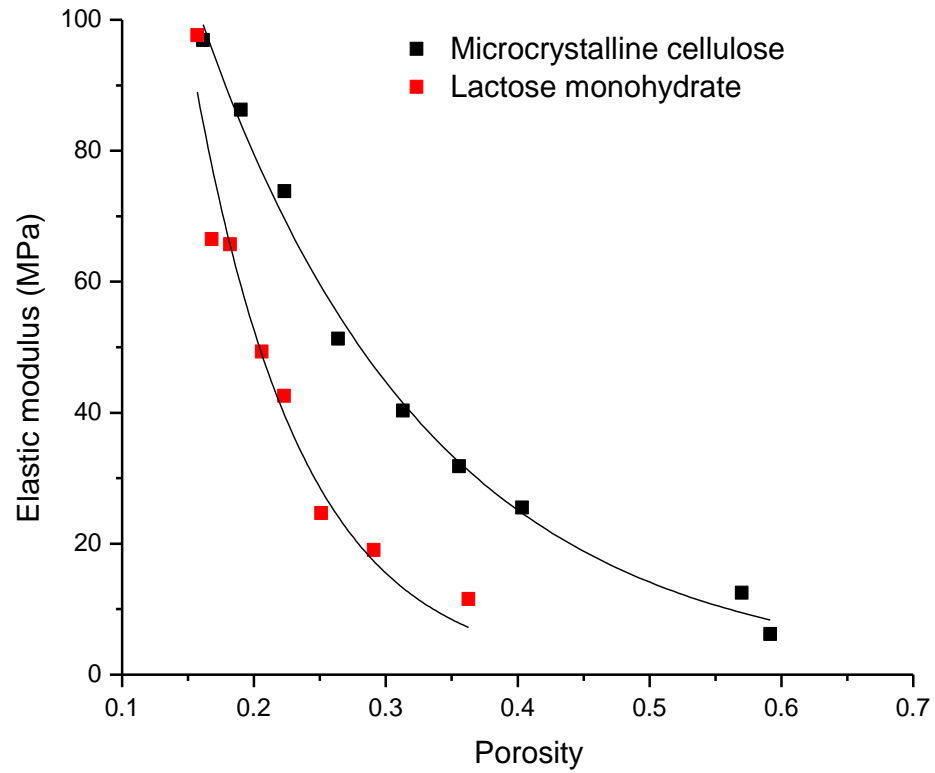


Figure 32: Effect of porosity on elastic modulus of microcrystalline cellulose and lactose monohydrate using Sprigg's equation (Eq. 32)

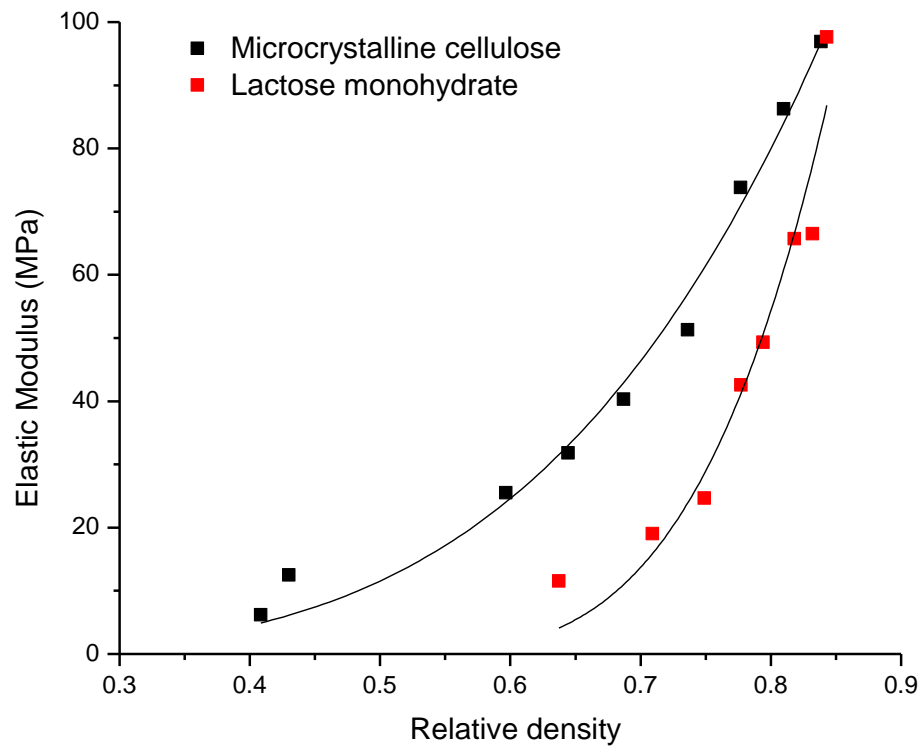


Figure 33: Effect of relative density on elastic modulus of microcrystalline cellulose and lactose monohydrate as per percolation model (Eq. 41)

3.3.4. Compressive strength and tensile strength at zero porosity

Compressive strength and tensile strength at zero porosity were computed by using Ryshkewitch Duckworth model (26). The data have been summarized in Table 11 and Table 12 along with the values of coefficient of determination and statistical parameters. It should be noted that both Sprigg's equation (Eq. 32) as well as Ryshkewitch Duckworth model (Eq. 29) is mathematically similar and is based on same exponential approximations. From Table 11, it can be observed that microcrystalline cellulose has highest compactibility compared to lactose monohydrate owing to its highly compactible nature.

In our previous study, percolation model was successfully applied to evaluate the compactibility of powder materials. Thus in the present study too, tensile strength and compressive strength at zero porosity was evaluated using percolation model assuming the value of $q = 2.7$. The compactibility of powder material was also evaluated using percolation model for both compressive strength and tensile strength by assuming value of critical exponent $q = 2.7$. The values of maximum tensile strength, σ_0 , computed using the concept of normalized relative density and assuming the value of critical exponent, $q = 2.7$ along with the R^2 values are summarized in Table 11 and Table 12. As expected, microcrystalline cellulose demonstrated higher compactibility by both mechanical strength (σ_0, σ_{cs0}) compared to lactose monohydrate due to its highly compactible nature. Moreover, it can be observed that percolation model shows superior fit in case of both the powder materials compared to Ryshkewitch-Duckworth model. Thus it can be inferred that assuming the value of critical exponent $q = 2.7$ can be used for predicting both mechanical strengths of tablet.

Table 11: Values of parameters of single component powders determined from compressive strength using percolation model (Eq. 42) and Ryshkewitch-Duckworth model (Eq. 29).

Material	Percolation model (Eq. 42)					Ryshkewitch Duckworth model (Eq. 29)				
	σ_{cs0}	ρ_c	R^2	Adj. R^2	RSS	σ_{cs0}	b	R^2	Adj. R^2	RSS
Microcrystalline cellulose	15.25	0.247	0.9914	0.9902	0.504	21.16	5.85	0.9952	0.9946	0.279
Lactose monohydrate	3.91	0.475	0.9655	0.9597	0.050	6.61	9.25	0.9832	0.9804	0.024

Table 12: Values of parameters of single component powders determined for tensile strength using percolation model (Eq. 40) and Ryshkewitch-Duckworth model (Eq. 29).

Material	Percolation model (Eq. 40)					Ryshkewitch Duckworth model (Eq. 29)				
	σ_0	ρ_c	R^2	Adj. R^2	RSS	σ_0	b	R^2	Adj. R^2	RSS
Microcrystalline cellulose	12.36	0.221	0.9984	0.9982	0.065	16.75	5.57	0.9906	0.9892	0.390
Lactose monohydrate	2.78	0.543	0.9715	0.9668	0.018	5.36	11.26	0.9683	0.9630	0.020

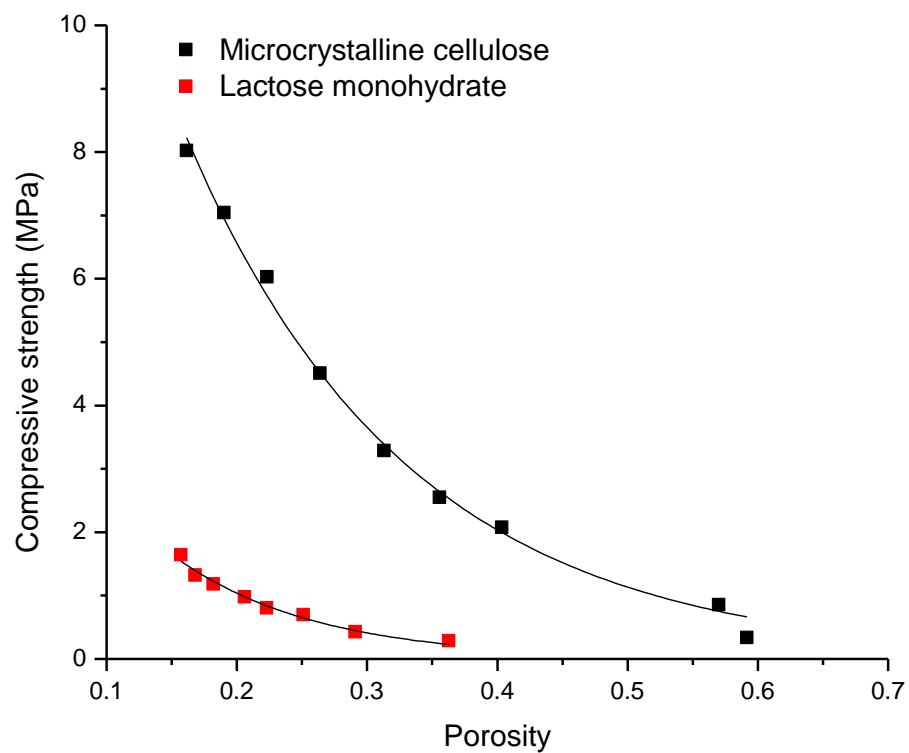


Figure 34: Effect of porosity on compressive strength of microcrystalline cellulose and lactose monohydrate using Ryshkewitch Duckworth equation (Eq.29)

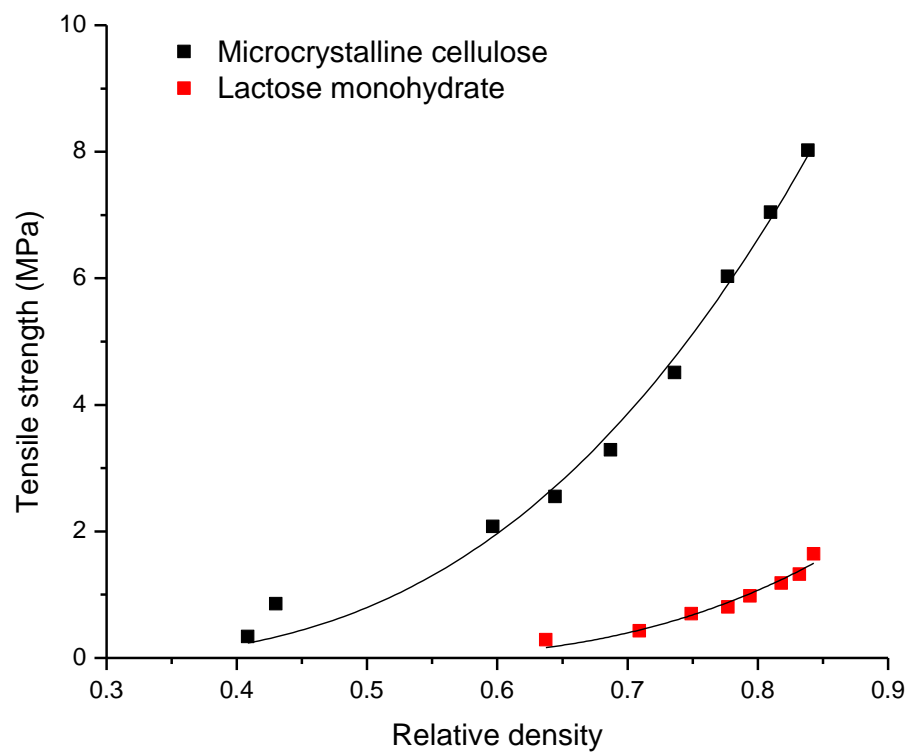


Figure 35: Effect of porosity on tensile strength of microcrystalline cellulose and lactose monohydrate using percolation model (Eq.40)

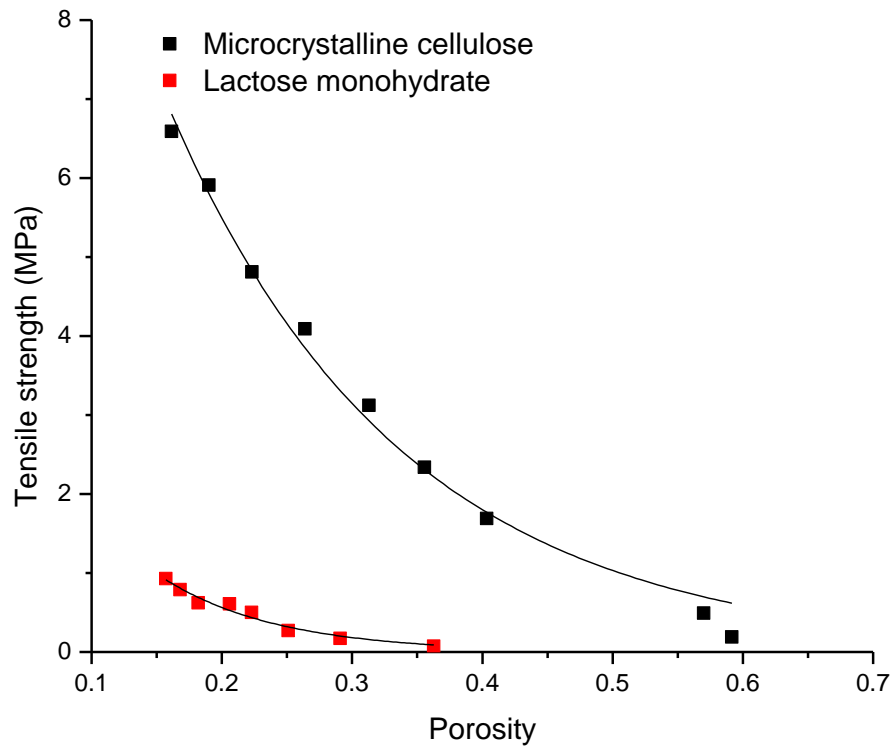


Figure 36: Effect of porosity on tensile strength of microcrystalline cellulose and lactose monohydrate using Ryshkewitch-Duckworth model (Eq.29)

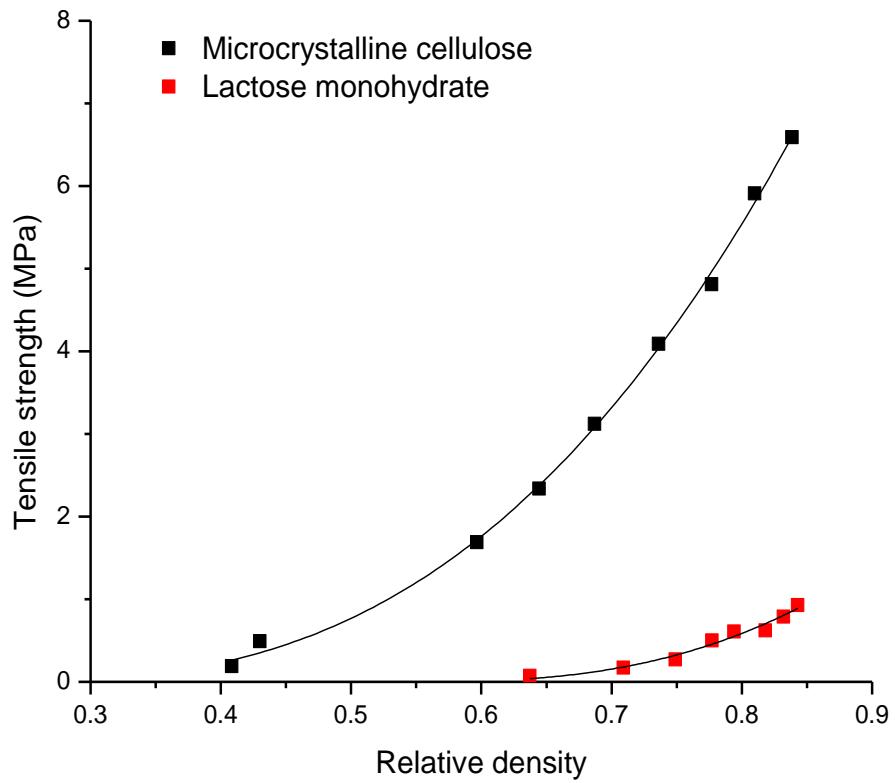


Figure 37: Effect of relative density on tensile strength of microcrystalline cellulose and lactose monohydrate using Percolation model (Eq.40)

3.3.5. Chapter Summary

A complete understanding of compaction cycle is essential for the tablet technologist to design a robust tablet formulation. In the present study, a systematic evaluation of compaction cycle which includes elastic and plastic deformation and fragmentation has been illustrated. Stress-strain curve of two powder materials of dissimilar deformation behavior was generated to calculate elastic modulus and compressive strength of powder materials. Additionally, tensile strength data were also generated to illustrate the radial strength of compacts. It was found that compression load had a linear relationship with elastic modulus, compressive strength and tensile strength. Thus with an increase in compression load increase in elastic modulus, compressive strength and tensile strength occurred for both the powder materials. Further to understand the relationship between these mechanical properties, compressive strength and tensile strength was plotted against the elastic modulus. A linear relationship between mechanical strength (compressive and tensile strength) with elastic modulus was observed indicating that these mechanical properties highly depend on each other. Further a correlation between compressive strength and tensile strength reveals the high anisotropy of lactose monohydrate compact. Further elastic modulus, compressive strength and tensile strength at zero porosity were computed using Sprigg's model as well as percolation model. Microcrystalline cellulose shows lower elastic modulus at zero porosity but higher compressive strength and tensile strength at zero porosity owing to its higher plasticity and well compactible nature by both the models studied. Thus in the present study, a systematic evaluation of mechanical properties of compacts has been successfully elucidated.

3.4. Chapter IV: A Closer Look at Tableting Process: An Order Out of Chaos

Millions of patients swallow one or more tablets each day as a medication. However, the tableting process is not yet fully understood. More than 17 equations have been proposed that empirically describe the tableting process (35, 96, 112-115). A high-speed tableting press is able to manufacture more than one million tablets per hour. The tablets need to be of highest quality showing an excellent content uniformity of the active pharmaceutical ingredient (API), the drug substance, which may be as low as 1 mg/tablet or less, showing a defined drug release in vitro, a defined disintegration time, a reasonable shelf-life of up to 5 years and an acceptable strength (tablet hardness, tensile strength) for packaging or further processing, such as coating. In addition, it is important that the tablets do not show any tableting process defects, such as sticking to the punches or cracks known as capping or lamination.

The primary substance particles represent a disordered system of powder or granules, i.e. processed powder, which contain the right amount of API and excipients (diluent, disintegrant, binder, lubricant, colorant, stabilizer etc). A disordered particulate system consists of solid particles but often behaves differently, more like a liquid or gas, and should probably be described as a fourth state of matter (22). The characterization of a disordered particulate system is still a challenge (82) since a long range order is missing and the local structure can often be only approximated with an estimated physical coordination number, z (83). Since the first use of percolation theory, it has always been assumed that there is no correlation or existence of dependence between segments in particularly defined systems. However, given the nature of disordered systems it can be

argued if the physical phenomenon of a system depends only on the random probability. Thus some kind of correlation, finite or infinite, may exist in such systems.

It has been earlier discussed how powder is 4th states of matter. Along with that, pharmaceutical powders further possess more disorderness due to the process of synthesis as well as multifunctionality. Moreover, transition of a powder bed into a tablet involves a number of steps and mechanisms. It commences with an application of a compaction force to a powder bed followed by inter-particle bonding by various mechanisms and deformations by elastic, plastic and brittle. Particles pass through one or several of these deformation phases during a compression process. These are more often concurrent than sequential as a single particle is likely to pass through multiple deformation cycles. Due to overlapping processes, the dominating volume reduction mechanism for most pharmaceutical materials are complex and often cannot be simply characterized as either elastic, plastic or fragmenting. Thus it can be hypothesized that with such kind of disordered nature of pharmaceutical powders, correlation does exist. Thus it becomes necessary to study the powder compaction in the light of correlated percolation phenomenon. Correlated percolation models are systems where sites in a lattice are occupied randomly by a given species, and then species are removed (bootstrap percolation) or added (diffusion percolation) according to the site's environment. As described earlier a powder component consists of solid particles along with pores. Thus essentially even a single component powder can be called as binary system consisting of powder particles and pores. With the application of stress, the pores are dissipated and powder particles occupy the spaces. Thus a correlated diffusion-based percolation phenomenon can be envisaged in powder compaction.

The primary particles are characterized by shape, size and size distribution. In case of small batches, the tablets are manufactured with a single punch press and in case of large batch sizes the pharmaceutical industry is using a high-speed rotary press with a lower and upper punch. The desired thickness of the tablet is achieved by the distance between the lower and upper punch during the compression cycle. The thickness of the tablet defines the density of the compact with $\rho_r = \text{relative density} = \text{solid fraction} = \text{ratio of apparent density/true density}$. Thus, the tablet porosity, $\varepsilon = 1 - \rho_r$ is an important quality attribute for relevant tablet properties, such as disintegration time, dissolution profile, of the drug substance and among others the hardness of the tablet (tensile strength, indentation hardness) (96). Before the final porosity is achieved, the punch force as the result of the tablet thickness and the material compressed (*actio = reactio*) leads to the stress distribution within the bed of particles in the die creating a pressure on the die wall. All the forces can be measured leading to a compact with a final porosity as a result of the maximum force and of the properties of the material (brittle, plastic, ductile hydrophilic, hydrophobic etc) compressed (116). In all cases the pharmaceutical ingredient particles (drug and auxiliary substances) are moved by the punches in z-direction closer to each other. Radial movement of the particles in direction to the center line of the punch hole is facilitated by the build-up of the die wall pressure and by pores in the neighborhood of the particles. Thus, during the tableting process, the pores are dissipating. Since the pores are randomly distributed the process of the occupation of the void space is governed by a stochastic process similar to heat diffusion. On the other hand, the stress between the upper and the lower punch is only transmitted if the particles touch each other to form a connective path between the punches, which is true in radial direction. With other words, the formation of a compact is

the result of the percolation of particles (50, 84). Since the die wall pressure is directly correlated to the punch pressure in z direction of the uniaxial compression, the tableting process corresponds to a diffusive correlated percolation. The percolation threshold for a 3D correlated percolation is $\rho_c = 0.634$ for a coordination number $z = 6$ and $\rho_c = 0.366$ for $z = 12$ and the value of its critical exponent, q for the correlated percolation is equal to 2.0 (85, 86). The critical exponent $q = 2$ being a universal value governs all diffusional processes, such as heat diffusion or drug dissolution (88, 89). It is important to realize that in a process far-from-equilibrium, the time plays an essential role being hidden in the variable z of the uniaxial tableting process since the tableting speed defines the time and the position of the punch. It is well known that the critical tablet quality attributes depend on the tableting speed (117) - a fact that needs to be considered in the framework of quality by design (QbD) already in the early development phase of a new medication (13). In this context, it is important to emphasize that the application of percolation theory should become part of the guidelines for the for industry since the knowledge of percolation thresholds (process thresholds, percolation thresholds of ingredients, such as the drug, a specific excipient, etc.) play a major role in formulation science and are part of critical quality attributes of the pharmaceutical product (118).

3.4.1. Spheres and powder materials

To test the hypothesis of correlated percolation phenomenon, powders with different deformation behavior, particle size and size distribution, crystalline nature, etc., were studied. In this context, three materials of spherical nature as well and their binary mixtures were studied. It was found that single component spheres of microcrystalline cellulose, sucrose and ibuprofen showed almost similar values of percolation threshold

values closer to the expected threshold of 0.634. Moreover the binary mixture of spheres (microcrystalline cellulose and sucrose, ibuprofen and sucrose) also demonstrated values of percolation threshold, ρ_c , similar to the expected value of 0.634. Here it should be noted that these spheres were of different deformation behavior as well compactibility, however, correlated percolation phenomenon can be observed in all cases. This can also be confirmed from higher goodness of fit (R^2) values and narrow confidence interval of the values (Table 13).

Further, the hypothesis was also tested for powder mixtures since they are of more disordered nature due to the absence of particular shape and structure along with other varied micromeritic properties. Among the powder components, it was found that carbamazepine, lactose monohydrate when plotted according to power law equation, percolation threshold was found closer to the expected threshold of $\rho_c = 0.634$. However, it was found that microcrystalline cellulose, crospovidone and croscarmellose sodium demonstrated lower value of threshold, ρ_c , that was close to 0.365 (Table 14). The difference in the values of percolation threshold is due to the difference in the coordination number. It is important to keep in mind that the percolation threshold depends on the coordination number, z , and on the formation of stable clusters. Thus a relationship between the crystal structure, i.e. type of crystal being related to different coordination numbers z (such as sc = “simple cubic”, fcc = “face center cubic” or bcc = “body centered cubic” and other structures) and the resulting percolation threshold can be expected. In other words, for a coordination number $Z > 6$, the percolation threshold will be lower than 0.634. Thus, the value of percolation threshold, $\rho_c = 0.634$ indicates a coordination number, $Z = 6$ while the value of $\rho_c = 0.365$ indicates $Z = 12$.

To systematically illustrate the change in percolation threshold or coordination number, an example of binary mixture of carbamazepine and microcrystalline cellulose was illustrated. Based on Figure 38, it can be observed the the shift in percolation threshold from higher values of carbamazepine to lower value of microcrystalline cellulose with an increase in the concentration of microcrystalline cellulose.

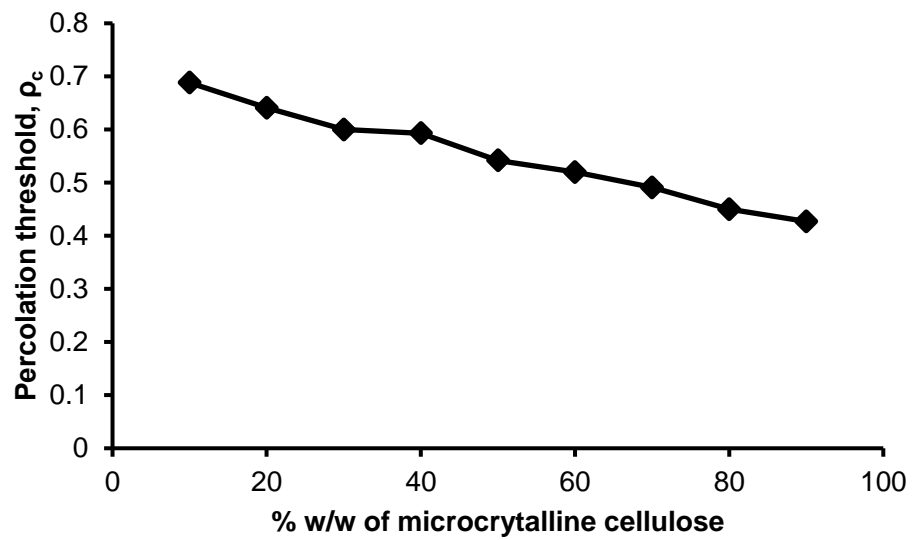


Figure 38: Percolation threshold of binary mixtures of carbamazepine and microcrystalline cellulose assuming the value of $q = 2$

3.4.2. Effect of particle size on percolation threshold

It is a well known concept that percolation threshold depends on the particle size and size distribution within the system. To study the effect of particle size on percolation threshold, four different grades of microcrystalline cellulose were studied. The nominal particle size as well as calculated percolation threshold values assuming the value of $q = 2$ are summarized in Table 15. It can be observed from Table 15 that all four grades of microcrystalline cellulose show the value of percolation threshold closer to $\rho_c = 0.366$ except for Avicel[®] PH 105 grade (20 μm) showing threshold of $\rho_c = 0.427$ which could be expected because of coordination number of $z = 8$.

To further confirm the hypothesis of correlated percolation phenomena in tableting process, microcrystalline cellulose was compressed using industrial scale rotary press. Microcrystalline cellulose (Avicel[®] PH 101) was compressed at tableting speed varying from 57600 tablets/hr to 162100 tablets/hr. The calculated percolation threshold values along with goodness of fit have been summarized in Table 16. It can be observed that calculated percolation threshold values at different tableting speed are closer to the value of Avicel[®] PH 101 calculated by single press punch with value of coordination number, $Z > 6$.

3.4.3. Effect of crystalline nature of microcrystalline cellulose on percolation threshold

It is widely known that polymorphic form of same materials can affect the physicochemical properties of substances including the hardness as well as other mechanical properties. Similarly the polymorphic form of a compound also has effect on

percolation threshold owing to difference in crystalline nature. In the present study, the effect of difference in the crystallinity was illustrated using two polymorphic forms of microcrystalline cellulose. Cellulose in general exists in four different crystal modifications (I, II, III, and IV). Among them form I and II are the most abundant and stable. Microcrystalline cellulose (Avicel PH 101, 101, 105, 200) is cellulose I type of polymorphic form and is most widely used excipient in solid dosage formulations. However, in recent years the polymorphic form type II has been introduced by mercerization of cellulose I using NaOH. MCC Sanaq Burst used in the present study is cellulose II type and consist of 47-57% of crystallinity compared to cellulose I type consisting of 77% crystallinity. Thus it would be of interest to understand the effect of crystalline nature on percolation threshold of microcrystalline cellulose. From Table 15 it can be observed that MCC Sanaq burst shows highest percolation threshold ($\rho_c = 0.567$) than other grades of microcrystalline cellulose (cellulose I). Thus, indicating significant effect of crystallinity on percolation threshold as well as coordination number of powder materials.

Table 13: Value of percolation threshold, ρ_c , calculated by assuming the value of critical exponent, $q = 2$.

Material	S	95% Confidence Interval	ρ_c	95% Confidence Interval	R^2
MCC Spheres 200	2.67	1.20 – 4.14	0.636	0.555 – 0.717	0.9418
Sucrose Starch Spheres	36.33	28.83 – 43.82	0.647	0.625 – 0.669	0.9923
Ibuprofen Spheres	14.83	10.34 – 19.32	0.631	0.631 – 0.713	0.9890
MCC spheres 200 + Sucrose-starch spheres (80:20)	12.42	- 4.39 – 29.23	0.735	0.593 – 0.877	0.7943
MCC spheres 200 + Sucrose-starch spheres (60:40)	17.23	8.41 – 26.05	0.675	0.615 – 0.735	0.9570
MCC spheres 200 + Sucrose-starch spheres (40:60)	41.72	22.32 – 61.13	0.715	0.672 – 0.757	0.9750
MCC spheres 200 + Sucrose-starch spheres (20:80)	61.06	23.08 – 99.04	0.727	0.680 – 0.772	0.9661
Ibuprofen + Sucrose-starch spheres (80:20)	14.96	11.25 – 18.66	0.640	0.606 – 0.674	0.9918
Ibuprofen + Sucrose-starch spheres (60:40)	22.01	17.27 – 26.76	0.671	0.646 – 0.695	0.9948
Ibuprofen + Sucrose-starch spheres (40:60)	22.13	17.05 – 27.20	0.671	0.646 – 0.697	0.9912
Ibuprofen + Sucrose-starch spheres (20:80)	26.46	18.49 – 34.43	0.688	0.659 – 0.717	0.9851

Table 14: Value of percolation threshold, ρ_c , calculated by assuming the value of critical exponent, $q = 2$.

Material	S	95% Confidence Interval	ρ_c	95% Confidence Interval	R^2
	Carbamazepine	8.59	4.09 – 13.09	0.659	0.609 – 0.709
Crospovidone	21.71	15.37 – 27.10	0.346	0.297 – 0.395	0.9747
Croscarmellose sodium	35.56	28.33 – 42.78	0.409	0.385 – 0.434	0.9799
Potassium Bromide (KBr)	16.99	13.86 – 20.12	0.542	0.519 – 0.563	0.9956
Lactose monohydrate	15.35	7.87 – 22.83	0.603	0.552 – 0.653	0.9688

Table 15: Calculated value of percolation threshold, ρ_c , calculated by assuming the value of critical exponent, $q = 2$ for various grades of microcrystalline cellulose.

Material	Nominal Particle size and Crystalline nature	S	95% Confidence Interval	ρ_c	95% Confidence Interval	R^2
MCC PH 105 (Avicel PH 105) (20 μm)	20 μm (Cellulose I)	47.18	38.22 – 56.14	0.427	0.399 – 0.455	0.9953
MCC PH 101 (Avicel PH 101) (50 μm)	50 μm (Cellulose I)	37.17	32.04 – 42.28	0.390	0.363 – 0.416	0.9956
MCC PH 102 (Avicel PH 102) (100 μm)	100 μm (Cellulose I)	27.99	25.19 – 30.80	0.352	0.331 – 0.373	0.9970
MCC PH 200 (Avicel PH 200) (200 μm)	200 μm (Cellulose I)	35.29	30.15 – 40.43	0.380	0.354 – 0.406	0.9960
MCC Sanaq Burst	110 (50-300 μm) (Cellulose II)	18.03	16.75 – 19.32	0.567	0.558 – 0.574	0.9977

Table 16: Calculated value of percolation threshold, ρ_c , calculated by assuming the value of critical exponent, $q = 2$ for microcrystalline cellulose (Avicel PH 101) and dicalcium phosphate (Emcompress) using industrial scale rotary press at different tableting speed.

Tablet (per hour) (TPH)	Microcrystalline cellulose (Avicel PH 101)			Dicalcium Phosphate (Emcompress)		
	S	ρ_c	R^2	S	ρ_c	R^2
57600*	30.83	0.432	0.7908	25.06	0.697	0.8961
60000*	NA	NA	NA	50.26	0.764	0.9822
96000*	32.37	0.424	0.9941	114.29	0.794	0.9953
120600**	50.38	0.452	0.9997	148.29	0.782	0.9958
162100**	58.24	0.481	0.9910	101.67	0.759	0.9790

* Compressed from Manesty (Press model - Betapress)

**Compressed from Fette (Press model - PT2090 IC)

3.4.4. A simple experimental set up for studying processes far-from-equilibrium conditions

The definition and the concept of time is a fascinating topic in the book of Ilya Prigogine and Isabelle Stengers “Order out of Chaos Man’s New Dialogue with Nature” and is worth discussion in reference to the compaction of a disordered particulate system (119). This “simple” pharmaceutical unit operation is a process far-from-equilibrium conditions and the experienced formulation scientist recommend the novice to wait 24 hours before measuring the quality attributes of the tablets manufactured. This advice cannot be based on the argument that formulation is an art and not a science since the advent of FDA’s Process Analytical Technology (PAT) Initiative but is the result of the tablet needing time to reach the equilibrium by relaxation processes (22). This time complies with the time defined by the second law of thermodynamics governing the process of aging. On the other hand, the time during the compaction process is defined by the tableting speed by the time of energy which flows into the cavity (die) by the position of the punch in z-direction. In this context, we have not only a geometrical correlated percolation phenomenon but in addition a time and space-time correlated percolation.

Thus, the tableting process is a result of the pressure of applying an energy/volume to the ensemble of disordered pharmaceutical particles far-from equilibrium conditions creating a dissipative structure - an order out of chaos (119). It is important to realize that this simple experimental set-up is not limited to the study of the tableting process but can be used for studying the effect of environmental effects on living organisms being in a process far-from equilibrium conditions. Thus, the effect of the amount of the volume specific energy due to the change of climate (temperature, humidity) and/or due to

anthropogenic installations, such as electric fields, can be studied on processes being far-from-equilibrium conditions, such as the growth of living organism (flora, fauna). In this context, it has to be kept in mind that the effects will be more pronounced far from equilibrium conditions, i.e. in the development phase of a living organism before achieving a dynamical equilibrium as an adult entity. This is a very simple experimental set up of a complex process which involves a disordered particulate system being governed by percolation theory.

3.4.5. Chapter Summary

Nature offers on one side plenty of initially disordered systems but on the other side the most exquisite jewels of highest order and beauty as a result of Prigogine's principle "Order out of chaos". Percolation theory with the concepts of percolation threshold and universal critical exponents allows a description of this phenomenon which is setting a counterpoint to the second law of thermodynamics. The phase transition which happens at the percolation threshold shows a fractal dimension and establishes a link to the fractal world of Mandelbrot (120, 121) emphasizing the very strong principle of self-similarity in nature. This principle is dominant and embracing all scales and the inorganic and organic world. Stephan Hawking explained that life needs a minimum of three dimensions (3D) (122). Therefore, no life can exist in a planar 2D world. Percolation theory provides us with a simple rational why life needs a minimum of 3D since in 3D exist 2 percolation thresholds with a common range that two different ingredients can percolate simultaneously. Thus, the influx of an ingredient in a 3D system can act as a switch, a function which is essential for the development of life. In this context, it can be anticipated

that nature's evolutionary process is using all existing physical laws of the standard cosmological model and beyond. For the moment, we can conclude that percolation theory describes optimally the Prigogine's process "Order out of chaos" (119) that the inflow of energy in a chaotic system leads to a higher order and correlated percolation phenomena can be found in very different disciplines and scales (123). Nano-science and nano-technology is only the beginning of a convergence of the disciplines of biology, chemistry and physics. This trend will be accelerated thanks to the study of processes far-from-equilibrium and thanks to the impact of the digital revolution, which embraces the so called exact sciences and the humanities being divided since many centuries.

Last but not the least, it is our task to preserve nature and its capacity to transform a chaotic world to a system of much higher order, such as the growth of wonderful crystals in the inorganic world and, last but not the least, the evolution of organic life.

3.5 Chapter V: Consolidation of Powder and Elucidation of Bonding Area and Bonding Strength Using Percolation Theory

The present section is based on the assumption that compressibility and compactibility are interdependent processes with one affecting the other. To prove this hypothesis, a systematic evaluation of the compaction behavior of pharmaceutical powders of different deformation behavior (carbamazepine, microcrystalline cellulose and lactose monohydrate) and their binary mixtures was studied using percolation theory.

3.5.1. A Modified model to determine compactibility of powder materials

Kuentz and Leuenberger developed an equation relating deformation hardness of powder materials with relative density of compact by combining differential form of Heckel equation (Eq. 48) with the theory of bonding and non bonding points in powder materials (69).

$$P = P_0 \left[\rho_c - \rho_r - \ln \left(\frac{1 - \rho_r}{1 - \rho_c} \right) \right] \quad (48)$$

Where P is the deformation hardness (MPa), P_0 is the magnitude of P at infinite compression stress, σ_c is compression stress applied to make the compact (MPa), ρ_r is relative density, and ρ_c is the percolation threshold of powder materials at which rigidity of compact starts.

In the present study, a modification of the above equation (Eq. 48) by replacing deformation hardness, P , of compact with its tensile strength, σ_t , is proposed. Although deformation hardness can be used to characterize mechanical strength of compact, it is

more suitable for characterizing deformation behavior or local plasticity of powder materials (124). Thus in the present study, tensile strength which depends on the diametrical crushing of tablet, is better indicator of mechanical strength of tablets. Thus Eq. 48 has been modified to define the tensile strength of compacts by substituting deformation hardness, P, with tensile strength, σ_t , and maximum deformation hardness, P_{\max} , with maximum tensile strength, σ_{\max} using Eq. 49

$$\sigma_t = \sigma_0 \left[\rho_c - \rho_r - \ln \left(\frac{1-\rho_r}{1-\rho_c} \right) \right] \quad (49)$$

Where, σ_t is tensile strength of the compact, σ_0 is tensile strength at zero porosity or relative density, $\rho_r \rightarrow 1$, and ρ_c is a percolation threshold of powder materials defining critical relative density that marks onset of the tensile strength of powder material.

3.5.2. Compressibility of powder materials and their binary mixtures

As discussed earlier, compressibility can be defined as the process of volume reduction of powder bed with respect to stress (compression load) applied. The phenomenon of compressibility in powder technology has been defined by various theories and equations. However, most of the equations suffer from limitations due to the theoretical assumptions associated with the theory and also due to compressibility being a overlapping process of several phenomenon. Moreover, given the complex heterogeneous and disorder nature of pharmaceutical powders, it becomes difficult to characterize the compressibility of powder. This can be attributed to the powder consisting of a high number of small solid particles with an irregular shape and, in many cases, the presence of

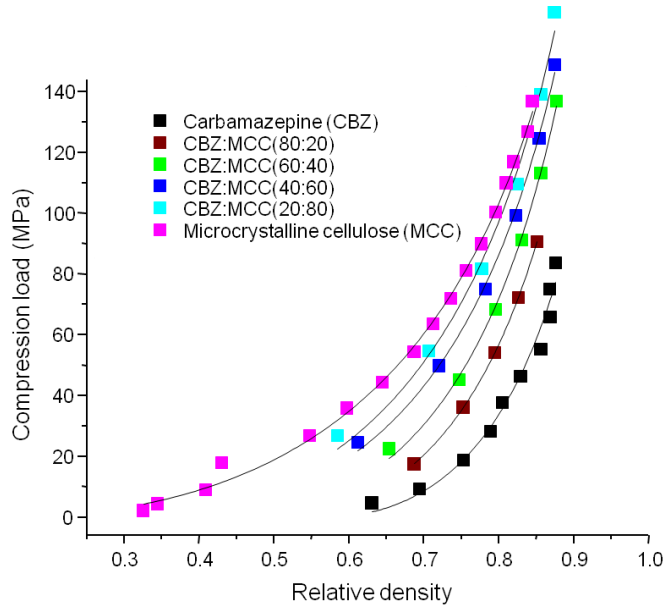
open and closed pores further complicates the scientific measurement of its dimensional values (specific surface area, true density etc.). Additionally, the high number of irregularly shaped particles with a high variation of particle size makes the scientific understanding of particle deformation behavior very tricky. A typical example of this complexity can be illustrated with an example of microcrystalline cellulose and lactose which is popularly characterized as plastic and brittle material, respectively. However, it has been reported that they tend to deviate from characteristic assumption of their densification properties with change in particle size and size distribution (125). Similarly, change in the polymorphic form of microcrystalline cellulose and lactose can also change the deformation behavior of both the powders significantly. Thus it becomes very difficult for a theory to assess deformation behavior of all kinds of pharmaceutical powder materials with difference in particle size, surface area and other micromeritics properties. In our previous study, we reported that bond and site percolation thresholds of powder materials can be a better approach for the evaluation of the deformation behavior as compared to the use of mean yield pressure, P_y , values derived from classical theories like Heckel equation (74). Similarly, we also found out that other classical theories, such as Kawakita and Walker models, although yield high goodness of fit (R^2), they too fail to characterize and differentiate the deformation behavior of powder materials at higher relative density. Thus a model with higher goodness of fit (R^2) and suitable to differentiate deformation behavior or compressibility of powder materials is desirable to study.

Paul and Sun (126) recently reported that modified Heckel equation proposed by Kuentz and Leuenberger can successfully characterize the compressibility of powder materials of different deformation behavior. Moreover, goodness of fit of modified Heckel

equation was also found superior compared to Heckel and Kawakita equations to characterize compressibility of powder materials. In the present study too, the compressibility of powder material and their binary mixtures has been characterized using modified Heckel equation (Eq. 23) (Figure 39). The calculated values of compressibility parameter, $1/c$, along with those of percolation threshold, ρ_{c1} , of powder materials have been summarized in Table 17. From Table 17, it can be observed that microcrystalline cellulose has highest values of c thus lowest $1/c$ values (170.06 MPa), followed by carbamazepine (375.94 MPa) and lactose monohydrate (595.23 MPa). Thus based on $1/c$ values it can be inferred that microcrystalline cellulose have higher plasticity followed by carbamazepine and lactose monohydrate. This deformation behavior concluded from modified Heckel equation is also consistent with reported literature. Plastic deformation and brittle fragmentation as compaction behavior of microcrystalline cellulose and lactose monohydrate, respectively, is well known (127). Also, Nokhodchi *et al.* (98) have reported poor compressibility of carbamazepine with possible elastic deformation and moderate brittle fragmentation as predominant mechanism of carbamazepine particles. Another model parameter of interest is the value of percolation threshold, ρ_{c1} , calculated from modified Heckel equation. In our previous studies, we have emphasized the importance of the percolation threshold, ρ_{c1} , values which can be used to characterize the material properties. It can be observed from Table 17 that lower the percolation threshold, ρ_{c1} , values coincide with lower $1/c$ values of powder materials and binary mixtures. As percolation threshold, ρ_c , values are the critical relative density that is required for the formation of first stable compact, a powder material with higher plasticity have lower percolation threshold, ρ_c , values due to faster transition of powder bed into compact.

Further, based on Table 17, it can also be observed that with increase in component of plastic material (microcrystalline cellulose), decrease in $1/c$ values can be observed (Figure 40). Similarly decrease in percolation threshold, ρ_{c1} , values can be observed in case of both types of binary mixtures (Figure 40). A shift in percolation threshold, ρ_c , values from higher to lower also confirms an increase in the plasticity of binary mixtures due to increase in the concentration of microcrystalline cellulose due to formation of infinite clusters of microcrystalline cellulose particles in binary mixtures at the expense of carbamazepine or lactose monohydrate particles.

(A)



(B)

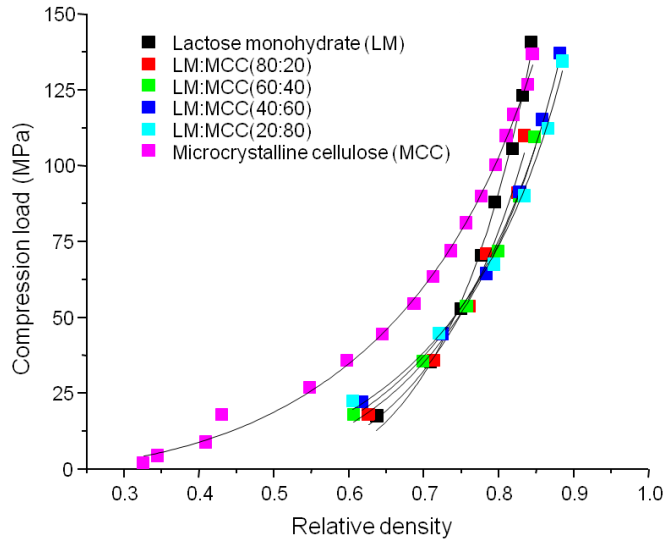


Figure 39: Compression load vs. relative density of binary mixtures using modified heckle equation (Eq. 23). (A) Binary mixture of carbamazepine and microcrystalline cellulose (CBZ:MCC). (B) Binary mixture of lactose monohydrate and microcrystalline cellulose (LM:MMC)

Table 17: Calculated compressibility and compactibility parameters of binary mixtures of carbamazepine (CBZ) and lactose monohydrate (LM) with microcrystalline cellulose (MCC).

Material	Compressibility parameters as per Eq. 23			Compactibility parameters as per Eq. 48			Compactibility parameters as per Eq. 40		
	1/C (Mpa)	ρ_c	R ²	σ_0 (MPa)	ρ_c	R ²	σ_0 (MPa)	ρ_c	R ²
Carbamazepine (CBZ)	375.94	0.584	0.9768	0.51	0.672	0.9458	1.13	0.606	0.9548
CBZ:MCC (80:20)	341.30	0.490	0.9999	1.06	0.659	0.9883	2.19	0.59	0.9953
CBZ:MCC (60:40)	314.46	0.427	0.9980	1.76	0.631	0.9992	3.37	0.524	0.9901
CBZ:MCC (40:60)	244.49	0.319	0.9982	3.05	0.549	0.9997	5.67	0.434	0.9956
CBZ:MCC (20:80)	239.81	0.276	0.9930	4.92	0.454	0.9972	9.01	0.348	0.9961
Lactose monohydrate (LM)	595.23	0.505	0.9954	1.36	0.635	0.9597	2.78	0.543	0.9687
LM: MCC (80:20)	361.01	0.438	0.9808	1.50	0.615	0.9695	2.91	0.512	0.9715
LM : MCC (60:40)	248.75	0.362	0.9948	2.76	0.579	0.9885	5.26	0.474	0.9935
LM :MCC (40:60)	224.72	0.332	0.9975	4.35	0.539	0.9933	8.18	0.431	0.9943
LM:MCC (20:80)	183.48	0.279	0.9951	5.77	0.462	0.9988	10.78	0.363	0.9946
Microcrystalline cellulose (MCC)	170.06	0.129	0.9974	7.50	0.335	0.9960	12.66	0.232	0.9982

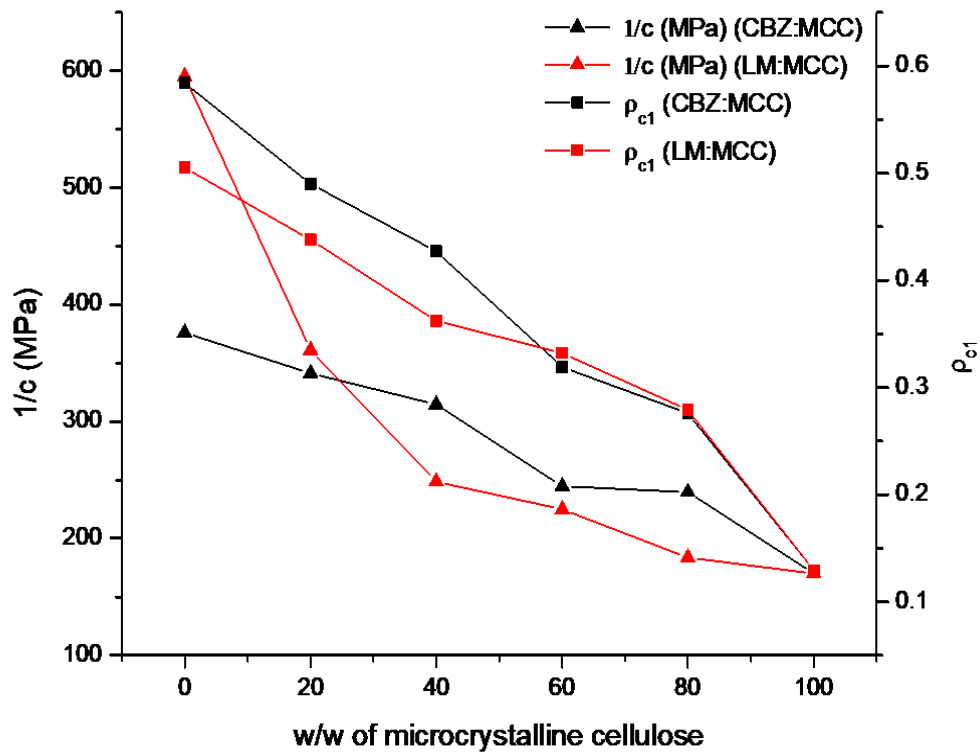


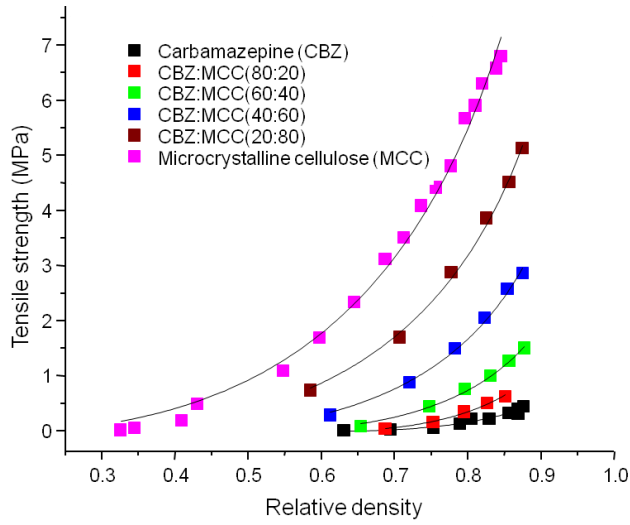
Figure 40: Relationship of compressibility parameters, $1/c$ (MPa) and percolation threshold, ρ_{c1} calculated by Eq. 23 of both model binary mixtures (carbamazepine and microcrystalline cellulose (CBZ: MCC) and lactose monohydrate and microcrystalline cellulose (LM: MCC) with increasing concentration of microcrystalline cellulose

3.5.3. Compactibility of powder materials and their binary mixtures

Compactibility of powder materials can be defined as strength of compact gained with application of stress. Powder particles undergo consolidation due to reduction in the distance between particles by application of stress. This reduction in compact volume brings the particles into close proximity to each other. This facilitates creation of bonds and makes the particles stick together into a coherent compact. It has been reported that three different bonding types are usually responsible for the consolidation of powder particles which includes intermolecular forces, solid bridges and mechanical interlocking (128). Among the intermolecular forces, van der Waals forces are more prevalent that helps in consolidation of particles together in a tablet along with certain degree of hydrogen bonds and electrostatic forces. However, the dominating bond type cannot be analyzed experimentally since it's usually combination of two or more mechanisms depending on various factors including the degree of compression and the inherent properties of the material (129). Due to these complexities, defining compactibility of powder material is difficult. In literature, various models have been proposed to study and define compactibility of powder materials. However like compressibility model, most of the models fail to define compactibility of powder materials of different deformation nature and do not have universal application. In the present study too, an attempt has been made to describe compactibility of powder materials and their binary mixtures using a new model (Eq. 49) based on a concept of percolation theory (Figure 41). The results of the calculated model parameters along with goodness of fit (R^2) values have been summarized in Table 17. From Table 17, it can be observed that microcrystalline cellulose has highest compactibility, σ_0 , followed by lactose monohydrate and carbamazepine. Moreover, as

expected the value of percolation threshold, ρ_{c2} , i.e. the critical relative density required to form a coherent compact was found to be lowest for microcrystalline cellulose followed by lactose monohydrate and carbamazepine. This result is in agreement with fundamentals of percolation theory that since microcrystalline cellulose forms a stable compact at lower relative density, formation of particle cluster and thus resultant consolidation will be higher with further increase in relative density of compact compared to lactose and carbamazepine. The same can also be confirmed from the results of compactibility of both the model binary mixtures. It can be observed that compactibility, σ_0 , of both the model binary mixtures increases with increase in weight fraction of microcrystalline cellulose owing to its good compactibility. However, the percolation threshold, ρ_{c2} , values were found to decrease and shift towards microcrystalline cellulose with an increase in its concentration.

(A)



(B)

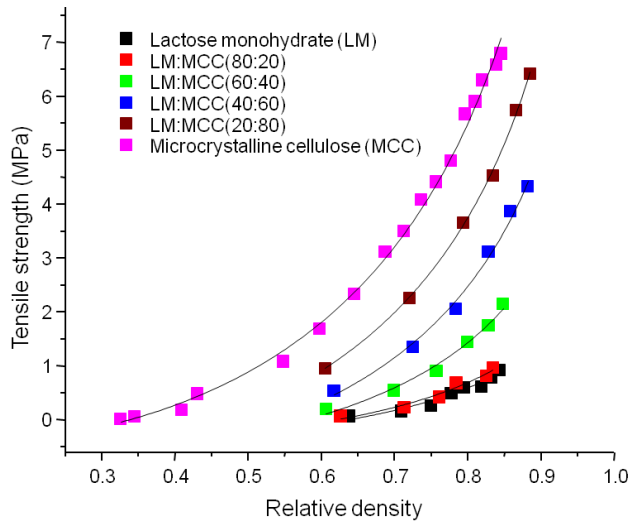
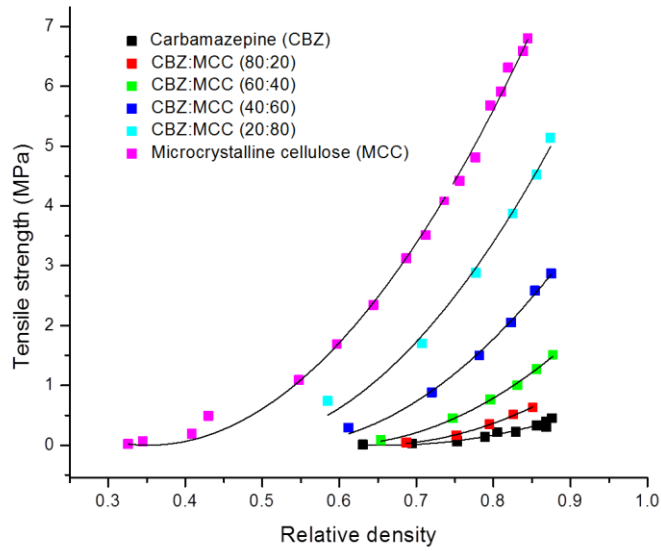


Figure 41: Tensile strength vs. relative density of binary mixtures using new model (Eq. 49). (A) Binary mixture of carbamazepine and microcrystalline cellulose. (B) Binary mixture of lactose monohydrate and microcrystalline cellulose

As discussed earlier, in our previous studies we found that power law equation in combination of effective medium approximations (Eq. 40), and was much superior to predict the compactibility, σ_0 , of powder materials and their complex binary mixtures compared to established classical theories (74). The value of critical exponent, q , was assumed as $q = 2.7$ as described in chapter II. The compactibility, σ_0 , and resultant percolation threshold, ρ_c , of powder of materials and their binary mixtures can be found out by plotting tensile strength, σ_t , vs. relative density, ρ_r , by assuming the value of critical exponent, $q = 2.7$ (Figure 42). The percolation model (Eq. 40) was found to have better prediction of powder materials of different deformation behavior due to consideration of percolation threshold, ρ_c in Eq. 40 and thus normalization of relative density of compact (Figure 42). In the present study also, compactibility of powder material was calculated by a new model (Eq. 49) proposed on the concept of fundamentals of percolation theory. Thus comparative evaluation between the two compactibility models (Eq. 40 and Eq. 49) has been made. The selection of the best model can be based on their fitting efficiency such as coefficient of determination values (R^2). However, based on values summarized in Table 17, it can be observed that obtained R^2 values are almost same for both the models, thus selection of best model was based on comparative evaluation using Akaike information criterion values test.

(A)



(B)

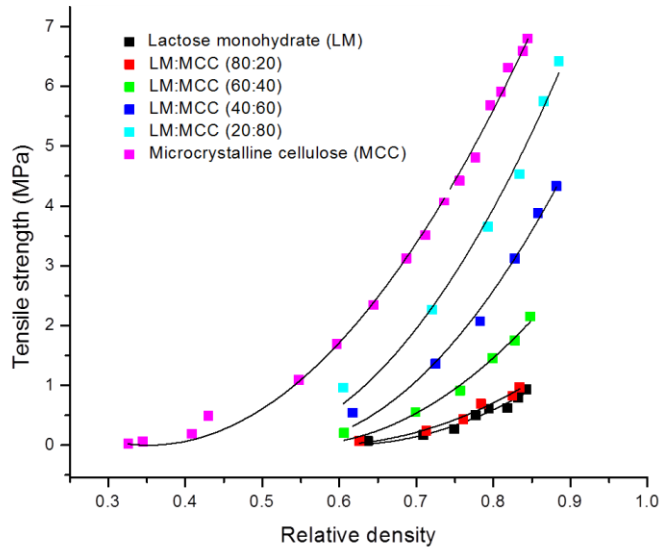


Figure 42: Tensile strength vs. relative density of binary mixtures using percolation model (Eq. 40). (A) Binary mixture of carbamazepine and microcrystalline cellulose. (B) Binary mixture of lactose monohydrate and microcrystalline cellulose

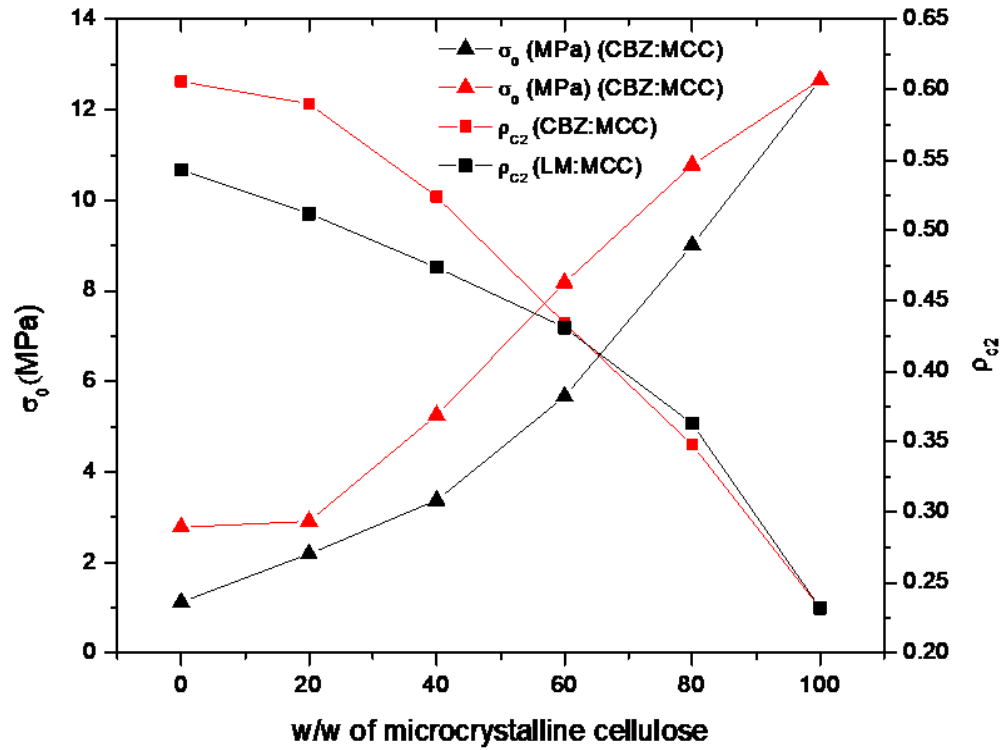


Figure 43: Relationship of compactibility parameters, σ_0 (MPa) and percolation threshold, ρ_{c2} calculated by Eq. 40 of both model binary mixtures (carbamazepine and microcrystalline cellulose (CBZ: MCC) and lactose monohydrate and microcrystalline cellulose: (LM: MCC) with increasing concentration of microcrystalline cellulose

Akaike information criterion is a statistical approach introduced by Akaike in 1974 for the selection and identification of best fit models from same set of data (130). As the number of fitting parameters usually dictates the goodness of fit model, Akaike information criterion is the best methodology to compare the fitness of model considering both numbers of data points along with residual sum of squares and fitting parameters involved as per the Eq. 50.

$$AIC = n \cdot \ln(RSS) + 2p \quad (50)$$

Where n is the number of data points, RSS is residual sum of squares and p is number of fitting parameters in the model. The calculated residual sum of square and AIC values by both compactibility equations (Eq. 40 and Eq. 49) have been summarized in Table 18. It can be observed that percolation model (Eq. 40) shows lower residual sum of square and AIC values compare to Eq. 49 in the case of single component mixtures and their binary mixtures. Thus it can be inferred from AIC study that both the models (Eq. 40 and Eq. 49) are statistically efficient and superior to characterize the mechanical properties of powder materials and their binary mixtures. Although the new model (Eq. 49) is also based on the relative increase in tensile strength of tablet with respect to relative density, one cannot differ that it also is based on concept of normalization of relative density, ρ_c , of compact similar to percolation model (69). Although, the trend of compactibility, σ_0 , and percolation threshold, ρ_c , values are almost similar with microcrystalline cellulose showing highest compactibility, σ_0 , and lowest percolation threshold, ρ_c values, the values calculated are different from both the models (Table 17). Moreover, it can be observed that compactibility values, σ_0 , calculated by percolation model (Eq. 40) were higher in case of both single component powder materials as well as their binary mixtures. This can be

attributed to the limitation of a new model (Eq. 49) being only valid for lower relative density due to first order approximations. Kuentz and Leuenberger too reported that Eq. 49 is more efficient in characterizing precise values of percolation threshold of powder material with respect to deformation hardness but had limitation of extrapolation to zero porosity for deformation hardness (69). From the Table 17, it can be observed that percolation threshold values, ρ_c , calculated by percolation model (Eq. 40) are almost similar to the values calculated by new model (Eq. 49). Kuentz and Leuenberger too reported that the new model (Eq. 49) although usually underestimated the maximum deformation hardness values, it was very efficient in calculating percolation threshold, ρ_c , of polymer tablets owing to its theoretical assumptions (69). Thus it can be concluded that percolation model (Eq. 40) assuming the value of $q=2$ is more efficient in characterizing both compactibility as well as percolation threshold of powder materials and binary mixtures, thus have wider application in characterizing the mechanical properties of tablets.

Table 18: Calculated Akaike Information Criterion (AIC) values for binary mixtures of carbamazepine and lactose with microcrystalline cellulose using Eq. 40 and Eq.49. The numbers of adjusting parameters (p) for both the model were 2.

Material	Eq. 49		Eq. 40	
	RSS	AIC	RSS	AIC
Carbamazepine (CBZ)	0.013	-55.73	0.009	-59.22
CBZ:MCC (80:20)	0.002	-8.96	0.001	-12.08
CBZ:MCC (60:40)	0.0008	0.3495	0.002	-30.16
CBZ:MCC (40:60)	0.011	-19.45	0.005	-24.26
CBZ:MCC (20:80)	0.032	-13.37	0.048	-10.90
Lactose Monohydrate (LM)	0.025	-33.88	0.018	-36.65
LM : MCC (80:20)	0.018	-16.67	0.014	-18.16
LM : MCC (60:40)	0.031	-13.47	0.018	-16.8
LM :MCC (40:60)	0.072	-8.46	0.062	-9.40
LM:MCC (20:80)	0.025	-14.70	0.11	-5.71
Microcrystalline cellulose (MCC)	0.385	-56.52	0.171	-70.25

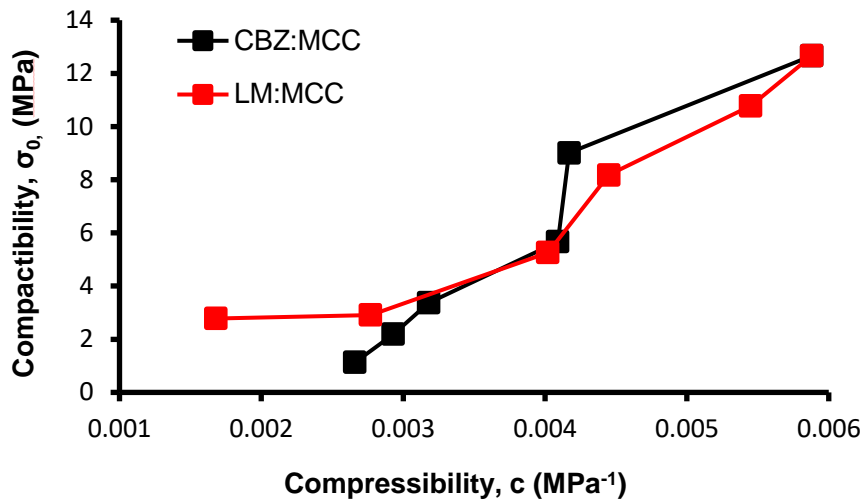
3.5.4. Elucidation of Bonding Area and Bonding Strength by Percolation Theory

Osei-Yeboah *et al.* while studying the compaction behavior of powder materials concluded that the degree of compaction as well as compact strength largely depends on bonding area and bonding strength (BABS) developed between particles of powder (110). Based on this theory, the successful tableting depends upon the presence of optimum level of bonding area and bonding strength in powder materials (131). Bonding area can be defined as bonding area or surface area available between two adjacent particles and bonding strength can be defined as strength of particles per unit area. Thus powder materials undergoing plastic deformation create large bonding area while brittle materials due to fragmentation of particles have higher bonding strength (131). Although a qualitative model, BABS can be studied theoretically by analyzing compressibility and compactibility of powder materials using various mathematical models. In the present study, an attempt to study compressibility and compactibility of three powder materials with different deformation behavior (plastic and brittle) and their binary mixtures in the context of BABS has been made. To elucidate BABS theory, compressibility, c , and compactibility, σ_0 , of powder material and their binary mixtures has been studied by establishing relationship between them. Based on the Figure 45A, it can be observed that with increase in compressibility, c , values there was increase in compactibility, σ_0 , values of both the model binary mixtures. Thus, indicating that higher the plasticity of powder materials higher would be the compactibility, σ_0 . A linear relationship between c and σ_0 with correlation coefficient ($R^2=0.9396$) was observed in case of binary mixtures of carbamazepine and microcrystalline cellulose. However an exponential relationship between c and σ_0 with correlation coefficient ($R^2=0.9444$) was observed in case of binary

mixtures of lactose monohydrate and microcrystalline cellulose (Figure 44A). The difference in the relationship in binary mixtures could be attributed to the dominant behavior of powder particles in mixture. In case of binary mixture of carbamazepine and microcrystalline cellulose, carbamazepine is moderately brittle thus an additive relationship in case of compressibility and compactibility could be observed. Whereas, in case of binary mixture of lactose monohydrate and microcrystalline cellulose, lactose monohydrate is much more brittle thus an exponential relationship between compressibility and compactibility with decrease in concentration of lactose monohydrate in binary mixtures can be observed. Further, to get more insight into the relationship between compressibility and compactibility, the calculated percolation threshold for both compressibility (ρ_{c1}) and compactibility (ρ_{c2}) have been plotted (Figure 44B) with R^2 value of 0.9656 and 0.9707 for carbamazepine and microcrystalline cellulose and lactose monohydrate and microcrystalline cellulose, respectively. A good linear relationship between both the percolation threshold (ρ_{c2} vs. ρ_{c1}) indicates that although the critical values of relative density, ρ_c , differ for compressibility and compactibility of powder materials, the process go hand in hand and interdependent from each other thus indicating that lower the compressibility threshold, ρ_{c1} , lower would be compactibility threshold, ρ_{c2} , and thus faster transition of a powder bed to a compact with higher mechanical strength. Hence degree of compactibility or strength gained by the powder particles depends on how fast the powder undergoes rearrangement and fragmentation or deformation. This is in line with the bonding area and bonding strength concept proposed by Osei-Yeboah *et al* (110). Thus it can be inferred from the present study that complex process of powder compaction

can be simplified and can be more profoundly understood by application of percolation theory.

(A)



(B)

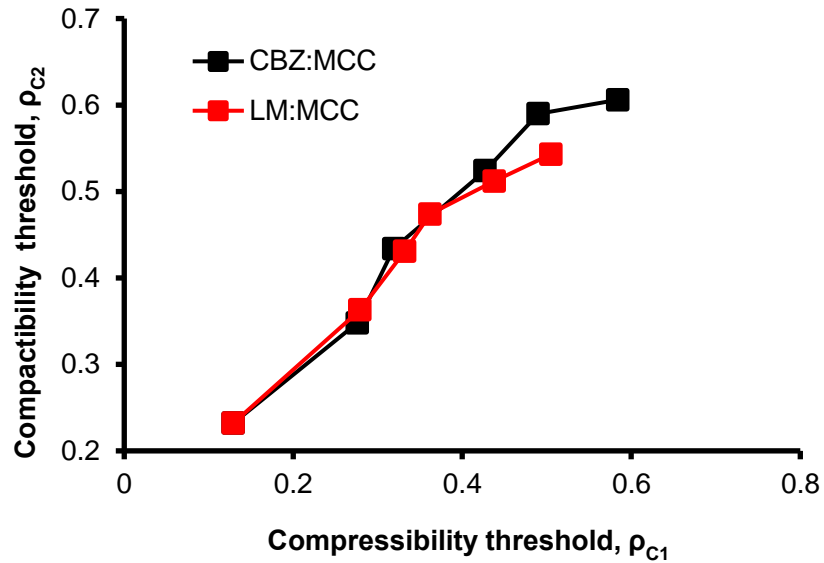


Figure 44: Elucidation of bonding area and bonding strength in both model binary mixtures of carbamazepine and microcrystalline cellulose (CBZ: MCC), lactose monohydrate and microcrystalline cellulose (LM: MCC). (A) Relationship between compressibility, c and compactibility. (B) Relationship between percolation thresholds of compressibility and compactibility

3.5.5. Chapter Summary

Powder deformation and subsequent gain of strength by particles is a complex and dynamic process. However, understanding powder compaction phenomenon is very important to develop a tablet formulation of acceptable mechanical strength and zero or near zero defects. Unfortunately, there is still lack of general understanding of powder compaction due to disorder and heterogeneous nature of pharmaceutical powders. In the present study, an attempt has been made to assess compressibility and compactibility of pharmaceutical powders which indicate reduction of powder volume and gain in the strength of compacts of three powder materials with different deformation behavior and their binary mixtures. It was found that modified Heckel equation in combination with percolation model is able to systematically define both compressibility and compactibility of powder materials with higher accuracy. It was also observed that the relationship between compressibility and compactibility parameters can also be used to understand bonding area and bonding strength between particles. Powder materials of binary mixtures with higher plasticity were found to possess more bonding surface area and thus higher bonding strength. This resulted in higher compactibility of binary mixtures consisting of plastic material like microcrystalline cellulose. However, this relationship between two parameters is not linear and is generally depended on the type and deformation characteristic of powder materials in the binary mixture. A linear relationship between percolation threshold for compressibility and compactibility also confirms that successful powder compaction depends on interplay of compressibility and compactibility phenomenon thus indicating degree of volume reduction of powder particles affecting the magnitude of interaction between particles.

4. Conclusions

The compression and compaction of powder materials is a complex phenomenon that is influenced by many factors, especially their physiochemical and mechanical properties. The process becomes even more complex when two or more powders, especially of dissimilar deformation behavior, are blended in the formulation which is almost always the case in tablet dosage formulations. It is therefore difficult to assess the compression and compaction phenomenon of powder materials by a single approach or a mathematical relationship. In the present thesis, the fundamentals of percolation phenomenon were applied to understand the compression and compaction behavior of pharmaceutical powders and spheres of different morphology, particle size, crystallinity and deformation behavior. The mechanical properties of compacts were analyzed by radial tensile strength, compressive strength and elastic modulus. A model developed on the fundamentals of percolation theory was found to predict the compaction behavior of both single component powder materials as well as their binary mixtures with higher accuracy compared to established classical models of powder compaction. Moreover, it was also found that bonding area and bonding strength can be very well understood by applications of percolation theory. A closer look at tableting process suggested the phenomena of 3-dimensional correlated diffusive percolation phenomena depending on the coordination numbers of particles when compacted. Thus from the above summarized sections in the thesis, it can be concluded that comprehensive application of percolation phenomenon in the study of compaction behavior of pharmaceutical powders is helpful in understanding the complexity of disordered pharmaceutical powders and their multicomponent mixtures.

References

1. CDER. 2014; Available from:
<http://www.fda.gov/downloads/Drugs/DevelopmentApprovalProcess/DrugInnovation/UCM430299.pdf>.
2. Mishra SM, Rohera BD. An integrated, quality by design (QbD) approach for design, development and optimization of orally disintegrating tablet formulation of carbamazepine. *Pharmaceutical Development and Technology*. 2017;22(7):889-903.
3. Çelik M. The past, present, and future of tableting technology. *Drug development and industrial pharmacy*. 1996;22(1):1-10.
4. Staniforth J. *Aulton's Pharmaceutics-The Design and Manufacture of Medicines*. New York: Churchill Livingstone. 2007.
5. Sun CC. Materials science tetrahedron—A useful tool for pharmaceutical research and development. *Journal of pharmaceutical sciences*. 2009;98(5):1671-87.
6. Charoo NA, Shamsheer AA, Zidan AS, Rahman Z. Quality by design approach for formulation development: a case study of dispersible tablets. *International journal of pharmaceutics*. 2012;423(2):167-78.
7. Lawrence XY. Pharmaceutical quality by design: product and process development, understanding, and control. *Pharmaceutical research*. 2008;25(4):781-91.
8. Garcia T, Cook G, Nosal R. PQLI key topics-criticality, design space, and control strategy. *Journal of Pharmaceutical Innovation*. 2008;3(2):60-8.
9. Guideline IHT. *Pharmaceutical Development Q8,(R2)*; US Department of Health and Human Services. Food and Drug Administration, Center for Drug Evaluation and Research (CDER): Rockville, MD. 2009.

10. Lionberger RA, Lee SL, Lee L, Raw A, Lawrence XY. Quality by design: concepts for ANDAs. *The AAPS journal*. 2008;10(2):268-76.
11. Verma S, Lan Y, Gokhale R, Burgess DJ. Quality by design approach to understand the process of nanosuspension preparation. *International journal of pharmaceutics*. 2009;377(1):185-98.
12. Lepore J, Spavins J. PQLI design space. *Journal of Pharmaceutical Innovation*. 2008;3(2):79-87.
13. Leuenberger H, Leuenberger MN. Impact of the digital revolution on the future of pharmaceutical formulation science. *European Journal of Pharmaceutical Sciences*. 2016;87:100-11.
14. Leane M, Pitt K, Reynolds G. A proposal for a drug product Manufacturing Classification System (MCS) for oral solid dosage forms. *Pharmaceutical development and technology*. 2015;20(1):12-21.
15. Kimura G, Puchkov M, Leuenberger H. An attempt to calculate in silico disintegration time of tablets containing mefenamic acid, a low water-soluble drug. *Journal of pharmaceutical sciences*. 2013;102(7):2166-78.
16. Leuenberger H, Rohera BD. Fundamentals of powder compression. II. The compression of binary powder mixtures. *Pharmaceutical research*. 1986;3(2):65-74.
17. Riippi M, Antikainen O, Niskanen T, Yliruusi J. The effect of compression force on surface structure, crushing strength, friability and disintegration time of erythromycin acistrate tablets. *European journal of pharmaceutics and biopharmaceutics*. 1998;46(3):339-45.

18. Rahman Z, Siddiqui A, Khan MA. Orally disintegrating tablet of novel salt of antiepileptic drug: formulation strategy and evaluation. *European Journal of Pharmaceutics and Biopharmaceutics*. 2013;85(3):1300-9.
19. Lawrence XY, Amidon G, Khan MA, Hoag SW, Polli J, Raju G, et al. Understanding pharmaceutical quality by design. *The AAPS journal*. 2014;16(4):771-83.
20. Berkowitz B, Balberg I. Percolation theory and its application to groundwater hydrology. *Water Resources Research*. 1993;29(4):775-94.
21. Holman L, Leuenberger H. The relationship between solid fraction and mechanical properties of compacts—the percolation theory model approach. *International journal of pharmaceutics*. 1988;46(1-2):35-44.
22. Leuenberger H, Lanz M. Pharmaceutical powder technology—from art to science: the challenge of the FDA's Process Analytical Technology initiative. *Advanced powder technology*. 2005;16(1):3-25.
23. Tripodi M, Puri V, Manbeck H, Messing G. Constitutive models for cohesive particulate materials. *Journal of agricultural engineering research*. 1992;53:1-21.
24. Leuenberger H. The compressibility and compactibility of powder systems. *International Journal of Pharmaceutics*. 1982;12(1):41-55.
25. Bassam F, York P, Rowe R, Roberts R. Young's modulus of powders used as pharmaceutical excipients. *International journal of pharmaceutics*. 1990;64(1):55-60.
26. Ryshkewitch E. Compression strength of porous sintered alumina and zirconia. *Journal of the American Ceramic Society*. 1953;36.

27. Higuchi T, Elowe L, Busse L. The physics of tablet compression. V. Studies on aspirin, lactose, lactose-aspirin, and sulfadiazine tablets. *Journal of the American Pharmaceutical Association*. 1954;43(11):685-9.
28. Mittal B. An elasto-viscoplastic constitutive formulation for dry powder compression analysis using finite elements. Pennsylvania: The Pennsylvania State University 2003.
29. Rankell AS, Higuchi T. Physics of tablet compression XV. Thermodynamic and kinetic aspects of adhesion under pressure. *Journal of pharmaceutical sciences*. 1968;57(4):574-7.
30. Hanus EJ, King LD. Thermodynamic effects in the compression of solids. *Journal of pharmaceutical sciences*. 1968;57(4):677-84.
31. Esezobo S, Pilpel N. The effect of temperature on the plasto-elasticity of some pharmaceutical powders and on the tensile strengths of their tablets. *Journal of Pharmacy and Pharmacology*. 1986;38(6):409-13.
32. Bogda M. Tablet compression: Machine theory, design, and process troubleshooting. *Encyclopedia of Pharmaceutical Technology*, Ed Swarbrick J, informa healthcare, New York, London. 2007;3614.
33. Michrafy A, Michrafy M, Kadiri M, Dodds J. Predictions of tensile strength of binary tablets using linear and power law mixing rules. *International journal of pharmaceutics*. 2007;333(1):118-26.
34. Kuentz M, Leuenberger H. A new theoretical approach to tablet strength of a binary mixture consisting of a well and a poorly compactable substance. *European journal of pharmaceutics and biopharmaceutics*. 2000;49(2):151-9.

35. Leuenberger H, Rohera BD. Fundamentals of powder compression. I. The compactibility and compressibility of pharmaceutical powders. *Pharmaceutical research*. 1986;3(1):12-22.
36. Wu C-Y, Best SM, Bentham AC, Hancock BC, Bonfield W. Predicting the tensile strength of compacted multi-component mixtures of pharmaceutical powders. *Pharmaceutical research*. 2006;23(8):1898-905.
37. Broadbent SR, Hammersley JM. Percolation processes. *Mathematical Proceedings of the Cambridge Philosophical Society*. 1957;53(03):629-41.
38. Berkowitz B, Ewing RP. Percolation theory and network modeling applications in soil physics. *Surveys in Geophysics*. 1998;19(1):23-72.
39. Christensen K. *Percolation theory*. Imperial College London, London. 2002:40.
40. Aharony A, Stauffer D. *Introduction to percolation theory*. Philadelphia, PA: Taylor & Francis; 2003.
41. Leuenberger H. The application of percolation theory in powder technology. *Advanced Powder Technology*. 1999;10(4):323-52.
42. Isichenko MB. Percolation, statistical topography, and transport in random media. *Reviews of modern physics*. 1992;64(4):961.
43. Leuenberger H, Ineichen L. Percolation theory and physics of compression. *European journal of pharmaceutics and biopharmaceutics*. 1997;44(3):269-72.
44. Stauffer D, Aharony A. *Introduction of Percolation Theory* Taylor and Francis Philadelphia, PA 1985.
45. Sahimi M. *Applications of percolation theory*. London: CRC Press; 1994.
46. Essam JW. Percolation theory. *Reports on Progress in Physics*. 1980;43(7):833.

47. Pinto G, Maaroufi A-K. Critical filler concentration for electro conductive polymer composites. Society of Plastics Engineers (SPE). 2011;10.
48. Vargas-Bernal R, Herrera-Pérez G, Calixto-Olalde ME, Tecpoyotl-Torres M. Analysis of DC electrical conductivity models of carbon nanotube-polymer composites with potential application to nanometric electronic devices. Journal of Electrical and Computer Engineering. 2013;2013.
49. Kirkpatrick S. Percolation and conduction. Reviews of modern physics. 1973;45(4):574.
50. Leuenberger H, Rohera B, Haas C. Percolation theory—a novel approach to solid dosage form design. International journal of pharmaceutics. 1987;38(1):109-15.
51. Leuenberger H, Leu R, Bonny J. Application of percolation theory and fractal geometry to tablet compaction. Drug development and industrial pharmacy. 1992;18(6-7):723-66.
52. Luginbühl R, Leuenberger H. Use of percolation theory to interpret water uptake, disintegration time and intrinsic dissolution rate of tablets consisting of binary mixtures. Pharmaceutica Acta Helvetiae. 1994;69(3):127-34.
53. Caraballo I, Fernández-Arévalo M, Holgado M, Rabasco A. Percolation theory: application to the study of the release behaviour from inert matrix systems. International journal of pharmaceutics. 1993;96(1):175-81.
54. Holman L. The compaction behaviour of particulate materials. An elucidation based on percolation theory. Powder technology. 1991;66(3):265-80.
55. Leuenberger H, Leu R. Formation of a tablet: a site and bond percolation phenomenon. Journal of pharmaceutical sciences. 1992;81(10):976-82.

56. Holman L, Leuenberger H. The relationship between solid fraction and mechanical properties of compacts—the percolation theory model approach. *International journal of pharmaceutics*. 1988;46(1):35-44.
57. Chelidze T. Percolation and fracture. *Physics of the Earth and Planetary Interiors*. 1982;28(2):93-101.
58. Kuentz M, Leuenberger H, Kolb M. Fracture in disordered media and tensile strength of microcrystalline cellulose tablets at low relative densities. *International journal of pharmaceutics*. 1999;182(2):243-55.
59. Wu C-Y, Best SM, Bentham AC, Hancock BC, Bonfield W. A simple predictive model for the tensile strength of binary tablets. *European Journal of Pharmaceutical Sciences*. 2005;25(2):331-6.
60. Tye CK, Sun CC, Amidon GE. Evaluation of the effects of tableting speed on the relationships between compaction pressure, tablet tensile strength, and tablet solid fraction. *Journal of pharmaceutical sciences*. 2005;94(3):465-72.
61. Fell J, Newton J. Determination of tablet strength by the diametral-compression test. *Journal of Pharmaceutical Sciences*. 1970;59(5):688-91.
62. Heckel R. Density-pressure relationships in powder compaction. *Trans Metall Soc AIME*. 1961;221(4):671-5.
63. Klevan I, Nordström J, Tho I, Alderborn G. A statistical approach to evaluate the potential use of compression parameters for classification of pharmaceutical powder materials. *European journal of pharmaceutics and biopharmaceutics*. 2010;75(3):425-35.

64. Kuentz M, Leuenberger H. Pressure susceptibility of polymer tablets as a critical property: a modified Heckel equation. *Journal of pharmaceutical sciences*. 1999;88(2):174-9.
65. Jetzer W, Johnson W, Hiestand E. Comparison of two different experimental procedures for determining compaction parameters. *International journal of pharmaceutics*. 1985;26(3):329-37.
66. Gentis ND, Betz G. Compressibility of binary powder formulations: investigation and evaluation with compaction equations. *Journal of pharmaceutical sciences*. 2012;101(2):777-93.
67. Ryshkewitch E. Compression strength of porous sintered alumina and zirconia. *Journal of the American Ceramic Society*. 1953;36(2):65-8.
68. Leu R, Leuenberger H. The application of percolation theory to the compaction of pharmaceutical powders. *International journal of pharmaceutics*. 1993;90(3):213-9.
69. Kuentz M, Leuenberger H. A new model for the hardness of a compacted particle system, applied to tablets of pharmaceutical polymers. *Powder technology*. 2000;111(1):145-53.
70. Aspnes D, Theeten J, Hottier F. Investigation of effective-medium models of microscopic surface roughness by spectroscopic ellipsometry. *Physical Review B*. 1979;20(8):3292.
71. Stroud D. The effective medium approximations: Some recent developments. *Superlattices and microstructures*. 1998;23(3-4):567-73.
72. Busignies V, Leclerc B, Porion P, Evesque P, Couarraze G, Tchoreloff P. Application of percolation model to the tensile strength and the reduced modulus of

- elasticity of three compacted pharmaceutical excipients. *European Journal of Pharmaceutics and Biopharmaceutics*. 2007;67(2):507-14.
73. Van Veen B, Van der Voort Maarschalk K, Bolhuis G, Frijlink H. Predicting mechanical properties of compacts containing two components. *Powder technology*. 2004;139(2):156-64.
74. Mishra SM, Rohera BD. *Mechanics of Tablet Formation: A Comparative Evaluation of Percolation Theory with Classical Concepts*. *Pharmaceutical Development and Technology*. 2019 (In Press):1-52.
75. Efros ALv. *Physics and geometry of disorder*. *Percolation Theory*. 1982.
76. Stauffer D. *Scaling theory of percolation clusters*. *Physics reports*. 1979;54(1):1-74.
77. Katsura S, Takizawa M. *Bethe lattice and the Bethe approximation*. *Progress of Theoretical Physics*. 1974;51(1):82-98.
78. Peierls R, editor. *On Ising's model of ferromagnetism*. *Mathematical Proceedings of the Cambridge Philosophical Society*; 1936: Cambridge University Press.
79. Ziman J. *Antiferromagnetism by the Bethe Method*. *Proceedings of the Physical Society Section A*. 1951;64(12):1108.
80. Burley D. *Closed form approximations for lattice systems*. *Phase transitions and critical phenomena*. 1972;2:329-74.
81. Guyon E, Roux S, Hansen A, Bideau D, Troadec J-P, Crapo H. *Non-local and non-linear problems in the mechanics of disordered systems: application to granular media and rigidity problems*. *Reports on Progress in Physics*. 1990;53(4):373.

82. Tian Z, Dong K, Yu A, editors. A method for structural analysis of disordered particle systems. AIP Conference Proceedings; 2013: AIP.
83. Bernal JD. A geometrical approach to the structure of liquids. *Nature*. 1959;183(4655):141.
84. Ziff RM, Torquato S. Percolation of disordered jammed sphere packings. *Journal of Physics A: Mathematical and Theoretical*. 2017;50(8):085001.
85. Grassberger P. Universality and asymptotic scaling in drilling percolation. *Physical Review E*. 2017;95(1):010103.
86. Chaves C, Koiller B. Universality, thresholds and critical exponents in correlated percolation. *Physica A: Statistical Mechanics and its Applications*. 1995;218(3-4):271-8.
87. Miranda A, Millán M, Caraballo I. Investigation of the influence of particle size on the excipient percolation thresholds of HPMC hydrophilic matrix tablets. *Journal of pharmaceutical sciences*. 2007;96(10):2746-56.
88. Bonny JD, Leuenberger H. Matrix type controlled release systems: I. Effect of percolation on drug dissolution kinetics. *Pharmaceutica Acta Helvetiae*. 1991;66(5-6):160-4.
89. Bonny J, Leuenberger H. Matrix type controlled release systems II. Percolation effects in non-swellable matrices. *Pharmaceutica Acta Helvetiae*. 1993;68(1):25-33.
90. Hartley HO. The modified Gauss-Newton method for the fitting of non-linear regression functions by least squares. *Technometrics*. 1961;3(2):269-80.
91. Brown AM. A step-by-step guide to non-linear regression analysis of experimental data using a Microsoft Excel spreadsheet. *Computer methods and programs in biomedicine*. 2001;65(3):191-200.

92. SigmaPlot Version 11.0. Systat Software, Inc., San Jose, California. 2008.
93. OriginLab C. OriginPro. Northampton; 2010.
94. Garekani HA, Ford JL, Rubinstein MH, Rajabi-Siahboomi AR. Effect of compression force, compression speed, and particle size on the compression properties of paracetamol. *Drug development and industrial pharmacy*. 2001;27(9):935-42.
95. Sonnergaard J. A critical evaluation of the Heckel equation. *International journal of pharmaceutics*. 1999;193(1):63-71.
96. Imbert C, Tchoreloff P, Leclerc B, Couarraze G. Indices of tableting performance and application of percolation theory to powder compaction. *European journal of pharmaceutics and biopharmaceutics*. 1997;44(3):273-82.
97. Li XH, Zhao LJ, Ruan KP, Feng Y, Ruan KF. The application of factor analysis to evaluate deforming behaviors of directly compressed powders. *Powder Technology*. 2013;247:47-54.
98. Nokhodchi A, Maghsoodi M, Hassan-Zadeh D, Barzegar-Jalali M. Preparation of agglomerated crystals for improving flowability and compactibility of poorly flowable and compactible drugs and excipients. *Powder technology*. 2007;175(2):73-81.
99. Patel S, Bansal AK. Prediction of mechanical properties of compacted binary mixtures containing high-dose poorly compressible drug. *International journal of pharmaceutics*. 2011;403(1):109-14.
100. Zuurman K, Van der Voort Maarschalk K, Bolhuis G. Effect of magnesium stearate on bonding and porosity expansion of tablets produced from materials with different consolidation properties. *International journal of pharmaceutics*. 1999;179(1):107-15.

101. Mohammed H, Briscoe B, Pitt K. A study on the coherence of compacted binary composites of microcrystalline cellulose and paracetamol. *European journal of pharmaceutics and biopharmaceutics*. 2006;63(1):19-25.
102. Busignies V, Leclerc B, Porion P, Evesque P, Couarraze G, Tchoreloff P. Investigation and modelling approach of the mechanical properties of compacts made with binary mixtures of pharmaceutical excipients. *European journal of pharmaceutics and biopharmaceutics*. 2006;64(1):51-65.
103. Gupta N, Ye R, Porfiri M. Comparison of tensile and compressive characteristics of vinyl ester/glass microballoon syntactic foams. *Composites Part B: Engineering*. 2010;41(3):236-45.
104. Sun W-J, Kothari S, Sun CC. The relationship among tensile strength, Young's modulus, and indentation hardness of pharmaceutical compacts. *Powder Technology*. 2018;331:1-6.
105. Kachrimanis K, Malamataris S. "Apparent" Young's elastic modulus and radial recovery for some tableted pharmaceutical excipients. *European journal of pharmaceutical sciences*. 2004;21(2):197-207.
106. Malamataris S, Hatjichristos T, Rees J. Apparent compressive elastic modulus and strength isotropy of compacts formed from binary powder mixes. *International journal of pharmaceutics*. 1996;141(1-2):101-8.
107. Kerridge J, Newton J. The determination of the compressive Young's modulus of pharmaceutical materials. *Journal of Pharmacy and Pharmacology*. 1986;38(S12):79P-P.

108. Spriggs R. Expression for effect of porosity on elastic modulus of polycrystalline refractory materials, particularly aluminum oxide. *Journal of the American Ceramic Society*. 1961;44(12):628-9.
109. Phani KK, Niyogi S. Young's modulus of porous brittle solids. *Journal of materials science*. 1987;22(1):257-63.
110. Osei-Yeboah F, Chang S-Y, Sun CC. A critical examination of the phenomenon of bonding area-bonding strength interplay in powder tableting. *Pharmaceutical research*. 2016;33(5):1126-32.
111. Kuentz M, Leuenberger H. Modified Young's modulus of microcrystalline cellulose tablets and the directed continuum percolation model. *Pharmaceutical development and technology*. 1998;3(1):13-9.
112. Leuenberger H. *Zur Theorie der Pulverkompensation*: Verlag nicht ermittelbar; 1980.
113. Kawakita K, Lüdde K-H. Some considerations on powder compression equations. *Powder technology*. 1971;4(2):61-8.
114. Comoglu T. An overview of compaction equations. *Journal of Faculty of Pharmacy*. 2007;36:123.
115. Panelli R, Ambrozio Filho F. Compaction equation and its use to describe powder consolidation behavior. *Powder metallurgy*. 1998;41(2):131-3.
116. Levin M, Tsygan L, Dukler S. Press simulation apparatus and methods. *Google Patents*; 2002.

117. Maneerojpakdee D, Mitrevej, A. (...), Sinchaipanid, N., Nowak, J., Leuenberger, H. An attempt to adopt the workflow of the automotive and aircraft industry for the design of drug delivery vehicles. *Pharm Tech Japan*. 2017;33,11:145 – 56.
118. Guidance for industry: Quality systems approach to pharmaceutical cGMP regulations. *Pharmaceutical CGMPs*. 2006.
119. Prigogine I, Stengers I. *Order out of chaos: Man's new dialogue with nature*: Verso Books; 2018.
120. Mandelbrot BB. *The Fractal Geometry of Nature*. Freeman New York. 1983.
121. Bonny J. Determination of fractal dimensions of matrix-type solid dosage forms and their relation with drug dissolution kinetics. *Eur J Pharm Biopharm*. 1993;39:31-7.
122. Stephen H. *Space and Time Warps*. Available from: <http://www.hawking.org.uk/space-and-time-warps.html>.
123. Coniglio A, Fierro A. Correlated percolation. arXiv preprint arXiv:160904160. 2016.
124. Jetzer W. Measurement of hardness and strength of tablets and their relation to compaction performance of powders. *Journal of pharmacy and pharmacology*. 1986;38(4):254-8.
125. Roberts R, Rowe R. The effect of the relationship between punch velocity and particle size on the compaction behaviour of materials with varying deformation mechanisms. *Journal of pharmacy and pharmacology*. 1986;38(8):567-71.
126. Paul S, Sun CC. The suitability of common compressibility equations for characterizing plasticity of diverse powders. *International journal of pharmaceutics*. 2017;532(1):124-30.

127. Narayan P, Hancock BC. The relationship between the particle properties, mechanical behavior, and surface roughness of some pharmaceutical excipient compacts. *Materials Science and Engineering: A*. 2003;355(1-2):24-36.
128. Augsburger LL, Hoag SW. *Pharmaceutical dosage forms-tablets*: CRC Press; 2016.
129. Adolfsson Å, Nyström C. Tablet strength, porosity, elasticity and solid state structure of tablets compressed at high loads. *International journal of pharmaceutics*. 1996;132(1-2):95-106.
130. Akaike H. A new look at the statistical model identification. *IEEE transactions on automatic control*. 1974;19(6):716-23.
131. Sun CC. Decoding powder tableability: roles of particle adhesion and plasticity. *Journal of Adhesion Science and Technology*. 2011;25(4-5):483-99.

Appendix

Nonlinear regression analysis using OriginPro.

Model: Percolation Model (Eq. 40)

Powder Component: Microcrystalline cellulose (Avicel® PH 102)

[General Information]

$$Y = A * ((x - C) / (1 - c))^q$$

Function Name = Percolation Model

Brief Description =

Function Source = N/A

Number of Parameters = 3

Function Type = User-Defined

Function Form = Expression

Path =

Number Of Independent Variables = 1

Number Of Dependent Variables = 1

[Fitting Parameters]

Names = A,q,c

Initial Values = 10(V),2(V),0.5(V)

Meanings = ?,?,?

Lower Bounds = --(I, Off),--(I, Off),--(I, Off)

Upper Bounds = --(I, Off),--(I, Off),--(I, Off)

Naming Method = User-Defined

Number Of Significant Digits = 0,0,0

Unit = ,,

[Independent Variables]

x =

[Dependent Variables]

y =

[Formula]

$A*((x-C)/(1-c))^q$

[Constraints]

[Initializations]

[After Fitting]

[Constants]

[Controls]

General Linear Constraints = 0

Initialization Scripts = off

Scripts After Fitting = off

Number Of Duplicates = N/A

Duplicate Offset = N/A

Duplicate Unit = N/A

Generate Curves After Fitting = Yes

Curve Point Spacing = Uniform on X-Axis Scale

Generate Peaks After Fitting = Yes

Generate Peaks During Fitting = Yes

Generate Peaks with Baseline = Yes

Paste Parameters to Plot After Fitting = Yes

Paste Parameters to Notes Window After Fitting = Yes

Generate Residuals After Fitting = No

Keep Parameters = No

Compile On Param Change Script = off

Enable Parameters Initialization = 1

[Compile Function]

Compile = 0

Compile Parameters Initialization = 1

OnParamChangeScriptsEnabled = 0.

[Parameters Initialization]

//Code to be executed to initialize parameters

[Origin C Function Header]

[Origin C Parameter Initialization Header]

[Derived Parameter Settings]

Unit =

Names =

Meanings =

[QuickCheck]

x=1

A=10

q=2

c=0.5

Nonlinear Curve Fit (NewFunction (User))

Notes

```

-----
Notes
-----
Description          Nonlinear Curve Fit
User Name            smish258
Model                NewFunction (User)
Number of Parameters 3
Number of Derived Parameters 0
Number of Datasets  1
Equation             A*((x-C)/(1-c))^q
Report Status        New Analysis Report
Special Input Handling

```

Input Data

```

-----
Dep/Indep      Data      Range      Weight Type
-----
B   x   Indep   [Book1]Sheet1!A  [1*:17*]
B   y   Dep     [Book1]Sheet1!B  [1*:17*]  No Weighting

```

Masked Data - Values Excluded from Computations

```

-----
Notes
-----
Masked Data - Values Excluded from Computations  No Masked Data

```

Bad Data (missing values) -- Values that are invalid and thus not used in computations

Notes

Bad Data (missing values) -- Values that are invalid and thus not used in computations No Missing Data

Parameters

Unit	A	q	c
Value	12.75439	2.7942	0.21643
Fixed	N	N	N
Standard Error	0.42102	0.34796	0.06008
t-Value	30.29395	8.03018	3.60251
Prob> t	3.64E-14	1.31E-06	0.00288
95% LCL	11.85139	2.0479	0.08758
95% UCL	13.65738	3.54051	0.34529
Dependency	0.96108	0.99673	0.99452
CI Half-Width	0.903	0.74631	0.12885
Lower Bound	--	--	--
Upper Bound	--	--	--

Reduced Chi-sqr = 0.0122022645834
 COD(R^2) = 0.99822062541359
 Iterations Performed = 6
 Total Iterations in Session = 6
 Fit converged - tolerance criterion satisfied.

Statistics

```

-----
                                     B
-----
Number of Points           17
Degrees of Freedom         14
Reduced Chi-Sqr            0.012202264583421
Residual Sum of Squares    0.1708317041679
R Value                    0.99910991658255
R-Square(COD)              0.99822062541359
Adj. R-Square              0.9979664290441
Root-MSE (SD)             0.11046386098368
Number of Iterations       6
Fit Status                  Succeeded(100)
  
```

Fit Status Code :
 100 : Fit converged - tolerance criterion satisfied.

Summary

A	Value	12.75439
A	Standard Error	0.42102
A	95% LCL	11.85139
A	95% UCL	13.65738
q	Value	2.7942
q	Standard Error	0.34796
q	95% LCL	2.0479
q	95% UCL	3.54051
c	Value	0.21643
c	Standard Error	0.06008
c	95% LCL	0.08758
c	95% UCL	0.34529
Statistics	Reduced Chi-Sqr	0.0122
Statistics	R-Square (COD)	0.99822
Statistics	Adj. R-Square	0.99797

ANOVA

		DF	Sum of Squares	Mean Square	F Value	Prob>F
B	Regression	3	287.75897	95.91966	7860.80776	0
B	Residual	14	0.17083	0.0122		
B	Uncorrected Total	17	287.9298			
B	Corrected Total	16	96.0066			

Covariance

B

```

-----
                A                q                c
-----
A  0.17725858851863    0.12926124256225    -0.020058953216936
q  0.12926124256225    0.12107804527362    -0.020576536554642
c  -0.020058953216936  -0.020576536554642    0.0036093879607006

```

Correlation

B

```

-----
                A                q                c
-----
A            1                0.88233190296934    -0.7930267544176
q    0.88233190296934    1                -0.98428936550146
c    -0.7930267544176    -0.98428936550146    1
  
```

Fitted value, confidence limit and prediction limit

Fitted curve plot		Confidence limit		Prediction limit	
Independent variable	Fitted value	95% Lower confidence limit	95% Upper confidence limit	95% Lower Prediction limit	95% Upper Prediction limit
0.3258	0.05201	-0.02394	0.12796	-0.19679	0.30081
0.3448	0.08137	-0.00775	0.17049	-0.17176	0.3345
0.4084	0.25051	0.13324	0.36778	-0.01385	0.51487
0.4299	0.33701	0.21615	0.45788	0.07105	0.60298
0.5473	1.14669	1.04138	1.25201	0.88742	1.40597
0.5967	1.69167	1.59395	1.78939	1.43539	1.94795
0.6444	2.35352	2.25648	2.45057	2.0975	2.60955
0.6871	3.06993	2.97261	3.16725	2.8138	3.32606
0.7118	3.54158	3.4466	3.63656	3.28633	3.79683
0.7361	4.04866	3.95884	4.13847	3.79528	4.30203
0.7563	4.50389	4.42006	4.58771	4.25257	4.7552
0.7769	5.00069	4.92226	5.07913	4.75113	5.25026
0.7957	5.48362	5.40496	5.56228	5.23399	5.73326
0.81	5.87031	5.78454	5.95608	5.61834	6.12228
0.8192	6.12809	6.03357	6.22261	5.87301	6.38317
0.8386	6.69525	6.57099	6.8195	6.42772	6.96278
0.8446	6.87723	6.7408	7.01365	6.60383	7.15062

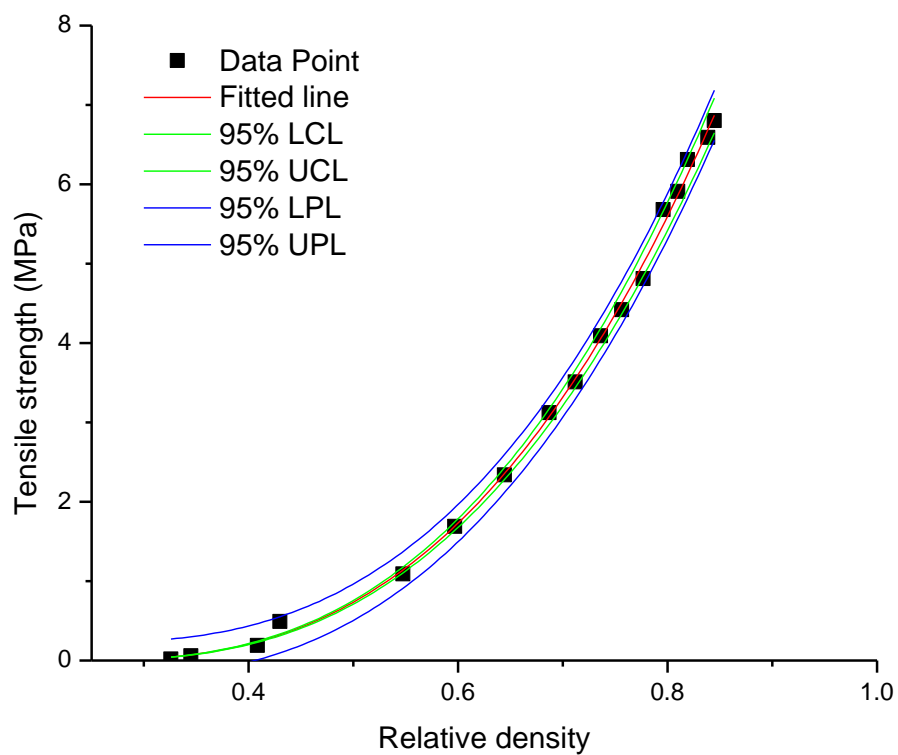


Figure 1: Plot depicting the relationship between tensile strength vs. relative density of microcrystalline cellulose using percolation model (Eq.40)

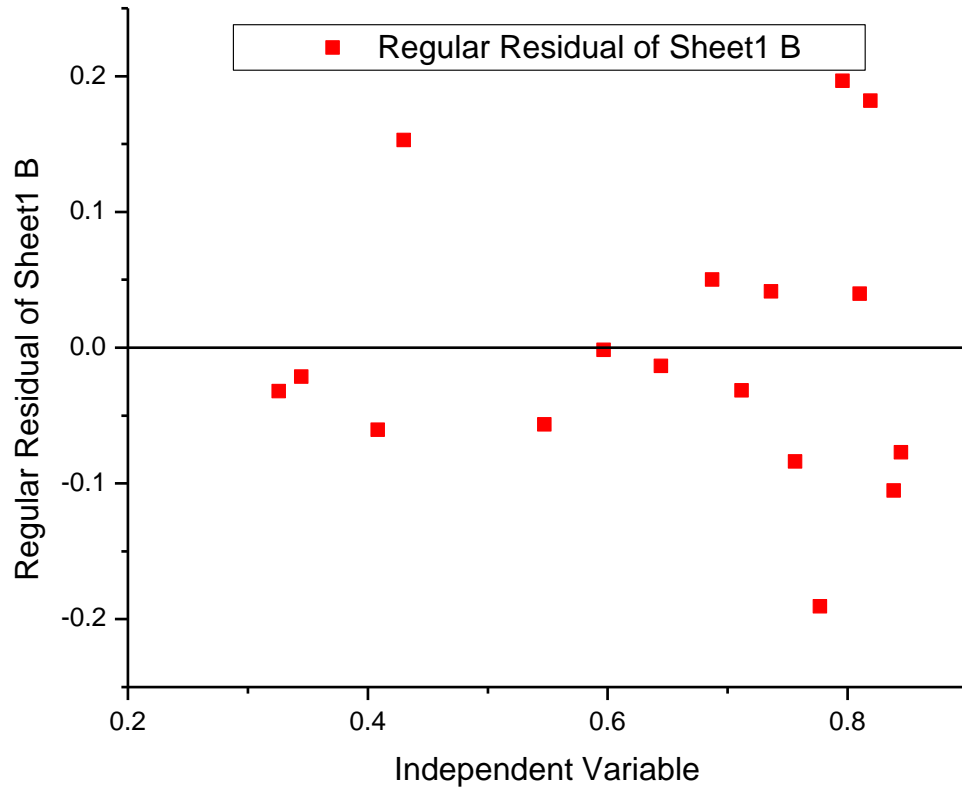


Figure 2: Residual graph for percolation model (Eq.40) using nonlinear regression analysis.

Residuals

Independent Variable	Regular Residual of Sheet1 B	Standardized Residual of Sheet1 B	Studentized Residual of Sheet1 B	Studentized Deleted Residual of Sheet1 B
0.3258	-0.03201	-0.28978	-0.30593	-0.29579
0.3448	-0.02137	-0.19347	-0.20881	-0.20153
0.4084	-0.06051	-0.54778	-0.63042	-0.6163
0.4299	0.15299	1.38494	1.61022	1.71897
0.5473	-0.05669	-0.51323	-0.57295	-0.5587
0.5967	-0.00167	-0.01511	-0.01658	-0.01598
0.6444	-0.01352	-0.12241	-0.13419	-0.12939
0.6871	0.05007	0.45327	0.49715	0.48335
0.7118	-0.03158	-0.28588	-0.31205	-0.30175
0.7361	0.04134	0.37427	0.40447	0.39205
0.7563	-0.08389	-0.7594	-0.81192	-0.80148
0.7769	-0.19069	-1.7263	-1.82946	-2.02096
0.7957	0.19638	1.77774	1.88464	2.10224
0.81	0.03969	0.35931	0.38546	0.37342
0.8192	0.18191	1.64674	1.79585	1.97258
0.8386	-0.10525	-0.95278	-1.11902	-1.13004
0.8446	-0.07723	-0.69911	-0.85511	-0.8464

VITA

Name: Saurabh M. Mishra

Baccalaureate Degree: KLES College of Pharmacy, Belgaum, India
Graduated: December 2012

Master's Degree: St. John's University, College of Pharmacy and
Health Sciences, Queens, NY
Graduated: July 2015